Foamy Virus Enzymes
Activity, Regulation and Resistance

Dissertation

zur Erlangung des Doktorgrades
der Fakultät für Biologie, Chemie und Geowissenschaften
an der Universität Bayreuth

Vorgelegt von
Diplom-Biochemiker
Maximilian Johannes Hartl

Bayreuth, 2009

Die vorliegende Arbeit wurde von August 2006 bis Oktober 2009 am Lehrstuhl für Struktur und Chemie der Biopolymere unter der Leitung von Prof. Dr. Birgitta Wöhrl angefertigt.

Vollständiger Abdruck der von der Fakultät für Biologie, Chemie und Geowissenschaften der Universität Bayreuth genehmigten Dissertation zur Erlangung des akademischen Grades eines Doktors der Naturwissenschaften (Dr. rer. nat.)

Promotionsgesuch eingereicht am: 21. Oktober 2009
Tag des wissenschaftlichen Kolloquiums: 19. März 2010

Prüfungsausschuss:
Prof. Dr. Birgitta Wöhrl (Erste Gutachterin)
Prof. Dr. Olaf Stemmann (Zweiter Gutachter)
Prof. Dr. Matthias Ullmann (Vorsitzender)
Prof. Dr. Franz X. Schmidt

„*Das Leben ist wert, gelebt zu werden, sagt die Kunst, die schönste Verführerin;*
das Leben ist wert, erkannt zu werden, sagt die Wissenschaft.“

Friedrich Nietzsche

Table of contents

Zusammenfassung

Foamy Viren oder Spumaretroviren gehören zur Familie der *Retroviridae*, unterscheiden sich jedoch deutlich von allen übrigen Retroviren (Orthoretroviren). Das Genom in infektiösen Viren besteht aus DNA und nicht aus RNA. Zudem wird Pol, das Vorläuferprotein der viralen Enzyme, von einer eigenen mRNA unabhängig von Capsid- und Matrix-Proteinen translatiert. Schließlich bleibt die virale Protease mit der Reversen Transkriptase verbunden, während sich die Proteasen von Orthoretroviren selbst abspalten. Gereifte Spumaretroviren enthalten somit ein Protease-Reverse Transkriptase (PR-RT) Protein, das drei katalytische Aktivitäten vereint: Proteolyse, DNA Polymerisation and RNase H Aktivität.

In dieser Arbeit wurden rekombinante PR-RTs von zwei verschiedenen Foamy Viren (dem Prototyp Foamy Virus und dem Simian Foamy Virus aus Makaken) gereinigt und miteinander verglichen. Unsere Ergebnisse zeigen, dass sich die enzymatischen Aktivitäten und die biophysikalischen Eigenschaften der beiden Proteine ähneln. Sie unterschieden sich jedoch bezüglich ihres Resistenzverhaltens gegenüber Azidothymidin. Dieser Nukleosidinhibitor ist in der Lage die Replikation von Foamy Viren zu hemmen, indem er die DNA Polymerisation terminiert. Während Prototyp Foamy Viren keine Resistenz gegen Azidothymidin entwickelten, gelang es, Azidothymidin-resistente Simian Foamy Viren zu isolieren. Vier Mutationen im Bereich der Reversen Transkriptase wurden identifiziert, die für diese Resistenz verantwortlich sind. Um den molekularen Mechanismus der Resistenz aufzuklären, wurden die entsprechenden rekombinanten PR-RT-Enzyme *in vitro* analysiert. Es wurde nachgewiesen, dass die Resistenz der Viren auf der Fähigkeit beruht, den bereits eingebauten Inhibitor mit Hilfe von ATP wieder zu entfernen.

Obwohl retrovirale Proteasen nur als Homodimere aktiv sind, zeigten analytische Ultrazentrifugation und Größenausschlußchromatographie, dass die PR-RTs des Simian Foamy Virus aus Makaken und des Prototyp Foamy Virus in Lösung als inaktive Monomere vorlagen. Die dreidimensionale Struktur der separaten Protease-Domäne des Simian Foamy Virus wurde durch Kernspinresonanzspektroskopie bestimmt. Sie weist die typische Faltung einer Monomeruntereinheit anderer retroviraler Proteasen auf. Darüber hinaus belegten Messungen paramagnetischer Relaxationsverstärkungen der Protease-Domäne mittels Kernspinresonanzspektroskopie die Ausbildung von transienten Homodimeren.

Diese Arbeit zeigt weiterhin, dass bestimmte purinreiche RNA-Sequenzen der Foamy Viren in der Lage sind, die Protease zu aktivieren. Chemische Analysen der entsprechenden RNA-Sekundärstrukturen deuteten auf die Ausbildung von charakteristischen Haarnadelschleifen-Strukturen hin. Retardations- und chemische Proteinquervernetzungsexperimente bewiesen

zudem die Ausbildung von stabilen PR-RT Dimeren in Gegenwart dieser RNA-Sequenzen. Auf Grundlage der vorgestellten *in vitro* Experimente wird ein Modell für den Ablauf des Zusammenbaus der Viruspartikel von Foamy Viren vorgeschlagen.

Summary

Foamy viruses or spumaretroviruses belong to the family of *retroviridae* but differ in several aspects from other retroviruses (orthoretroviruses). Viral particles contain DNA not RNA. The Pol protein, the precursor of the viral enzymes, is translated from a separate mRNA independently of the capsid and matrix proteins. The protease remains covalently bound to the reverse transcriptase, while in orthoretroviruses the protease is cleaved off autocatalytically. Thus, in mature spumaretroviruses a protease-reverse transcriptase protein (PR-RT) with three different catalytic activities is found: proteolysis, DNA polymerization and RNase H activity.

In this work, the recombinant PR-RTs from the prototype foamy virus and a simian foamy virus isolate from macaques were purified and compared. The biophysical and enzymatic properties of the two enzymes were similar. However, their behavior towards the nucleoside inhibitor azidothymidine is different. This nucleoside analog inhibits the replication of foamy viruses by terminating polymerization. Prototype foamy virus was not able to develop resistance against azidothymidine, but we succeeded in the generation of an azidothymidine-resistant simian foamy virus. Up to four mutations within the reverse transcriptase were found to be necessary to confer high resistance against azidothymidine. To characterize the mechanism of resistance, the corresponding recombinant PR-RTs were investigated *in vitro*. The data reveal that the azidothymidine resistance is based on the excision of the incorporated inhibitor in the presence of ATP.

Retroviral proteases are only active as homodimers. In this work, analysis of the PR-RT of prototype foamy virus and simian foamy virus isolated from macaques by analytical ultracentrifugation and size exclusion chromatography indicate, that foamy virus proteases are stable and inactive monomers in solution. The three-dimensional structure of the simian foamy virus protease domain was determined by nuclear magnetic resonance spectroscopy and revealed the typical folding of a monomer subunit of retroviral proteases. Furthermore, nuclear magnetic resonance analysis by paramagnetic relaxation enhancement suggested the formation of transient protease homodimers under native conditions.

Finally, it is shown that polypurine rich sequences of the foamy virus RNA are able to activate protease activity. Chemical analysis of the secondary structure of these RNA sequences indicated a characteristic hairpin loop structure. Retardation and protein crosslinking experiments prove the formation of stable PR-RT dimers in the presence of the polypurine RNA sequences. Based on these *in vitro* data we propose a model for foamy virus assembly.

1 Introduction

1.1 Foamy viruses

Until the 1960s the "Central Dogma" of molecular biology, meaning that there is an irreversible flow of information in the cell from deoxyribonucleic acid (DNA) to ribonucleic acid (RNA) to protein, was incontrovertible. However, this changed with the discovery of reverse transcription in retroviruses confirming an earlier proposal, which postulated that retroviruses indeed generate DNA copies of their RNA genome (Temin, 1964; Baltimore, 1970; Temin & Mizutani, 1970). All retroviruses share this unique behavior.

Since many retroviruses cause diseases in animals as well as in humans, researchers always have had a special interest in this family of viruses. Representatives are the oncogenic murine leukemia virus (MLV) and, most famous, the human immunodeficiency virus (HIV) causing the **a**cquired **i**mmuno**d**eficiency **s**yndrome (AIDS). On the other hand, a distinct group of retroviruses, the so-called foamy viruses (FVs) (Figure 1.1), have not been associated with any disease and thus appear to be less dangerous (reviewed in Meiering & Linial, 2001).

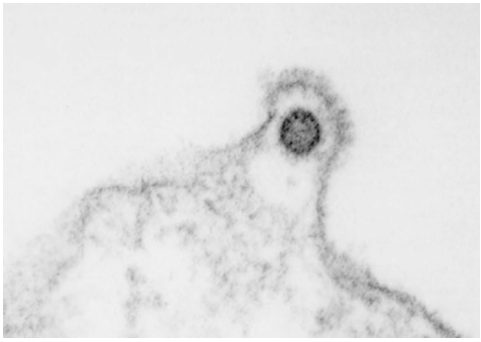

Figure 1.1: Electron microscopy of Prototype FV budding from the plasma membrane of human embryonic lung fibroblasts (Meiering & Linial, 2001)**.**

Phylogenetically, FVs are set apart from all other retroviruses (Figure 1.2) and form their own subfamily of *Spumaretrovirinae* (spumaretroviruses). All remaining retroviruses are combined in the second subfamily of *Orthoretrovirinae* (orthoretroviruses) (Rethwilm, 2005). FVs are widespread in vertebrates, especially in apes. Transmission occurs through biting and licking. They are the oldest known vertebrate RNA viruses having existed for at least 65 million years in primate populations (Switzer *et al.*, 2005).

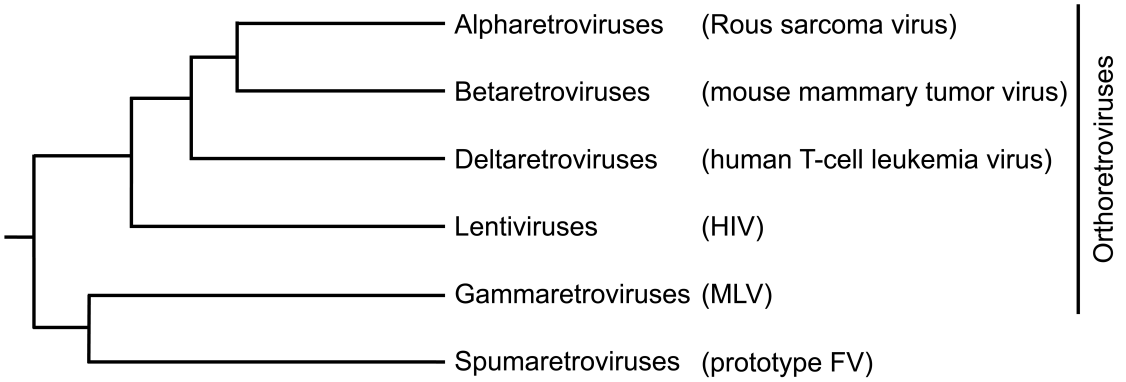

Figure 1.2: Phylogenetic tree of retroviruses.
The tree is based on the RT sequence of the viruses depicted in parenthesis (modified from Coffin *et al.*, 1997).

FVs can infect humans, but there appears to be no human-to-human transfections and patients stay healthy. Humans reported to be infected with FVs have either been bitten by an ape or have been infected working with FVs in a laboratory (reviewed in Meiering & Linial, 2001). Still, FVs integrate their genes into the host cell's genome as all retroviruses do. These features make FVs a potential tool as vectors in molecular biology carrying recombinant genetic material and possibly for gene therapeutic approaches as well. Moreover, prominent characteristics in the FV replication and life cycle might enable us to better understand retroviral behavior in general.

Research on FVs focuses on two different species: a simian FV derived from macaques (SFVmac) and the prototype FV (PFV), originally isolated from humans but most probably originating from chimpanzee (Herchenröder *et al.*, 1994). The main focus of this work is put on these species as well.

1.2 Virus and life cycle

The most obvious difference between FVs and orthoretroviruses is that infectious FV particles contain double-stranded DNA instead of single-stranded RNA (Figure 1.3) (Moebes *et al.*, 1997; Yu *et al.*, 1999; Roy *et al.*, 2003). In fact this has been the main reason to establish a special subfamily for FVs. Consequently, this means that reverse transcription of the viral RNA into DNA has to occur during assembly or budding of the virus particle – at a late time point in the viral life cycle. In orthoretroviruses virions harbor RNA and reverse transcription occurs early in the life cycle (Goff, 2007).

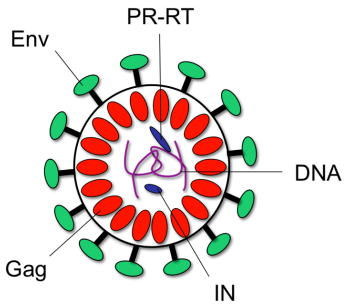

Figure 1.3: The FV virion.
In this schematic figure the relative locations of the viral proteins in the viral particle are shown. DNA is shown in purple, Env in green, Gag in red and the proteins resulting from protease cleavage of Pol in blue. PR-RT: protease-reverse transcriptase; IN: integrase.

The organization of the FV genome is typical for complex retroviruses (Figure 1.4). Long terminal repeats (LTR) enframe the complete genetic information. Three characteristic retroviral genes are found in the genome:

- *gag* (capsid and matrix proteins),
- *pol* (viral enzymes) and
- *env* (envelope glycoproteins).

These genes are transcribed from a promoter (P) in the 5' LTR region. Interestingly, each of these genes is translated from a separate mRNA. This is in clear contrast to all other retroviruses where Gag and Pol are derived from the same mRNA. Translation in FVs therefore leads to the polyproteins Gag, Pol and Env, whereas in orthoretroviruses Gag, Gag-Pol and Env are synthesized (Rethwilm, 2003; Rethwilm, 2005; Linial, 2007). To obtain mature virus particles, a protease (PR) has to cleave the polyproteins into the different proteins. This is either catalyzed by the viral protease PR (Gag and Pol) or by cellular PRs (Env). Remarkably, there is only a single PR cleavage site within the Pol polyprotein of FVs located between the reverse transcriptase (RT) and integrase (IN). A second cleavage site

separating PR and RT, which is present in orthoretroviruses, is missing (Pfrepper *et al.*, 1998; Flügel & Pfrepper, 2003). Thus, the FV enzymes consist of a combined PR-RT and a separate IN (Figure 1.4).

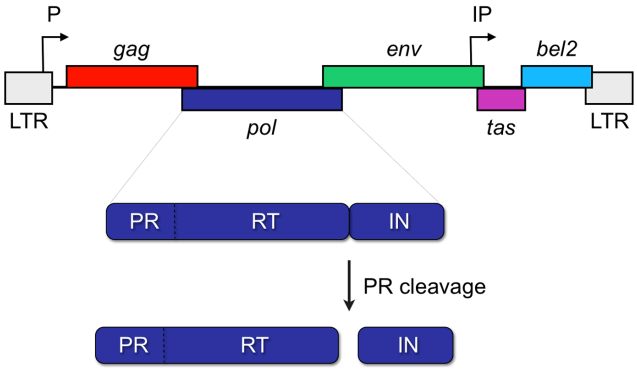

Figure 1.4: FV genome and Pol polyprotein.
Top: Organization of the FV genome and coding regions together with the 5' and 3' promoter (right-angled arrows). Bottom: The Pol polyprotein including protease (PR), reverse transcriptase (RT) and integrase (IN) and its processing by PR.

Typical for FV is a second internal promoter (IP) located in the *env* gene. Starting from this promoter *tas* and *bel2* are transcribed resulting in the two nonstructural proteins Tas and Bet. Bet is translated from a spliced mRNA of *tas* and *bel2* (Löchelt *et al.*, 1994). While Tas is a transactivator of transcription (Mergia *et al.*, 1990; Rethwilm *et al.*, 1991) the function of Bet is yet unclear but the protein might be an antagonist of the APOBEC 3C protein, which is part of the cellular immune response (Löchelt *et al.*, 2005; Russell *et al.*, 2005; Perkovic *et al.*, 2009).

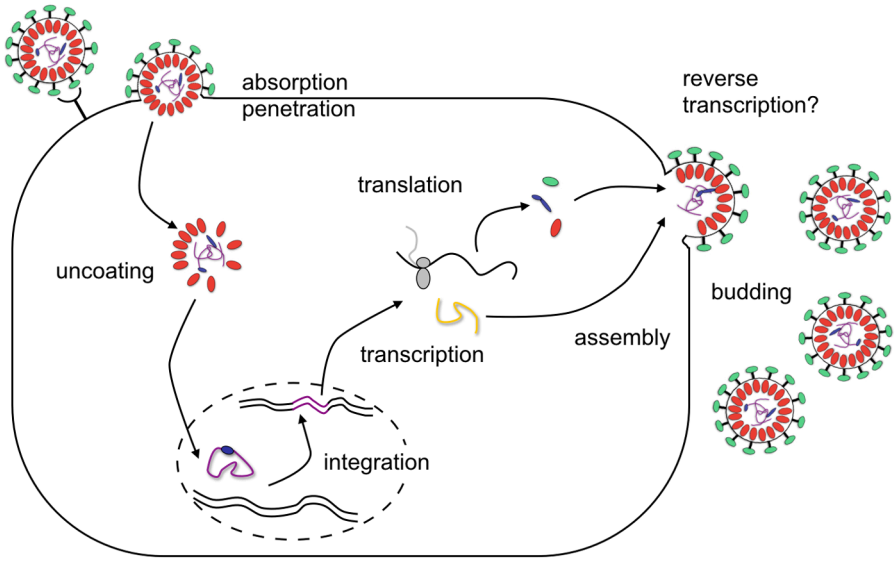

Figure 1.5: Schematic life cycle of FV.
Viral DNA is indicated in purple, genomic RNA in yellow, Env in green, Gag in red and Pol in blue. (Budding of viral particles from the membrane of the endoplasmatic reticulum is not shown.) A detailed description is given in the text below.

Figure 1.5 gives an overview of the life cycle of FVs. First, DNA-containing virions bind to a yet unknown receptor and penetrate the cell. Uncoating is achieved by cleavage of Gag by cellular protease. The viral DNA and IN are imported into the nucleus where integration of the DNA into the host cell genome is catalyzed by the viral IN enzyme. The integrated provirus serves as a template for transcription and translation of the viral RNA and proteins by viral and cellular factors (reviewed in Linial, 2007).

So far, assembly of the virus particle is poorly understood. Capsid formation appears to occur in the cytoplasm (Eastman & Linial, 2001) and glycoproteins are added on either the membrane of the endoplasmatic reticulum or the plasma membrane (Goepfert *et al.*, 1999; Meiering & Linial, 2001). However, it is still unclear at which time point RNA is reverse transcribed and how assembly of the viral RNA, the Gag and especially the Pol proteins works. The latter is a problem, which is not faced by orthoretroviruses, as Gag and Pol are expressed as a fusion protein. Orthoretroviral Gag harbors a localization signal and therefore localization of Pol is achieved simultaneously (Coffin *et al.*, 1997).

Recently, two components critical for incorporation of Pol into the FV virion were identified. It has been shown that the C-terminus of Gag is required for Pol encapsidation (Stenbak & Linial, 2004; Lee & Linial, 2008). Additionally, Peters *et al*. (2008) demonstrated that parts of the viral nucleic acid sequence play an important role for the same process. These sequences are located in the central polypurine tract (cPPT) within the *pol* open reading frame. In FVs as well as lentiviruses the cPPT is present in addition to the 3' polypurine tract (PPT) upstream of the 3' LTR (Kupiec *et al.*, 1988; Arhel *et al.*, 2006). The PPT is important for synthesis of the viral DNA. In the FV cPPT there are four polypurine rich sequences (A-D), whose lengths vary between nine to twelve bases. While the role of D is unclear, C is required for regulation of gene expression, and encapsidation of Pol is dependent on A and B (Peters *et al.*, 2008). At the end of the FV life cycle, viral particles bud from the cell.

Although it is not exactly known at which time point the polyproteins are processed or reverse transcription of the genomic RNA occurs, in infectious viral particles all these processes are finished. Characteristic for FV particles is an immature looking core and prominent surface spikes (Linial, 2007).

1.3 Reverse transcriptases

The key enzyme within the retroviral life cycle is the RT. It is responsible for synthesis of double-stranded DNA starting from a single-stranded RNA template – a rather complex procedure. Thereby three different reactions have to be catalyzed:

- RNA-dependent DNA polymerization,
- DNA-dependent DNA polymerization and
- cleavage of the RNA strand in an RNA/DNA hybrid.

While synthesis of DNA is catalyzed by the RT's polymerase activity, cleavage of RNA is due to the RNase H domain at the C-terminus of the RT.

For synthesis of double stranded DNA a transfer RNA (tRNA) primer has to bind to the viral primer binding site (PBS) of the (+) strand RNA (Figure 1.6, step 1). FVs use the cellular $tRNA_{Lys1,2}$ (Maurer *et al.*, 1988), while other retroviruses make use of other tRNAs (e. g. $tRNA_{Lys3}$ in HIV-1 (Raba *et al.*, 1979; Wain-Hobson *et al.*, 1985)). Polymerization of the (-)-strand DNA starts at the PBS and stops when the end of the 5' LTR is reached (step 2). Thus, this region forms an RNA/DNA hybrid and serves as a substrate for RNase H. Degradation of the RNA in the hybrid leads to a single stranded stretch of DNA, whose "repeated" sequence (R') is complementary to the "repeated" sequence (R) in the 3' LTR of the RNA and thus the two R regions can hybridize (first jump, step 3) (Goff, 2007).

Polymerization of the (-)-strand DNA can be completed, while the RNase H simultaneously degrades the RNA in the resulting hybrid (step 4). However, not all of the copied RNA is degraded. The PPT RNA is not cleaved by the RNase H and is used as a primer for DNA (+)-strand synthesis. Polymerization of the (+)-strand DNA stops after 18 bases of the tRNA primer have been copied and the first modified nucleotide of the tRNA is reached. The RNase H degrades the RNA of the tRNA/DNA hybrid (step 5). Removal of the tRNA primer creates a single stranded (+)-strand DNA stretch that is complementary to the PBS of the (-) DNA (step 6). Hence, these two parts can bind to each other (second jump, step 7). Now polymerization of the both DNA strands can be completed (step 8) (Goff, 2007).

In consequence the RNA is converted into double stranded DNA. Caused by the two jumps during replication the sequences upstream of the PBS and downstream of the PPT are doubled and form the LTRs on both sides of the DNA. The LTRs not only ensure the correct transcription of the viral DNA since the LTR encodes the viral promoter, but they are also recognized by the viral IN and are of great importance in the integration process.

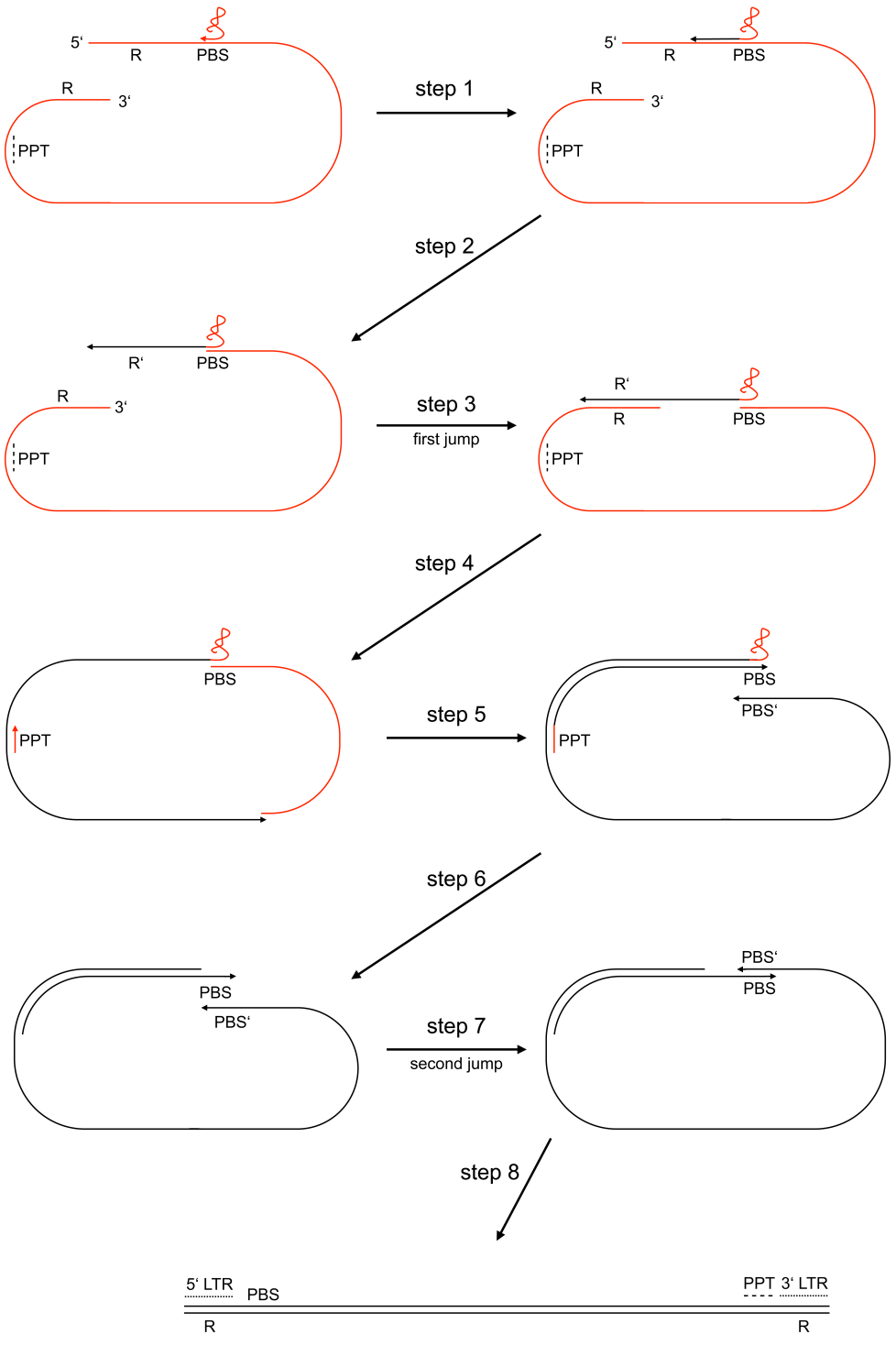

Figure 1.6: Reverse transcription of the retroviral genome.
The retroviral genome and the cell-derived tRNA are shown in red, the DNA strands produced are depicted in black. LTR: long terminal repeats; PPT: polypurine tract; R: repeated sequence of the LTR; PBS: primer binding site; sequences complementary to R and PBS are designated R’ and PBS’, respectively. For detailed explanation see text above.

1.3.1 The polymerase domain of the PR-RT enzyme

The polymerase domain of the RT can synthesize a DNA copy from a DNA or RNA template. *In vitro*, the primer used for this reaction can be either DNA or RNA. The structure of the polymerase domain of retroviral RTs is similar to that of other polymerases (e.g. T7 and Klenow polymerase) and resembles a right hand (Figure 1.7). Consequently, the subdomains were called fingers, palm and thumb. The domain connecting the polymerase and RNase H domains was named "connection domain" (Coffin *et al.*, 1997).

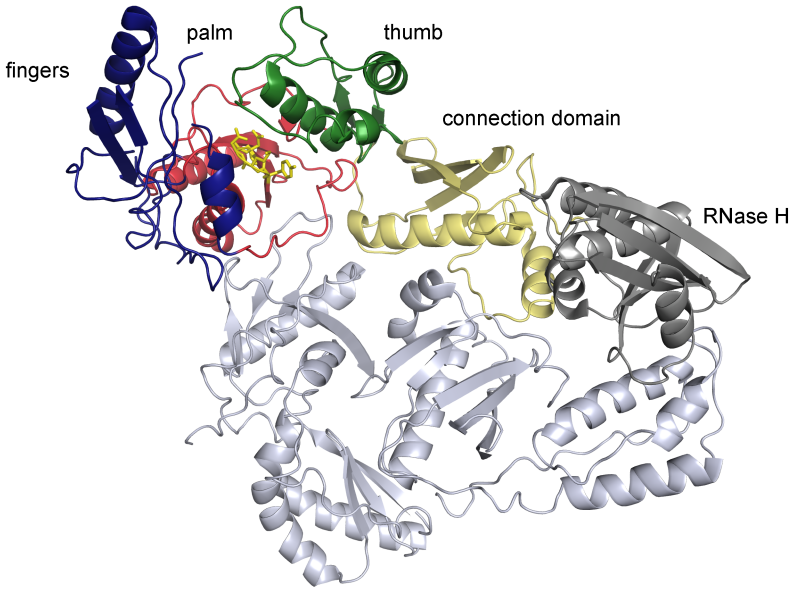

Figure 1.7: Crystal structure of the HIV-1 RT.
The two subunits (p51 and p66) of HIV-1 RT are displayed. p51 is shown in light grey, the subdomains of p66, which are named based on the analogy to a right hand, are color coded: fingers (blue), palm (red), thumb (green), connection domain (light yellow) and RNase H (black). The polymerase active site Tyr-Met-Asp-Asp is highlighted as yellow sticks (picture generated from PDB 1HMV with MacPyMOL).

The overall folding of the polymerase domain is similar across all retroviral species (Coffin *et al.*, 1997; Goff, 2007). However, while in some species the RT is a heterodimer (e.g. p66 and p51 in HIV) the RT of FV and MLV consists of a single polypeptide chain. The active site with the conserved Tyr-X-Asp-Asp motif is located in the palm subdomain. The central part surrounding the active site represents the phylogenetically most conserved portion of the retroviral genome (Coffin *et al.*, 1997). The two Asp residues of this motif in combination with a third Asp bind two divalent metal ions and catalyze polymerization with a carboxylate-chelate two-metal-ion catalytic mechanism (reviewed in Sarafianos *et al.*, 2009). The active site sequence present most frequently is Tyr-Met-Asp-Asp, but in FVs and MLV Tyr-Val-Asp-Asp is found (Linial, 2007). Surprisingly, in FVs a Val to Met amino acid exchange

showed only minor differences in RT activity *in vitro* but completely abolished virus infectivity (Rinke *et al.*, 2002).

In HIV, the thumb region appears to be rather flexible and moves about 30° upon substrate binding. In its closed form it touches the tip of the fingers (Rodgers *et al.*, 1995; Hsiou *et al.*, 1996). Primer/template binding of RT can be imagined as a right hand closing around the substrate like a grip. Binding of the primer/template perfectly positions the 3' end of the primer at the active site of the polymerase (Jacobo-Molina *et al.*, 1993). An incoming deoxynucleotide-triphosphate (dNTP) then binds to the nucleotide-binding site. This is followed by a conformational change of the protein where the finger domain closes down on the dNTP (Huang *et al.*, 1998). Thus, the α-phosphate of the dNTP is aligned with the 3' hydroxyl group of the primer. The chemical reaction catalyzed by bivalent metal ions leads to the formation of a phosphodiester bond between the incoming nucleotide and the primer (Steitz, 1998). The pyrophosphate (PP_i) generated is released by an opening of the fingers. Translocation of the primer finally results in a free nucleotide-binding site and polymerization can proceed.

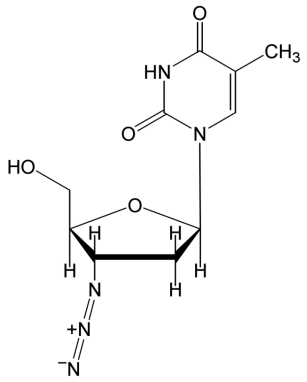

Figure 1.8: Chemical Structure of the nucleoside inhibitor azidothymidine (AZT).

Since human cells do not depend on RT, anti-retroviral therapy – in particular AIDS therapy - early concentrated on inhibiting RT activity of the virus. To date several therapeutic agents targeting RT are available. Interestingly, only the two nucleoside inhibitors tenofovir and azidothymidine (AZT, 3'-azido-3'-deoxythymidine, Figure 1.8) are known to inhibit FV RT (Moebes *et al.*, 1997; Rosenblum *et al.*, 2001; Lee *et al.*, 2006). AZT is similar in structure to the nucleoside thymidine, but lacks the 3' hydroxyl group. Thus, polymerization is terminated after incorporation of AZT-5'-monophosphate (AZTMP) into the synthesized DNA chain. Unfortunately, HIV is able to escape AZT treatment by developing resistance.

Two different mechanisms of resistance have been shown for HIV- 1 and 2. HIV-2 RT can distinguish between AZT-5'-triphosphate (AZTTP) and thymidine-5'-triphosphate (TTP)

(Boyer *et al.*, 2006) by as few as two mutations located in the RT gene (Q151M/I/L and K70R) (Rodes *et al.*, 2000). The situation for HIV-1 is more complex and is still discussed to some extent. Altogether, high level AZT resistance in HIV-1 is achieved by five mutations in the RT gene (M41L, D67N, K70R, T215Y/F and K219E/Q) (Larder & Kemp, 1989). The mechanism of resistance is based on the excision of incorporated AZTMP, which reactivates polymerization. The excision reaction was proposed to take place either in the presence of inorganic PP_i representing the back reaction of polymerization (Arion *et al.*, 1998) or in the presence of adenosine-5'-triphosphate (ATP) (Meyer *et al.*, 1998; Meyer *et al.*, 1999).

1.3.2 The RNase H domain of the PR-RT enzyme

As mentioned before the RNase H domain of retroviral RTs is responsible for degradation of the RNA in an RNA/DNA hybrid. Removal of the tRNA primer and the PPT are special functions of the RNase H. Activity and specificity of the RNase H are finely tuned.

The tertiary folding of retroviral RNase H domains is similar to other known RNase H proteins like RNase HI of *Escherichia coli* (*E. coli*) or *Thermus thermophilus*. In principle, the RNase H domains consist of 5 β-strands and 4 to 5 α-helices (Figure 1.9). When comparing various RNase H domains, the presence or absence of a positively charged so-called C-helix is the most obvious difference (reviewed in Schultz & Champoux, 2008). The C-helix can be found in FV and MLV, but not in HIV. The exact function of this helix is unclear. It has been suggested to have structural importance in MLV RNase H (Telesnitsky *et al.*, 1992; Lim *et al.*, 2002) and to participate in effective substrate binding in *E. coli* RNase H (Kanaya *et al.*, 1991). Interestingly, HIV RNase H expressed separately was shown to be inactive. However, a recombinant HIV RNase H harboring the C-helix of MLV at the N-terminus was active (Stahl *et al.*, 1994; Keck & Marqusee, 1995).

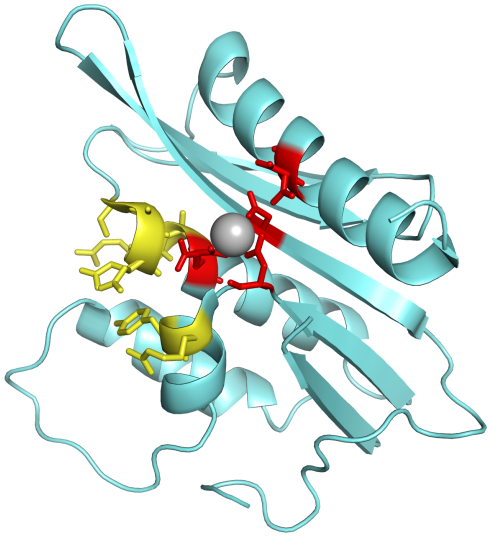

Figure 1.9: Crystal structure of the RNase H domain of MLV.
The RNase H domain of Moloney MLV lacking the C-helix is shown. The conserved acidic residues of the active site are shown in red, a coordinated Mg^{2+} ion is depicted in grey and the residues belonging to the primer grip are highlighted in yellow (picture generated from PDB 2HB5 with MacPyMOL).

The second important region of the RNase H is called primer grip. This region is found in all retroviral RNase H domains structurally investigated so far. It contributes significantly to the positioning and binding of the substrate at both the DNA polymerase and RNase H active site. Contacts between the primer grip of the RNase H and the nucleotides of the DNA strand, base paired with RNA, are formed at positions -4 to -9 relative to the scissile phosphate (Sarafianos *et al.*, 2001). Close to the primer grip is the active site of the RNase H. It is highly conserved and consists of a Glu and three Asp. The distance between the polymerase and the RNase H active site is about 17 to 18 base pairs. Most likely, two divalent metal ions, Mg^{2+} and/or Mn^{2+} are coordinated and are required for RNase H activity. Recent studies suggest that one ion activates a nucleophilic water molecule, the second ion stabilizes the transition state intermediate (Schultz & Champoux, 2008).

1.4 Retroviral proteases

In FVs, PR is part of the multifunctional PR-RT enzyme emerging from Pol after IN is cleaved off. In orthoretroviruses PR is expressed as part of a Gag-Pol polyprotein but is excised from the precursor by cuts performed at its C- and N-terminus. Depending on the virus, mature PR therefore is either present as a separate protein or as part of PR-RT.

Without any known exceptions retroviral PRs belong to the well-characterized family of aspartic PRs (Katoh *et al.*, 1987; Katoh *et al.*, 1989). This family also includes mammalian PRs like rennin and pepsin. Eukaryotic PRs consist of two highly similar domains. In contrast, retroviral PRs are active as symmetric homodimers (Pearl & Taylor, 1987). Upon dimerization two Asp residues each originating from one monomer constitute the active site. Analysis of different structures of retroviral PRs shows that even though there are large differences in the amino acid sequence, the overall folds are quite similar (Figure 1.10a) (Wlodawer *et al.*, 1989; Wlodawer & Gustchina, 2000; Dunn *et al.*, 2002).

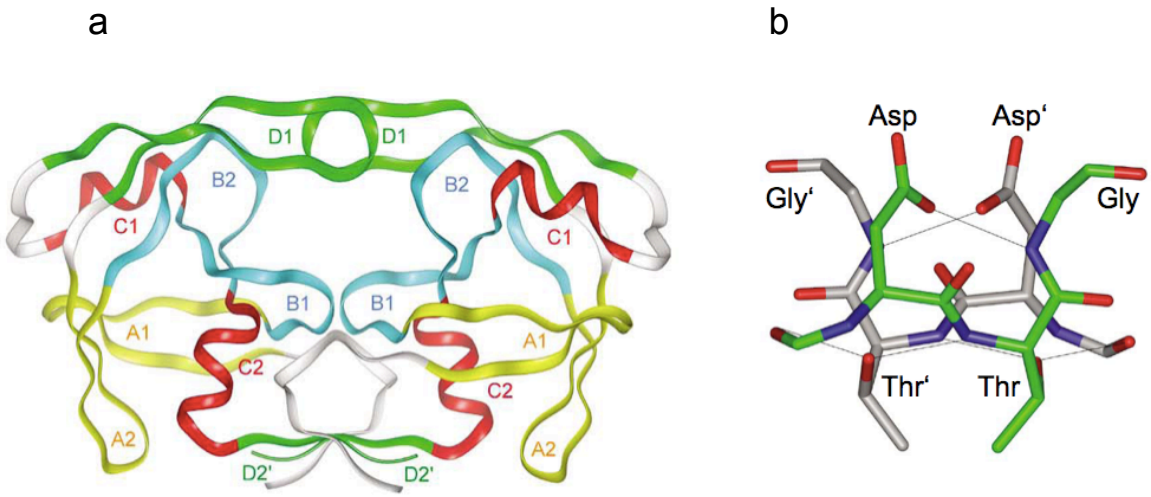

Figure 1.10: Structural template and amino acid orientation in the active site of retroviral PRs. (**a**) Cartoon overview of the typical folding of the symmetric homodimer of retroviral PRs. The active site is formed by the two B1 loops. D1 is also-called "flap". (**b**) The rigid network structure of the "fireman's grip" involves the Asp-Thr-Gly triad of the active site. One subunit is shown in green, the second subunit in grey, amino acids of the second subunit are labeled with a (‘). Hydrogen bonds are depicted as thin lines (modified from Dunn *et al.*, 2002).

Four structural elements are characteristic for retroviral PRs but may vary slightly in different species. A hairpin (A1) is followed by a large B1 loop containing the catalytic Asp, then a short helix (C1) forms the connection to a second large hairpin, which is called "flap" (D1). A monomer is formed by duplication of this hairpin-loop-helix-hairpin motif (A2, B2, C2 and D2). Thus an active, dimeric retroviral PR consists of a single structural motif, which is

repeated four times. For dimerization, the contacts in the flap region, the active site and most importantly a four stranded β-sheet formed by the N- and C-terminal regions are significant.
The structures of retroviral PRs solved so far show a distinct orientation of the residues in the conserved Asp-Ser/Thr-Gly active site motif (Fig. 1.10b). The active site is stabilized by a rigid network of hydrogen bonds, the so-called "fireman's grip". The γO of the conserved Thr, which is replaced by Ser in FV and Rous sarcoma virus, is bridged with a hydrogen bond to the main chain NH of the Thr within the opposing monomer. Moreover, it donates a hydrogen bond to the mainchain carbonyl group oxygen one residue prior to the catalytic Asp on the opposite active site loop. In consequence, the carboxylate groups of the two catalytic Asp are almost co-planar. They are bridged by a water molecule, which is required for hydrolysis of the peptide bond in the substrate (reviewed in Davies, 1990). Studies showed that stabilization of the dimer is strongly depending on the presence of a Thr in the active site motif. Exchange of Thr to Ser in HIV-1 PR significantly destabilized the dimer (Ingr *et al.*, 2003).
Regulation of PR activity is essential within the retroviral life cycle. Premature processing of the polyproteins prior to virus assembly would result in incomplete packaging whereas a loss of PR activity would lead to immature viral particles. Recent results for HIV-1 revealed a possible mechanism for PR regulation. The uncleaved PR within the Gag-Pol polyprotein appears to lack proper activity due to inefficient dimerization (Tang *et al.*, 2008). Localization of Gag-Pol in the cell during virus assembly by the Gag packaging signal activates PR und thus enables viral maturation. For this regulation of HIV-1 PR activity the Gag sequence at the N-terminus of PR - the so-called transframe region - is important. Elongation of HIV-1 PR at the N-terminus *in vitro* alters PR activity dramatically (Tessmer & Kräusslich, 1998; Louis *et al.*, 1999; Louis *et al.*, 2000; Pettit *et al.*, 2003; Chiu *et al.*, 2006; Louis *et al.*, 2007), while C-terminal extensions do not have any significant effects (Wondrak *et al.*, 1996; Cherry *et al.*, 1998a; Cherry *et al.*, 1998b). Therefore a „free" N-terminus of HIV-1 PR appears to be needed for proper formation of the four-stranded β-sheet formed by both N- and C-termini.
However, regulation of PR activity in FV has to be different. Pol expression in FV is independent of Gag and PR does not harbor an N-terminal extension. Moreover, contradicting results regarding the dimerization state of FV PR have been published. An early publication by Benzair *et al.* (1982) described SFVmac PR to be monomeric, while Pfrepper *et al.* (1998) predicted a dimeric PFV PR. In summary, regulation of FV PR is an interesting and promising field for research.

2 Objectives

Some of the main differences between FV and other retroviruses are related either to the synthesis or the activity of PR-RT, which is key to the retroviral life cycle and therefore its behavior is of broad interest. This work focuses on the catalytic activities of PFV and SFVmac PR-RT, the molecular basis of resistance of SFVmac against AZT and the regulation of PR activity in PFV and SFVmac.

The first aim of this work is to analyze the biochemical and biophysical behavior of PFV and SFVmac PR-RT. Thus, the recombinant PR-RTs should be purified and their secondary structure as well as their enzymatic activities (proteolytic activity, DNA polymerization and RNase H activity) compared *in vitro*.

A major problem in retroviral therapy is resistance of the viruses against drug treatment. HIV, for example, is able to escape treatment with the nucleoside inhibitor AZT. Details on how this resistance works are still being discussed. As AZT is one of two known inhibitors of FV replication, it is the goal of this thesis to use FV as a model organism to investigate AZT resistance of retroviruses. The objective of this study is to generate AZT resistant FV *in vivo* and to elucidate the molecular processes involved in resistance *in vitro*.

Retroviral PRs are crucial for correct processing of the viral proteins and thus for the retroviral life cycle. In FVs, where expression and processing of PR differs from other retroviruses, little was known about their PRs. This thesis investigates the structure and the factors important for the regulation of FV PRs.

3 Synopsis

3.1 Comparison of foamy virus PR-RT catalytic activities

PR and RT of FVs are unique among retroviral enzymes. In contrast to the *Orthoretrovirinae*, PR and RT are located in a single polypeptide chain – even after maturation of the viral particle is complete (Pfrepper *et al.*, 1998; Flügel & Pfrepper, 2003). Therefore, the PR-RT enzyme harbors the essential catalytic activities associated with PR and RT: proteolysis as well as DNA polymerase and RNase H activity. PR-RT plays a central role in the viral life cycle and thus is of great interest in FV research.

So far *in vivo* as well as *in vitro* studies of FV PR-RT focused mainly on two species: one from a human isolate (PFV), probably originally derived from chimpanzees, and one of simian origin (SFVmac). In this work, the PR-RT of PFV and SFVmac were compared with biophysical and biochemical methods to elucidate their differences and similarities.

Recombinant PFV and SFVmac PR-RT were analyzed by circular dichroism and both enzymes appeared to be predominantly folded. In addition, similar α-helical and β-sheet contents were predicted for both enzymes (publication A, Figure 1A and Table 1).

Protease

To detect proteolytic activity a substrate was designed by inserting the SFVmac Pol cleavage site, which is located between RT and IN, between the immunoglobulin binding domain B1 of the streptococcal protein G (GB1) and the green fluorescent protein (GFP). Upon cleavage of the GB1-GFP fusion protein the resulting GB1 and GFP products were analyzed by gel electrophoresis. Surprisingly, the salt concentration in the assay had to be elevated to 2 to 3 M NaCl to obtain proteolytic activity (publication A and E). Nevertheless, comparable activity was observed for the two different PR-RTs (Figure 3.1) although the substrate constructed to test PR activity harbored the SFVmac Pol cleavage site (YVVH↓CNTT), which differs from the PFV Pol cleavage site (YVVR↓CNTT) by one amino acid.

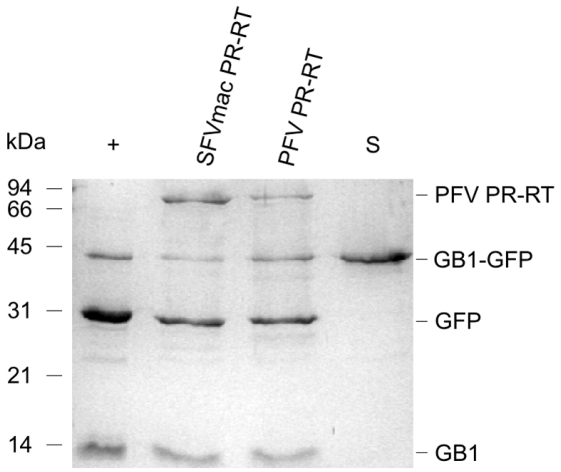

Figure 3.1: PR activity assays of SFVmac and PFV PR-RT.
10 µM of the substrate GB1-GFP harboring the SFVmac Pol cleavage site between GB1 and GFP was incubated with 10 µM PFV or SFVmac PR-RT at 37 °C for 16 h in 50 mM Na_2HPO_4/NaH_2PO_4 pH 7.4, 0.5 mM DTT and 3 M NaCl. Reaction products were analyzed by 19 % sodium dodecylsulfate polyacrylamide gelelectrophorseis. +: positive control; S: uncleaved substrate. The sizes of standard proteins are indicated on the left (Publication A, Figure 2).

Polymerase

RTs can make use of either a DNA- or RNA-strand as a template for DNA synthesis. Both activities are indispensable for transforming the single-stranded viral RNA genome into the double-stranded DNA needed for integration. Without proper polymerization activity retroviruses cannot replicate and inhibition of RT is a powerful tool in antiretroviral therapy.

Characterization of the polymerization activity of the PR-RTs from PFV and SFVmac was performed using a DNA primer and a homopolymeric RNA (poly(rA)) or a heteropolymeric DNA substrate (single-stranded M13-DNA), respectively. In both experiments no significant differences in the behavior of PFV and SFVmac PR-RT were observed. Michaelis-Menten parameters obtained from polymerization on the homopolymeric poly(rA) substrate in the presence of radioactively labeled TTP were virtually identical (publication A, Table 2). Time dependent primer elongation on the heteropolymeric single-stranded M13 substrate revealed similar polymerization behavior (publication A, Figure 4). Moreover, K_D-values for binding to a DNA/DNA or DNA/RNA substrate were determined. Despite a somewhat higher affinity of PFV PR-RT for the DNA/RNA substrate (10 nM) all values measured were in a similar range of 30 to 45 nM (publication A, Table 2; publication C, Table 2). In conclusion, the polymerization behavior of PFV and SFVmac PR-RT did not differ significantly.

RNase H

The third activity associated with PR-RT is the digestion of RNA in a DNA/RNA hybrid catalyzed by the RNase H domain. RNase H activity is needed in the replication process of retroviruses to remove the RNA-strand from the DNA/RNA hybrid to enable polymerization of the DNA (+)-strand.

RNase H activity of PFV and SFVmac PR-RT was analyzed using two different substrates. First Michaelis-Menten parameters were measured with a blunt ended DNA/RNA substrate containing a fluorescent dye at the 3' end of the RNA and a quencher at the 5' end of the DNA (publication A, Table 3). Additionally, endonucleolytic RNase H cleavage sites were identified using a 40mer RNA/24mer DNA substrate (publication A, Figure 5B). The results indicate that the kinetic parameters and the cleavage sites of the two enzymes are comparable. In summary, it was shown in this work that PFV and SFVmac PR-RT exhibit similar biophysical and biochemical properties *in vitro*.

3.2 Resistance of foamy virus against azidothymidine

Since most retroviruses are associated with serious diseases, the inhibition of retroviral replication is a major goal in retrovirus research. Thus, the RT enzyme is an ideal target for antiretroviral therapy, because its catalytic activity is pivotal for virus replication. Regrettably, retroviruses and especially HIV are able to escape drug treatment by developing resistance. Treatment of patients therefore requires new and better drugs. Understanding the mechanism involved in drug resistance is key for the development of new drugs. To our knowledge FVs are not pathogenic (reviewed in Meiering & Linial, 2001). Nevertheless, FV could serve as a model organism to elucidate the mechanisms of resistance against selected drugs important for other retroviral species.

AZT is one of two nucleoside inhibitors known to impair FV replication (Moebes *et al.*, 1997; Rosenblum *et al.*, 2001; Lee *et al.*, 2006). AZT terminates DNA polymerization due to its 3' azido group (Figure 1.8), which leads to DNA chain termination. In recent years a lot of effort has been put into characterizing the resistance of HIV against AZT. Surprisingly, AZT resistance in HIV-1 and HIV-2 is based on different mechanisms. In resistant HIV-2 the RT can discriminate between the incorporation of the natural nucleotide thymidine-5'-monophosphate (TMP) and AZTMP (Boyer *et al.*, 2006), while HIV-1 RT removes incorporated AZTMP from an already terminated primer. The latter gave rise to a number of questions, since PP_i (Arion *et al.*, 1998) and ATP (Meyer *et al.*, 1998; Meyer *et al.*, 1999) were discussed as possible factors necessary for the excision of AZTMP (Figure 3.2).

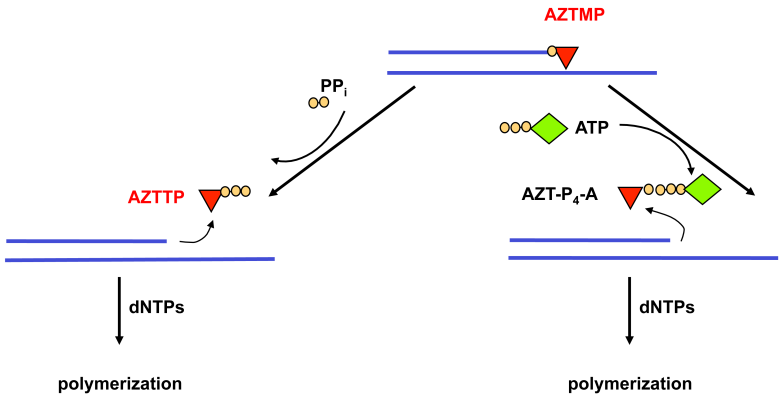

Figure 3.2: Schematic representation of AZTMP removal from a terminated primer.
Removal of AZTMP by RT from an AZTMP terminated primer in resistant HIV-1 was suggested to be catalyzed either in the presence of PP_i (left) (Arion *et al.*, 1998) or ATP (right) (Meyer *et al.*, 1998; Meyer *et al.*, 1999). While removal of AZTMP with PP_i restores AZTTP, excision with ATP leads to formation of the dinucleotide 3'-azido-3'-deoxythymidin-(5')-tetraphospho-(5')-adenosine (AZT-P_4-A). DNA is shown as blue lines, phosphate as orange circles, adenosine as a green square and AZT as a red triangle.

Publication B describes the attempt to generate AZT resistant PFV and SFVmac. Four non-silent mutations leading to AZT resistance in the RT gene of SFVmac were identified:

K211I, I224T, S345T and E350K.

Viruses containing these four mutations showed no replication defects in the absence of AZT and were able to replicate in the presence of AZT concentrations as high as 1 mM. In contrast, generation of AZT resistant PFV failed. Remarkably, even though the sequence identity of PFV and SFVmac PR-RT exceeds 90 % and their biophysical as well as biochemical behavior are highly similar (see 3.1), insertion of the resistance mutations from SFVmac into the PFV RT gene did not result in AZT resistant PFV (publication B, Table 2, Virus M108).

After having identified the AZT resistance mutations in SFVmac the molecular mechanism of resistance was investigated (publication C). Two different SFVmac PR-RTs resistant to AZT were tested *in vitro* and compared with wildtype (WT) PR-RTs:

- *mt4*, harboring all four mutations (K211I, I224T, S345T, E350K), and
- *mt3* (K211I, S345T, E350K), lacking the I224T mutation.

WT SFVmac PR-RT has a polymorphism at the amino acid at position 224 of the PR-RT gene and either Ile or Thr can be found. AZT resistant SFVmac always contained a Thr at position 224. In the absence of AZT a recombinant virus containing the *mt3* mutations replicated only poorly, but the virus tolerated the addition of 50 µM AZT to the medium (publication B, Table 2, virus BK37-IITK). The mutation I224T was identified *in vitro* to be important for polymerization activity of SFVmac PR-RT in the absence of AZTTP (Figure 3.3a; see also publication C, Table 1). WT PR-RT activity was threefold higher than that of mutant *mt3*, however polymerization activity of *mt3* could be restored by introducing the fourth mutation. This finding implies that the I224T mutation does not contribute to the mechanism of AZT resistance itself, but is needed to increase polymerization activity of PR-RT in resistant viruses. The *in vivo* results confirm this interpretation.

To investigate whether AZT resistance is based on the discrimination between AZTMP and TMP at the level of incorporation either a homopolymeric poly(rA)/oligo(dT) or a heteropolymeric single-stranded M13 DNA substrate was used (Figure 3.3a and b, respectively). Polymerization was analyzed in the absence and in the presence of increasing amounts of AZTTP. Despite the fact that SFVmac harboring the mutations corresponding to *mt4* or *mt3* replicated in the presence of high AZT concentrations (publication B, Table 2), the mutant recombinant PR-RTs purified from *E. coli* were sensitive to the addition of AZTTP. Compared to the WT PR-RT, polymerization activities of the mutant enzymes measured on the homopolymeric substrate with different AZTTP concentrations were impaired

(Figure 3.3a). Polymerization on M13 DNA in the presence of AZTTP led to termination products, which got shorter when higher AZTTP concentrations were applied. Similar to the activities on poly(rA)/oligo(dT) *mt4* and *mt3* appeared to be somewhat more affected by AZTTP than the WT (Figure 3.3b).

These experiments argue against a mechanism of resistance based on discrimination between AZTMP and TMP. They are reminiscent of HIV-1 RT (Krebs *et al.*, 1997), where the AZT resistance was also not visible in steady-state polymerization assays or during pre-steady-state analyses and could only be detected with an AZTMP-terminated primer/template substrate (Arion *et al.*, 1998; Meyer *et al.*, 1998; Meyer *et al.*, 1999).

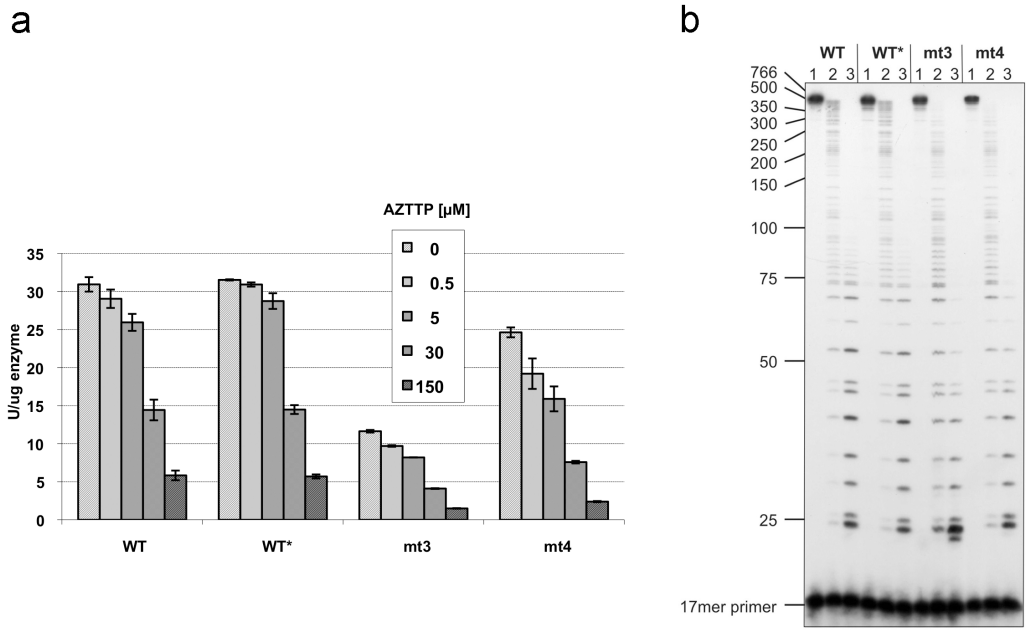

Figure 3.3: Polymerization activities in the presence of AZTTP.
(**a**) Specific activities were measured on 6 nM of poly(rA)/oligo(dT) with 12 nM of various SFVmac PR-RTs as indicated, 150 µM TTP and 0, 0.5, 5, 30 or 150 µM AZTTP. The reaction was stopped after 10 min at 37 °C. (**b**) Chain termination by AZTMP incorporation during DNA polymerization with 6 nM M13 single-stranded DNA, 150 µM dNTP and 85 nM SFVmac PR-RTs within 10 min at 37 °C. Either no AZTTP (lanes 1), 5 µM (lanes 2) or 50 µM (lanes 3) of AZTTP was added. DNA size markers are indicated on the left.
*: Indicates a mutation in PR-RT leading to loss of proteolytic activity. This D24A mutation does not influence polymerization activities (Publication C, Figure 2).

It has been shown for AZT resistant HIV-1 RT that AZTMP can be excised from an AZTMP-terminated primer/template either in the presence of PP_i or ATP (Figure 3.2) (Arion *et al.*, 1998; Meyer *et al.*, 1998; Meyer *et al.*, 1999). To test these two possibilities an AZTMP terminated primer/template was incubated with the WT or mutated PR-RTs in the presence of PP_i or ATP. Excision of AZTMP from the terminated and [^{32}P] labeled primer leads to a DNA

product one nucleotide shorter than the AZTMP-primer. The reaction products were separated by denaturing gel electrophoresis and quantified by densitometry. Time dependent experiments undoubtedly showed that excision reactions with PP_i were relatively slow and did not differ between the WT and mutant PR-RTs. In contrast, excision in the presence of ATP did not result in deblocking of the terminated primer with WT PR-RT, but the *mt4* and *mt3* PR-RTs were able to reactivate polymerization (Figure 3.4).

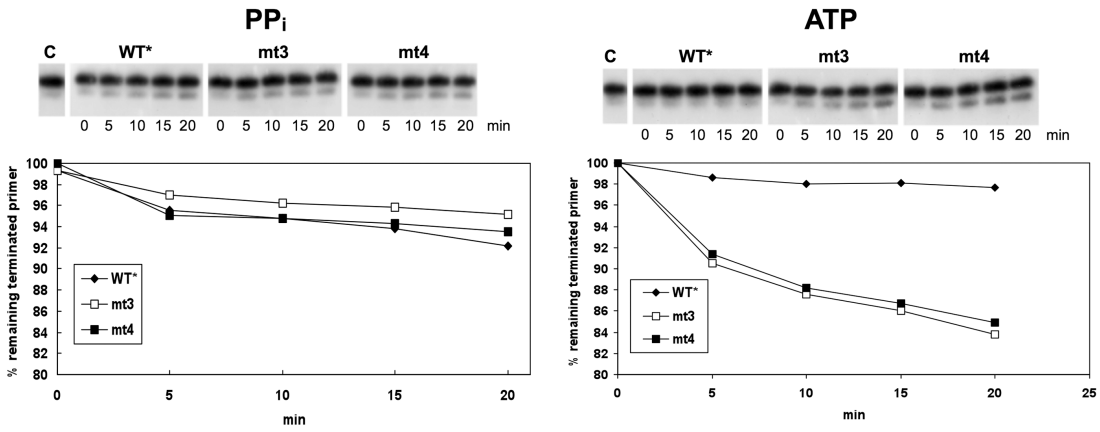

Figure 3.4: Time dependent AZTMP removal in the presence of PP_i or ATP.
Top: In a mixture containing 10 nM of an AZTMP-terminated primer/template labeled with [^{32}P] at the 5' end of the primer either 100 µM $NaPP_i$ (left) or 5 mM ATP (right) were present. Reactions were started by addition of 20 nM of the different PR-RTs and stopped at the time points indicated. The upper bands represent the AZTMP-primer, the lower bands the reactivated primer without AZTMP. Lane C: no enzyme added. Bottom: Densitometric quantification of AZTMP removal by PP_i or ATP. The percentage of remaining terminated primer is shown.*: Indicates a mutation in PR-RT leading to loss of proteolytic activity. This D24A mutation does not influence polymerization activities (publication C, Figures 3 and 4).

The results obtained in this work clearly show that the mechanism of AZT resistance of SFVmac is based on the excision of incorporated AZTMP in the presence of ATP. Interestingly, excision of AZTMP in HIV-1 has been associated with the selection of an aromatic amino acid (Phe or Tyr) at position 215 (see chapter 1.3.1). It was suggested that the adenine moiety of the incoming ATP forms π-π interactions with the aromatic ring of the exchanged amino acid (Boyer *et al.*, 2001; Boyer *et al.*, 2002a; Boyer *et al.*, 2002b; Sarafianos *et al.*, 2002; Smith *et al.*, 2005). However, in AZT resistant SFVmac no mutation leading to an aromatic amino acid is selected. Consequently, in SFVmac either an aromatic amino acid present at a different position serves to bind ATP or the mechanism of ATP binding or ATP-mediated excision differs from that of HIV-1. Unfortunately, the sequences of SFVmac and HIV-1 RT reveal a homology of only 21 %. Thus, it is difficult to identify a putative aromatic amino acid homologous to Phe or Tyr 215 in AZT resistant HIV-1 RT. Structural data are necessary to clarify this problem.

3.3 Regulation of protease activity in foamy viruses

3.3.1 Transient dimerization of foamy virus protease

Despite the fact that retroviral PRs play a crucial role in virus maturation und thus in infectivity of retroviruses, little is known about their regulation. However, PR activity has to be regulated, because premature processing of the polyproteins would result in packaging defects. On the other hand, incomplete processing would lead to non-infectious viral particles. It has been shown in this work (chapter 3.1) that PFV and SFVmac PR activity is only achieved under very high salt concentrations of 2 to 3 M NaCl – conditions, which are very likely not present *in vivo*. Analysis of PFV and SFVmac PR-RT revealed monomeric proteins (publication E, Figure 3 and publication A, Figure 1B, respectively), although all retroviral PRs investigated so far have been shown to be only active as homodimers (Pearl & Taylor, 1987). A separately expressed and purified 12.6 kDa PR-domain of SFVmac (SFVmac PRshort) behaved like a monomer also (publication E, Figure 2) even though catalytic activity was measurable and comparable to SFVmac PR-RT.

These results are consistent with a previous publication on SFVmac PR-RT by Benzair *et al*. (1982) and contradict Pfrepper *et al*. (1997), who predicted a dimeric PFV PR. Solution structure determination of SFVmac PRshort by nuclear magnetic resonance (NMR) spectroscopy (publication D and E) further confirmed the monomeric status of FV PRs (Figure 3.5; see also Publication E, Figures 5 and 6).

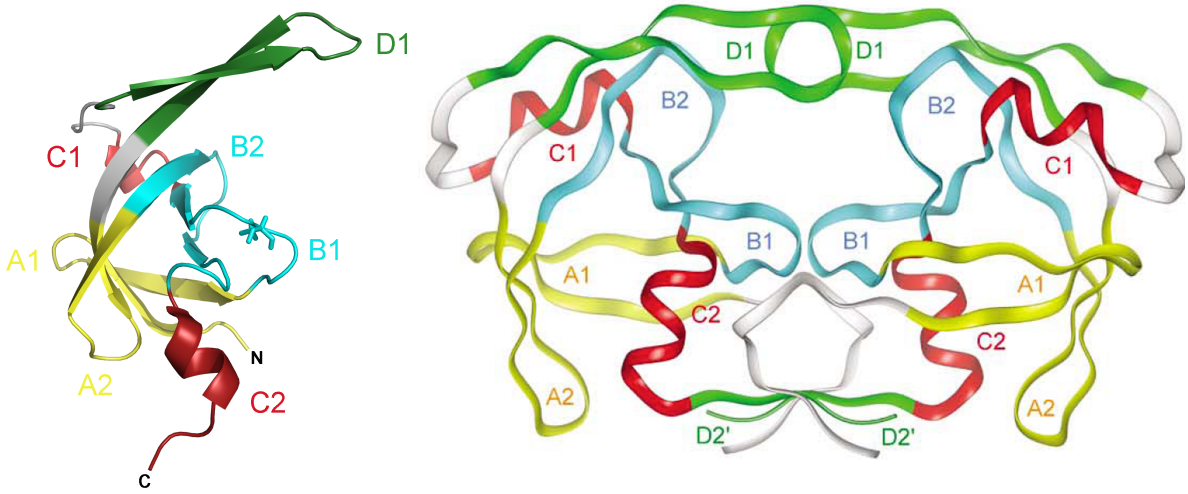

Figure 3.5: Solution structure of SFVmac PRshort in comparison to a structural template of retroviral PRs.
(**a**) A cartoon representation of the SFVmac PRshort monomer is shown. The catalytic Asp of the active site motif is displayed in stick mode. (**b**) Cartoon overview of the typical folding of the symmetric homodimer of retroviral PRs (Dunn *et al*., 2002). The active site is formed by the two B1 loops.

The solution structure of SFVmac PRshort reveals a monomeric protein but the folding is highly similar to the monomer subunits of known retroviral PR dimers (Dunn *et al.*, 2002). Starting from the N-terminus a characteristic hairpin-loop-helix-hairpin motif (A1, B1, C1 and D1) is followed by an additional hairpin-loop-helix motif (A2, B2 and C2). This is rather typical for retroviral PRs (Figure 3.5b; see also chapter 1.4). The main differences between the SFVmac PRshort structure and the dimeric retroviral PR structures solved so far are found at the dimerization interface. Contacts between the subunits in homodimeric PRs are formed at the active site loop (B1) containing the "fireman's grip", the D1 hairpin or "flap" region and the N- and C-termini (see chapter 1.4) (Dunn *et al.*, 2002). ^{15}N relaxation data characterize the D1 hairpin to be quite flexible on the ps-ns timescale (publication E, Figure 6). The most flexible region in the SFVmac PRshort structure, however, are the N- and C-termini. In the symmetric homodimer of retroviral PRs the termini form a four-stranded intermonomeric β-sheet, which contributes significantly to the stability of the dimer (Ishima *et al.*, 2001). Consequently, since SFVmac PRshort is monomeric, this β-sheet is missing. Thus, the catalytic center cannot be formed, because both subunits contribute essential residues to form the active site, e.g. the catalytic Asp and the residues of the fireman's grip (see chapter 1.4, Figure 1.10b).

Structural data and quaternary structure analysis raise the question how catalytic activity of FV PRs is achieved. Folding of the monomer subunit indicates that the active form of FV PR is also the dimer. To confirm this hypothesis SFVmac PR-RT and PRshort activity was tested in the presence of cholic acid, a putative dimerization inhibitor of HIV-1 PR (publication F, Figures 1 and 2). Publication F shows binding of cholic acid at the proposed dimerization interface of SFVmac PRshort with a K_D of approximately 5 mM and loss of proteolytic activity of SFVmac PR-RT and PRshort in the presence of cholic acid with an IC_{50} value of about 0.7 mM and 0.6 mM, respectively. These data imply dimerization of FV PRs.

Specific transient dimerization of SFVmac PRshort was finally proven by paramagnetic relaxation enhancement (PRE). In this experiment two species of SFVmac PRshort were mixed. One SFVmac PRshort species was ^{15}N-labeled and corresponding signals were measured by NMR. An SFVmac PRshort which was randomly labeled at the ε-amino groups of its Lys residues with the spin label 1-oxyl-2,2,5,5-tetramethylpyrroline-3-carboxylate N-hydroxysuccinimide ester (oxyl-1-NHS) was added to the ^{15}N-labeled species. Contacts between amide protons of the ^{15}N species and the spin label of the second species, lead to a dramatic enhancement of transverse relaxation rates of the protons close to the spin label. For SFVmac PRshort amino acids with increased relaxation rates were found to be explicitly

located within or close to the proposed dimerization interface (Figure 3.6; see also publication F, Figures 3 and 4). Amide protons of residues far from the dimerization interface did not exhibit significant changes in transversal relaxation rates, demonstrating that transient dimerization of SFVmac PRshort is structure specific.

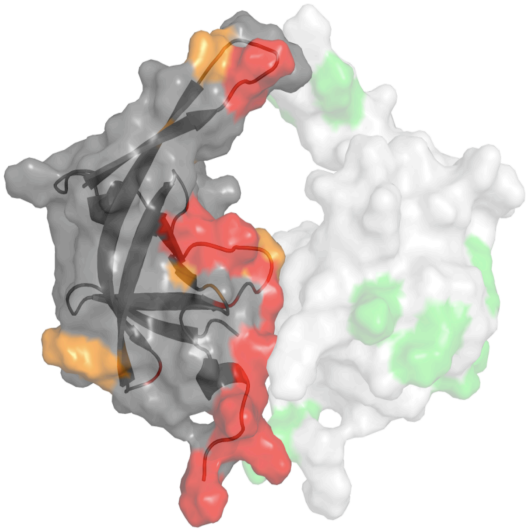

Figure 3.6: Transient contacts formed by SFVmac PRshort.
Model of a hypothetical SFVmac PRshort dimer. The left half of the dimer represents the ^{15}N labeled monomer with color-coded PREs upon addition of spin labeled PRshort. PREs > 20 Hz are colored in red and PREs > 10 Hz in orange. Spin labeled Lys residues are highlighted in green on the right monomer subunit (publication F, Figure 3c).

3.3.2 Activation of foamy virus protease by nucleic acid sequences

The data presented so far have shown that the PR of PFV and SFVmac PR-RT is inactive under low salt conditions due to inefficient dimerization. Activity was only measured at high salt concentrations of 2 to 3 M NaCl (see chapter 3.1). It is obvious that these conditions do not reflect the situation in living cells but somehow create an environment that facilitates dimerization, probably by hydrophobic interaction of the two monomers. Recently, transient dimerization of the HIV-1 PR in the Gag-Pol precursor was shown (Tang *et al.*, 2008). This mechanism prevents activation of PR before virus assembly. Packaging of the Pol proteins in HIV-1 is mediated by RNA binding of Gag within the Gag-Pol polyprotein (reviewed in Goff, 2007) and this process probably activates PR. Since FVs express Gag and Pol independently, Pol packaging and PR regulation have to be different.

The aim of this work is to clarify how regulation of PR activity is achieved in FV. During virus assembly the inactive PR-RT of FV has to be activated due to dimerization and therefore components important for encapsidation of Pol might play an essential role in PR

regulation as well. Apart from the C-terminus of Gag (Lee & Linial, 2008) special nucleic acid sequences on the viral RNA have been determined to be important for Pol uptake (Heinkelein *et al.*, 2002b; Peters *et al.*, 2008). Two cis-acting sequences, CasI and CasII, have been identified to play a role in the transfer of FV vectors (Erlwein *et al.*, 1998; Heinkelein *et al.*, 2002a; Heinkelein *et al.*, 2002b; Linial & Eastman, 2003), indicating an important function in virus assembly.

The cPPT, which accomodates the A to D elements, is included in this CasI-CasII sequence (Figure 3.7a). It has been shown that the A, B, C and D elements of the cPPT are critical for Pol uptake *in vivo* (Peters *et al.*, 2008) (see chapter 1.2).

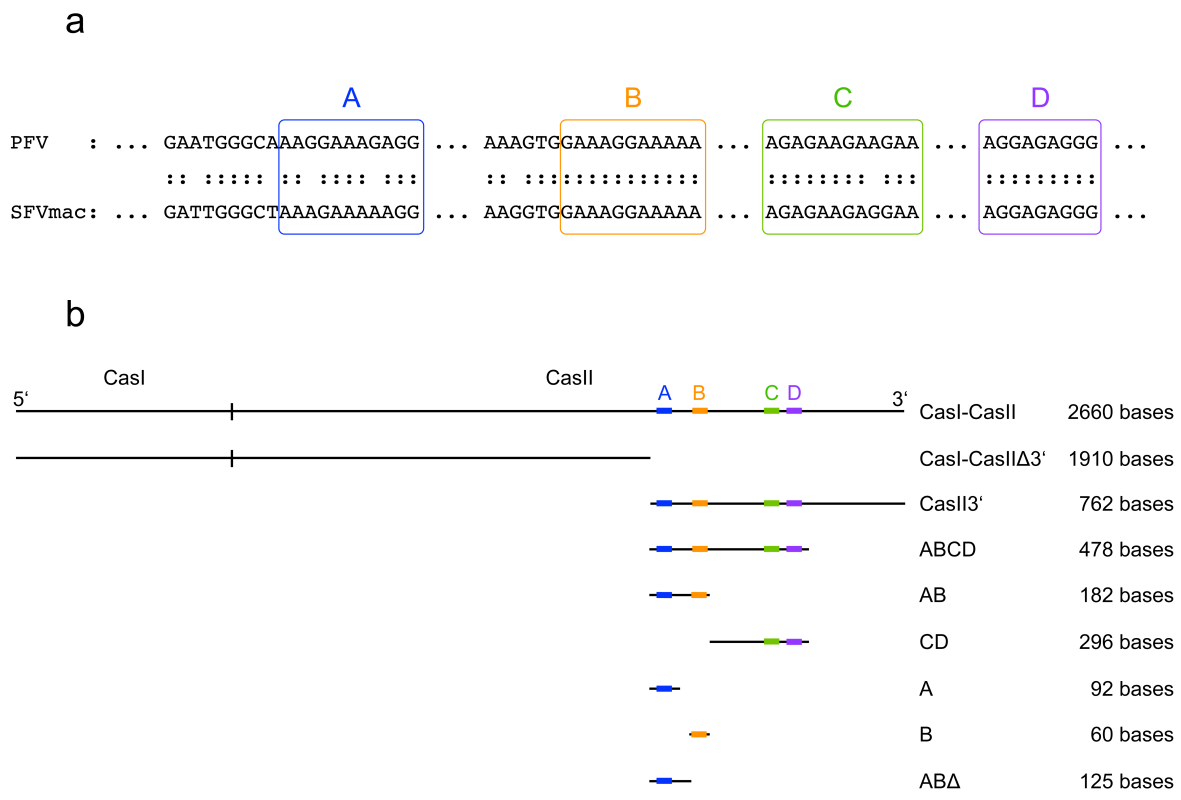

Figure 3.7: Comparison of PFV and SFVmac purine rich elements and schematic representation of RNA fragments used.
(**a**) Representation of the polypurine rich sequences of PFV and SFVmac. The core sequences are highlighted. (**b**) Overview of the RNAs examined for PR activation. The relative positions of the polypurine sequences A to D and the lengths of different RNAs are displayed (publication G, Figure 1).

In publication G different RNA sequences derived from PFV CasI-CasII were tested for their ability to activate proteolytic activity of PFV and SFVmac PR-RT (Figure 3.7b). Although RNAs in general had a small stimulatory effect on PR, truncation of the CasI-CasII RNA at the 5' and the 3' end revealed that the A- and B-element of the cPPT are the essential factors for PR regulation (Figure 3.8; see also publication G, Figure 2).

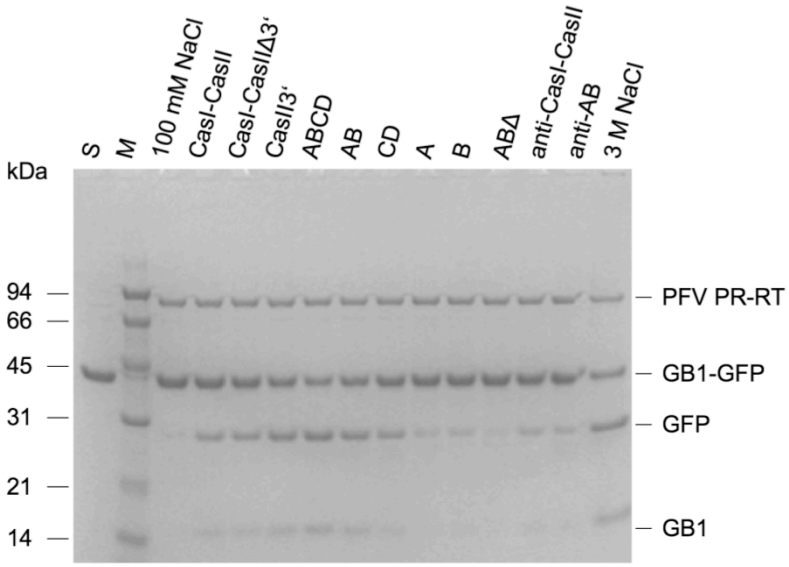

Figure 3.8: Proteolytic activities of PFV PR-RT in the presence of various RNAs.
Activity assays were performed with 0.5 µM of RNA as indicated, 2.5 µM PFV PR-RT and 10 µM substrate GB1-GFP (see 3.1) at 37 °C for 2 h in 50 mM Na_2HPO_4/NaH_2PO_4 pH 6.4 and 100 mM NaCl. Reaction products were separated on 10 % BisTris gels. S: uncleaved substrate; M, molecular weight standard. The sizes of the standard proteins are indicated on the left (publication G, Figure 2a).

Analysis of the secondary structure of AB-RNA by selective 2' hydroxyl acylation analyzed by primer extension (SHAPE) revealed a distinct folding of the polypurine elements A and B. Both are located in a hairpin loop structure where the region at the 3' side of the loop is almost exclusively formed by purines (publication G, Figure 3). PPT structures in HIV have been demonstrated to form distinct secondary structures with bents and deviations from typical Watson-Crick base pairs (Fedoroff *et al.*, 1997; Sarafianos *et al.*, 2001). Although definite data of the PFV RNA-AB structure are missing, a distinct folding of the AB-element of the FV cPPT can be assumed (publication G, Figure 3).

Binding of PFV and SFVmac PR-RT to RNA was analyzed by electrophoretic mobility shift assays (EMSAs). Shifts corresponding to multiple binding of the PR-RTs were obtained independently of the RNA sequence (publication G, Figure 4). Crosslinking experiments revealed that in the presence of RNA dimers and even tetramers are formed (publication G, Figure 5). Protein crosslinking and EMSA are in good agreement with PR activity assays, where all RNA sequences had at least a low stimulatory effect on PR activity. However, RNA containing the A- and B-element is required to form stable PR-RT dimers with high proteolytic activity.

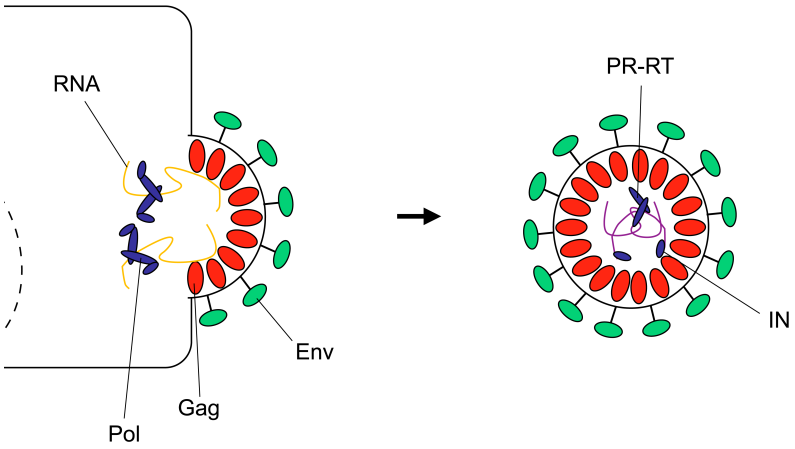

Figure 3.9: Model of FV assembly.
A model for the assembly of FV at the plasma membrane is shown. Binding of Pol to the AB-element within the cPPT of the viral RNA results in Pol uptake (Heinkelein *et al.*, 2002a; Peters *et al.*, 2008). The RNA binds to the C-terminus of Gag (Lee & Linial, 2008). Simultaneously, Pol dimerization is achieved which leads to PR activation (publication G). Pol is cleaved into PR-RT and IN, cleavage of Gag is not shown. The time point of reverse transcription remains unclear, but in infectious viral particles the RNA is reverse transcribed into DNA by PR-RT. Pol is shown in blue, Gag in red, Env in green, RNA in yellow and DNA in purple.

From the data presented in this work a model for FV assembly can be proposed (Figure 3.9). Due to inefficient dimerization the PR in Pol is inactive in the cytoplasm of the host cell (publication F). While packaging of the viral RNA is mediated by the C-terminus of Gag (Lee & Linial, 2008), binding of Pol to the AB-element of the cPPT of the viral RNA (Heinkelein *et al.*, 2002b; Peters *et al.*, 2008) leads to correct localization and proper dimerization of Pol (publication G). PR is activated and through cleavage of Gag and Pol mature viral particles are obtained. In this model the exact time point of reverse transcription is still missing. Further studies on PR-RT and especially Pol are needed to answer this question.

4 List of abbreviations

AIDS	acquired immunodeficiency syndrome
ATP	adenosine-5'-triphosphate
AZT	3'-azido-3'-deoxythymidine
AZTMP	3'-azido-3'-deoxythymidine -5'-monophosphate
AZTTP	3'-azido-3'-deoxythymidine -5'-triphosphate
AZT-P_4-A	3'-azido-3'-deoxythymidine-(5')-tetraphospho-(5')-adenosine
cPPT	central polypurine tract
DNA	deoxyribonucleic acid
dNTP	deoxynucleotide-triphosphate
E. coli	*Escherichia coli*
EMSA	electrophoretic mobility shift assay
FV	foamy virus
HIV	human immunodeficiency virus
GB1	immunoglobulin binding domain B1 of the streptococcal protein G
GFP	green fluorescent protein
IN	integrase
IP	internal promoter
LTR	long terminal repeats
MLV	murine leukemia virus
mRNA	messenger ribonucleic acid
NMR	nuclear magnetic resonance
P	promoter
PBS	primer binding site
PFV	prototype foamy virus
PP_i	pyrophosphate
PPT	polypurine tract
PR	protease
SFVmac PRshort	PR domain of SFVmac
PRE	paramagnetic relaxation enhancement
R	repeated region
RNA	ribonucleic acid
RT	reverse transcriptase
SHAPE	selective 2' hydroxyl acylation analyzed by primer extension

SFVmac	simian foamy virus from macaques
tRNA	transfer ribonucleic acid
TMP	thymidine-5’-monophosphate
TTP	thymidine-5’-triphosphate
WT	wildtype

5 References

Arhel N, Munier S, Souque P, Mollier K und Charneau P (2006) Nuclear import defect of human immunodeficiency virus type 1 DNA flap mutants is not dependent on the viral strain or target cell type. J Virol **80:** 10262-10269

Arion D, Kaushik N, McCormick S, Borkow G und Parniak MA (1998) Phenotypic mechanism of HIV-1 resistance to 3'-azido-3'-deoxythymidine (AZT): increased polymerization processivity and enhanced sensitivity to pyrophosphate of the mutant viral reverse transcriptase. Biochemistry **37:** 15908-15917

Baltimore D (1970) RNA-dependent DNA polymerase in virions of RNA tumour viruses. Nature **226:** 1209-11

Benzair AB, Rhodes-Feuillette A, Emanoil-Ravicovitch R und Peries J (1982) Reverse transcriptase from simian foamy virus serotype 1: purification and characterization. J Virol **44:** 720-724

Boyer PL, Sarafianos SG, Arnold E und Hughes SH (2002a) The M184V mutation reduces the selective excision of zidovudine 5 '-monophosphate (AZTMP) by the reverse transcriptase of human immunodeficiency virus type 1. J Virol **76:** 3248-3256

Boyer PL, Sarafianos SG, Arnold E und Hughes SH (2002b) Nucleoside analog resistance caused by insertions in the fingers of human immunodeficiency virus type 1 reverse transcriptase involves ATP-mediated excision. J Virol **76:** 9143-9151

Boyer PL, Sarafianos SG, Arnold E und Hughes SH (2001) Selective excision of AZTMP by drug-resistant human immunodeficiency virus reverse transcriptase. J Virol **75:** 4832-4842

Boyer PL, Sarafianos SG, Clark PK, Arnold E und Hughes SH (2006) Why Do HIV-1 and HIV-2 Use Different Pathways to Develop AZT Resistance? PLoS Pathog **2:** e10

Cherry E, Liang C, Rong L, Quan Y, Inouye P, Li X, Morin N, Kotler M und Wainberg MA (1998a) Characterization of human immunodeficiency virus type-1 (HIV-1) particles that express protease-reverse transcriptase fusion proteins. J Mol Biol **284:** 43-56

Cherry E, Morin N und Wainberg MA (1998b) Effect of HIV constructs containing protease-reverse transcriptase fusion proteins on viral replication. AIDS **12:** 967-975

Chiu HC, Wang FD, Chen YM und Wang CT (2006) Effects of human immunodeficiency virus type 1 transframe protein p6* mutations on viral protease-mediated Gag processing. J Gen Virol **87:** 2041-2046

Coffin JM, Hughes SH, Varmus HE (1997) Retroviruses. Cold Spring Harbor Press, New York

Davies DR (1990) The structure and function of the aspartic proteinases. Annu Rev Biophys Biophys Chem **19:** 189-215

Dunn BM, Goodenow MM, Gustchina A und Wlodawer A (2002) Retroviral proteases. Genome Biol **3:** 1465-6914

Eastman SW, Linial ML (2001) Identification of a conserved residue of foamy virus Gag required for intracellular capsid assembly. J Virol **75:** 6857-6864

Erlwein O, Bieniasz PD und McClure MO (1998) Sequences in pol are required for transfer of human foamy virus-based vectors. J Virol **72:** 5510-5516

Fedoroff OY, Ge Y und Reid BR (1997) Solution structure of r (gaggacug):d (CAGTCCTC) hybrid: implications for the initiation of HIV-1 (+)-strand synthesis. J Mol Biol **269:** 225-239

Flügel RM, Pfrepper KI (2003) Proteolytic processing of foamy virus Gag and Pol proteins. Curr Top Microbiol Immunol **277:** 63-88

Goepfert PA, Shaw K, Wang G, Bansal A, Edwards BH und Mulligan MJ (1999) An endoplasmic reticulum retrieval signal partitions human foamy virus maturation to intracytoplasmic membranes. J Virol **73:** 7210-7217

Goff SP (2007) Retroviridae: The Retroviruses and Their Replication. In DM Knipe, PM Howley, eds, Fields Virology. Lippincott Williams & Wilkins, Philadelphia, pp 1999-2069

Heinkelein M, Dressler M, Jarmy G, Rammling M, Imrich H, Thurow J, Lindemann D und Rethwilm A (2002a) Improved primate foamy virus vectors and packaging constructs. J Virol **76:** 3774-3783

Heinkelein M, Leurs C, Rammling M, Peters K, Hanenberg H und Rethwilm A (2002b) Pregenomic RNA is required for efficient incorporation of pol polyprotein into foamy virus capsids. J Virol **76:** 10069-10073

Herchenröder O, Renne R, Loncar D, Cobb EK, Murthy KK, Schneider J, Mergia A und Luciw PA (1994) Isolation, cloning, and sequencing of simian foamy viruses from chimpanzees (SFVcpz): high homology to human foamy virus (HFV). Virology **201:** 187-199

Hsiou Y, Ding J, Das K, Clark AD,Jr, Hughes SH und Arnold E (1996) Structure of unliganded HIV-1 reverse transcriptase at 2.7 A resolution: implications of conformational changes for polymerization and inhibition mechanisms. Structure **4:** 853-860

Huang HF, Chopra R, Verdine GV und Harrison SC (1998) Structure of a covalently trapped catalytic complex of HIV-1 reverse transcriptase: implications for drug design. Science **282:** 1669-1675

Ingr M, Uhlikova T, Strisovsky K, Majerova E und Konvalinka J (2003) Kinetics of the dimerization of retroviral proteases: the "fireman's grip" and dimerization. Protein Sci **12:** 2173-2182

Ishima R, Ghirlando R, Tozser J, Gronenborn AM, Torchia DA und Louis JM (2001) Folded monomer of HIV-1 protease. J Biol Chem **276:** 49110-49116

Jacobo-Molina A, Ding J, Nanni RG, Clark AD,Jr., Lu X, Tantillo C, Williams RL, Kamer G, Ferris AL, Clark P, Hizi A, Hughes SH und Arnold E (1993) Crystal structure of human immunodeficiency virus type 1 reverse transcriptase complexed with double-stranded DNA at 3.0 A resolution shows bent DNA. Proc Natl Acad Sci U S A **90:** 6320-6324

Kanaya S, Katsuda-Nakai C und Ikehara M (1991) Importance of the positive charge cluster in *Escherichia coli* ribonuclease HI for the effective binding of the substrate. J Biol Chem **266:** 11621-11627

Katoh I, Ikawa Y und Yoshinaka Y (1989) Retrovirus protease characterized as a dimeric aspartic proteinase. J Virol **63:** 2226-2232

Katoh I, Yasunaga T, Ikawa Y und Yoshinaka Y (1987) Inhibition of retroviral protease activity by an aspartyl proteinase inhibitor. Nature **329:** 654-656

Keck JL, Marqusee S (1995) Substitution of a highly basic helix/loop sequence into the RNase H domain of human immunodeficiency virus reverse transcriptase restores its Mn (2+)-dependent RNase H activity. Proc Natl Acad Sci U S A **92:** 2740-2744

Krebs R, Immendörfer U, Thrall SH, Wöhrl BM und Goody RS (1997) Single-step kinetics of HIV-1 reverse transcriptase mutants responsible for virus resistance to nucleoside inhibitors zidovudine and 3-TC. Biochemistry **36:** 10292-10300

Kupiec JJ, Tobaly-Tapiero J, Canivet M, Santillana-Hayat M, Flügel RM, Peries J und Emanoil-Ravier R (1988) Evidence for a gapped linear duplex DNA intermediate in the replicative cycle of human and simian spumaviruses. Nucleic Acids Res **16:** 9557-9565

Larder BA, Kemp SD (1989) Multiple mutations in HIV-1 reverse transcriptase confer high-level resistance to zidovudine (AZT). Science **246:** 1155-1158

Lee CC, Ye F und Tarantal AF (2006) Comparison of growth and differentiation of fetal and adult rhesus monkey mesenchymal stem cells. Stem Cells Dev **15:** 209-220

Lee EG, Linial ML (2008) The C terminus of foamy retrovirus Gag contains determinants for encapsidation of Pol protein into virions. J Virol **82:** 10803-10810

Lim D, Orlova M und Goff SP (2002) Mutations of the RNase H C helix of the Moloney murine leukemia virus reverse transcriptase reveal defects in polypurine tract recognition. J Virol **76:** 8360-8373

Linial M (2007) Foamy Viruses. In DM Knipe, PM Howley, eds, Fields Virology. Lippincott Williams & Wilkins, Philadelphia, pp 2245-2262

Linial ML, Eastman SW (2003) Particle assembly and genome packaging. Curr Top Microbiol Immunol **277:** 89-110

Löchelt M, Flügel RM und Aboud M (1994) The human foamy virus internal promoter directs the expression of the functional Bel 1 transactivator and Bet protein early after infection. J Virol **68:** 638-645

Löchelt M, Romen F, Bastone P, Muckenfuss H, Kirchner N, Kim YB, Truyen U, Rosler U, Battenberg M, Saib A, Flory E, Cichutek K und Munk C (2005) The antiretroviral activity of APOBEC3 is inhibited by the foamy virus accessory Bet protein. Proc Natl Acad Sci U S A **102:** 7982-7987

Louis JM, Ishima R, Torchia DA und Weber IT (2007) HIV-1 protease: structure, dynamics, and inhibition. Adv Pharmacol **55:** 261-298

Louis JM, Weber IT, Tozser J, Clore GM und Gronenborn AM (2000) HIV-1 protease: maturation, enzyme specificity, and drug resistance. Adv Pharmacol **49:** 111-146

Louis JM, Wondrak EM, Kimmel AR, Wingfield PT und Nashed NT (1999) Proteolytic processing of HIV-1 protease precursor, kinetics and mechanism. J Biol Chem **274:** 23437-23442

Maurer B, Bannert H, Darai G und Flügel RM (1988) Analysis of the primary structure of the long terminal repeat and the gag and pol genes of the human spumaretrovirus. J Virol **62:** 1590-1597

Meiering CD, Linial ML (2001) Historical perspective of foamy virus epidemiology and infection. Clin Microbiol Rev **14:** 165-176

Mergia A, Shaw KE, Pratt-Lowe E, Barry PA und Luciw PA (1990) Simian foamy virus type 1 is a retrovirus which encodes a transcriptional transactivator. J Virol **64:** 3598-3604

Meyer PR, Matsuura SE, Mian AM, So AG und Scott WA (1999) A mechanism of AZT resistance: an increase in nucleotide-dependent primer unblocking by mutant HIV-1 reverse transcriptase. Mol Cell **4:** 35-43

Meyer PR, Matsuura SE, So AG und Scott WA (1998) Unblocking of chain-terminated primer by HIV-1 reverse transcriptase through a nucleotide-dependent mechanism. Proc Natl Acad Sci U S A **95:** 13471-13476

Moebes A, Enssle J, Bieniasz PD, Heinkelein M, Lindemann D, Bock M, McClure MO und Rethwilm A (1997) Human foamy virus reverse transcription that occurs late in the viral replication cycle. J Virol **71:** 7305-7311

Pearl LH, Taylor WR (1987) A structural model for the retroviral proteases. Nature **329:** 351-354

Perkovic M, Schmidt S, Marino D, Russell RA, Stauch B, Hofmann H, Kopietz F, Kloke BP, Zielonka J, Strover H, Hermle J, Lindemann D, Pathak VK, Schneider G, Löchelt M, Cichutek K und Munk C (2009) Species-specific inhibition of APOBEC3C by the prototype foamy virus protein bet. J Biol Chem **284:** 5819-5826

Peters K, Barg N, Gärtner K und Rethwilm A (2008) Complex effects of foamy virus central purine-rich regions on viral replication. Virology **33:** 51-60

Pettit SC, Gulnik S, Everitt L und Kaplan AH (2003) The dimer interfaces of protease and extra-protease domains influence the activation of protease and the specificity of GagPol cleavage. J Virol **77:** 366-374

Pfrepper KI, Löchelt M, Schnölzer M und Flügel RM (1997) Expression and molecular characterization of an enzymatically active recombinant human spumaretrovirus protease. Biochem Biophys Res Commun **237:** 548-553

Pfrepper KI, Rackwitz HR, Schnölzer M, Heid H, Löchelt M und Flügel RM (1998) Molecular characterization of proteolytic processing of the Pol proteins of human foamy virus reveals novel features of the viral protease. J Virol **72:** 7648-7652

Raba M, Limburg K, Burghagen M, Katze JR, Simsek M, Heckman JE, Rajbhandary UL und Gross HJ (1979) Nucleotide sequence of three isoaccepting lysine trnas from rabbit liver and sv40-transformed mouse fibroblasts. Eur J Biochem **97:** 305-318

Rethwilm A (2005) Foamy Viruses. In V ter Meulen, BWJ Mahy, eds, Topley & Wilson's Microbiology and Microbial Infections - Virology Vol 10, Vol.2. Hodder Arnold, London, pp 1304-1321

Rethwilm A (2003) The replication strategy of foamy viruses. Curr Top Microbiol Immunol **277:** 1-26

Rethwilm A, Erlwein O, Baunach G, Maurer B und ter Meulen V (1991) The transcriptional transactivator of human foamy virus maps to the bel 1 genomic region. Proc Natl Acad Sci U S A **88:** 941-945

Rinke CS, Boyer PL, Sullivan MD, Hughes SH und Linial ML (2002) Mutation of the catalytic domain of the foamy virus reverse transcriptase leads to loss of processivity and infectivity. J Virol **76:** 7560-7570

Rodes B, Holguin A, Soriano V, Dourana M, Mansinho K, Antunes F und Gonzalez-Lahoz J (2000) Emergence of drug resistance mutations in human immunodeficiency virus type 2-infected subjects undergoing antiretroviral therapy. J Clin Microbiol **38:** 1370-1374

Rodgers DW, Gamblin SJ, Harris BA, Ray S, Culp JS, Hellmig B, Woolf, DJ, Debouck C und Harrison SC (1995) The structure of unliganded reverse transcriptase from the human immunodeficiency virus type 1. Proc Natl Acad Sci U S A **92:** 1222-1226

Rosenblum LL, Patton G, Grigg AR, Frater AJ, Cain D, Erlwein O, Hill CL, Clarke JR und McClure MO (2001) Differential susceptibility of retroviruses to nucleoside analogues. Antivir Chem Chemother **12:** 91-97

Roy J, Rudolph W, Juretzek T, Gärtner K, Bock M, Herchenröder O, Lindemann D, Heinkelein M und Rethwilm A (2003) Feline foamy virus genome and replication strategy. J Virol **77:** 11324-11331

Russell RA, Wiegand HL, Moore MD, Schafer A, McClure MO und Cullen BR (2005) Foamy virus Bet proteins function as novel inhibitors of the APOBEC3 family of innate antiretroviral defense factors. J Virol **79:** 8724-8731

Sarafianos SG, Clark AD,Jr., Das K, Tuske S, Birktoft JJ, Ilankumaran P, Ramesha AR, Sayer JM, Jerina DM, Boyer PL, Hughes SH und Arnold E (2002) Structures of HIV-1 reverse transcriptase with pre- and post-translocation AZTMP-terminated DNA. EMBO J **21:** 6614-6624

Sarafianos SG, Das K, Tantillo C, Clark AD,Jr., Ding J, Whitcomb JM, Boyer PL, Hughes SH und Arnold E (2001) Crystal structure of HIV-1 reverse transcriptase in complex with a polypurine tract RNA:DNA. EMBO J **20:** 1449-1461

Sarafianos SG, Marchand B, Das K, Himmel DM, Parniak MA, Hughes SH und Arnold E (2009) Structure and function of HIV-1 reverse transcriptase: molecular mechanisms of polymerization and inhibition. J Mol Biol **385:** 693-713

Schultz SJ, Champoux JJ (2008) RNase H activity: structure, specificity, and function in reverse transcription. Virus Res **134:** 86-103

Smith AJ, Meyer PR, Asthana D, Ashman MR und Scott WA (2005) Intracellular substrates for the primer-unblocking reaction by human immunodeficiency virus type 1 reverse transcriptase: detection and quantitation in extracts from quiescent- and activated-lymphocyte subpopulations. Antimicrob Agents Chemother **49:** 1761-1769

Stahl SJ, Kaufman JD, Vikic-Topic S, Crouch RJ und Wingfield PT (1994) Construction of an enzymatically active ribonuclease h domain of human immunodeficiency virus type 1 reverse transcriptase. Protein Eng **7:** 1103-1108

Steitz TA (1998) A mechanism for all polymerases. Nature **391:** 231-232

Stenbak CR, Linial ML (2004) Role of the C terminus of foamy virus Gag in RNA packaging and Pol expression. J Virol **78:** 9423-9430

Switzer WM, Salemi M, Shanmugam V, Gao F, Cong ME, Kuiken C, Bhullar V, Beer BE, Vallet D, Gautier-Hion A, Tooze Z, Villinger F, Holmes EC und Heneine W (2005) Ancient co-speciation of simian foamy viruses and primates. Nature **434:** 376-380

Tang C, Louis JM, Aniana A, Suh JY und Clore GM (2008) Visualizing transient events in amino-terminal autoprocessing of HIV-1 protease. Nature **455:** 693-696

Telesnitsky A, Blain SW und Goff SP (1992) Defects in Moloney murine leukemia virus replication caused by a reverse transcriptase mutation modeled on the structure of *Escherichia coli* RNase H. J Virol **66:** 615-622

Temin HM (1964) Nature of the provirus of Rous sarcoma. National Cancer Institute Monograph **17:** 557-570

Temin HM, Mizutani S (1970) RNA-dependent DNA polymerase in virions of Rous sarcoma virus. Nature **226:** 1211-3

Tessmer U, Kräusslich HG (1998) Cleavage of human immunodeficiency virus type 1 proteinase from the N-terminally adjacent p6* protein is essential for efficient Gag polyprotein processing and viral infectivity. J Virol **72:** 3459-3463

Wain-Hobson S, Sonigo P, Danos O, Cole S und Alizon M (1985) Nucleotide sequence of the AIDS virus, LAV. Cell **40:** 9-17

Wlodawer A, Gustchina A (2000) Structural and biochemical studies of retroviral proteases. Biochim Biophys Acta **1477:** 16-34

Wlodawer A, Miller M, Jaskolski M, Sathyanarayana BK, Baldwin E, Weber IT, Selk LM, Clawson L, Schneider J und Kent SB (1989) Conserved folding in retroviral proteases: crystal structure of a synthetic HIV-1 protease. Science **245:** 616-621

Wondrak EM, Nashed NT, Haber MT, Jerina DM und Louis JM (1996) A transient precursor of the HIV-1 protease. Isolation, characterization, and kinetics of maturation. J Biol Chem **271:** 4477-4481

Yu SF, Sullivan MD und Linial ML (1999) Evidence that the human foamy virus genome is DNA. J Virol **73:** 1565-1572

6 List of publications

Publication A

Maximilian J. Hartl, Florian Mayr, Axel Rethwilm and Birgitta M. Wöhrl (2010): Biophysical and enzymatic properties of the simian and prototype foamy virus reverse transcriptases. *Retrovirology* **7**:5.

PFV full length DNA was provided by Axel Rethwilm. I established the cloning and purification of PFV PR-RT and SFVmac PR-RT. Circular dichroism of PFV and SFVmac PR-RT was analyzed by Florian Mayr. Florian Mayr and myself characterized protease and RNase H activities. I performed the polymerization assays and K_D measurements. The project was planned and supervised by Birgitta M. Wöhrl. Birgitta M. Wöhrl and I wrote the manuscript.

Publication B

Benedikt Kretzschmar*, Ali Nowrouzi*, Maximilian J. Hartl, Kathleen Gärtner, Tatiana Wiktorowicz, Ottmar Herchenröder, Sylvia Kanzler, Wolfram Rudolph, Ayalew Mergia, Birgitta M. Wöhrl and Axel Rethwilm (2007): AZT-resistant foamy virus. *Virology* **370**, 151-157.
* both authors contributed equally to this study

Benedikt Kretzschmar, Ali Nowrouzi, Axel Rethwilm and his group did the main work in this publication in collaboration with Ayalew Mergia. I provided purified SFVmac PR-RT for generation of polyclonal antisera in close cooperation with Birgitta M. Wöhrl. Birgitta M. Wöhrl and I contributed to writing the manuscript.

Publication C

Maximilian J. Hartl, Benedikt Kretzschmar, Anne Frohn, Ali Nowrouzi, Axel Rethwilm and Birgitta M. Wöhrl (2008): AZT resistance of simian foamy virus reverse transcriptase is based on the excision of AZTMP in the presence of ATP. *Nucleic Acids Research* **36**, 1009-1016.

I cloned the SFVmac PR-RT genes and established the expression and purification of recombinant WT and mutant SFVmac PR-RTs. Furthermore, I performed all experiments in this publication. Benedikt Kretzschmar and Axel Rethwilm provided the information and the DNA clones containing the mutations needed for AZT resistance in SFVmac. Anne Frohn purified two of the PR-RT mutants. Birgitta M. Wöhrl planned and supervised the project and wrote the manuscript with my participation.

Publication D

Maximilian J. Hartl, Birgitta M. Wöhrl and Kristian Schweimer (2007): Sequence-specific ^{1}H, ^{13}C and ^{15}N resonance assignments and secondary structure of a truncated protease from simian foamy virus. *Biomolecular NMR Assignment* **1**, 175-177.

I cloned, purified and tested the activity of SFVmac PRshort. NMR measurements and analysis were performed by myself under the supervision of Kristian Schweimer. Birgitta M. Wöhrl and Kristian Schweimer wrote the manuscript.

Publication E

Maximilian J. Hartl, Birgitta M. Wöhrl, Paul Rösch and Kristian Schweimer (2008): The solution structure of the simian foamy virus protease reveals a monomeric protein. *Journal of Molecular Biology* **381**, 141-149.

I performed the protein purifications, activity assays and determination of the monomer/dimer status of the SFVmac PR-RT and PRshort. Analytical ultracentrifugation was done in close cooperation with Stephan Uebel (*Max Planck Institut für Biochemie*, Martinsried, Germany). NMR measurements, analysis and structure calculation were done by Kristian Schweimer and

myself. Birgitta M. Wöhrl planned and supervised the project. Paul Rösch discussed the data and participated in writing the manuscript. Kristian Schweimer, Birgitta M. Wöhrl and I wrote the manuscript.

Publication F

Maximilian J. Hartl, Kristian Schweimer, Martin H. Reger, Stephan Schwarzinger, Jochen Bodem, Paul Rösch and Birgitta M. Wöhrl (2010): Formation of transient dimers by a retroviral protease. *Biochemical Journal* **427**, 197-203.

The influence of the dimerization inhibitor cholic acid on SFV PR-RT and PRshort was investigated by myself. Kristian Schweimer helped to analyze the NMR data. Jochen Bodem pervormed *in vivo* experiments with cholic acid and SFVmac. Initial spin label experiments were done by Martin Reger and Stephan Schwarzinger. I planned, performed and analyzed further PRE experiments with the support of Kristian Schweimer. Birgitta M. Wöhrl planned and supervised the project. Paul Rösch provided conceptual input and participated in wirting the manuscript. Kristian Schweimer, Birgitta M. Wöhrl and I wrote the manuscript.

Publication G

Maximilian J. Hartl and Birgitta M. Wöhrl (2009): Regulation of foamy virus protease by RNA – a unique mechanism among retroviruses. *in preparation*.

I performed and planned the experiments. Birgitta M. Wöhrl planned and supervised the project. Both authors wrote the manuscript.

7 Publication A

Maximilian J. Hartl, Florian Mayr, Axel Rethwilm and Birgitta M. Wöhrl (2010): Biophysical and enzymatic properties of the simian and prototype foamy virus reverse transcriptases. *Retrovirology* **7**:5.

Hartl et al. Retrovirology 2010, 7:5
http://www.retrovirology.com/content/7/1/5

RETROVIROLOGY

RESEARCH Open Access

Biophysical and enzymatic properties of the simian and prototype foamy virus reverse transcriptases

Maximilian J Hartl[1], Florian Mayr[1], Axel Rethwilm[2], Birgitta M Wöhrl[1*]

Abstract

Background: The foamy virus Pol protein is translated independently from Gag using a separate mRNA. Thus, in contrast to *orthoretroviruses* no Gag-Pol precursor protein is synthesized. Only the integrase domain is cleaved off from Pol resulting in a mature reverse transcriptase harboring the protease domain at the N-terminus (PR-RT). Although the homology between the PR-RTs from simian foamy virus from macaques (SFVmac) and the prototype foamy virus (PFV), probably originating from chimpanzee, exceeds 90%, several differences in the biophysical and biochemical properties of the two enzymes have been reported (i.e. SFVmac develops resistance to the nucleoside inhibitor azidothymidine (AZT) whereas PFV remains AZT sensitive even if the resistance mutations from SFVmac PR-RT are introduced into the PFV PR-RT gene). Moreover, contradictory data on the monomer/dimer status of the foamy virus protease have been published.

Results: We set out to purify and directly compare the monomer/dimer status and the enzymatic behavior of the two wild type PR-RT enzymes from SFVmac and PFV in order to get a better understanding of the protein and enzyme functions. We determined kinetic parameters for the two enzymes, and we show that PFV PR-RT is also a monomeric protein.

Conclusions: Our data show that the PR-RTs from SFV and PFV are monomeric proteins with similar biochemical and biophysical properties that are in some aspects comparable with MLV RT, but differ from those of HIV-1 RT. These differences might be due to the different conditions the viruses are confronted with in dividing and non-dividing cells.

Background

Foamy viruses (FVs) belong to the family *retroviridae*, but differ in several aspects from *orthoretrovirinae*: (a) reverse transcription occurs before the virus leaves the host cell [1,2], (b) the *pol*-gene is expressed from a separate mRNA [3-5], and (c) the viral protease is not cleaved off from the Pol polyprotein. Only the integrase is removed from Pol [6,7]. Thus, the FV reverse transcriptase harbors a protease, polymerase and RNase H domain (PR-RT) (for review see [8,9]).

Only recently, studies have focused on the biochemistry of the PR-RTs of FVs. Although the PR-RTs from simian foamy virus from macaques (SFVmac) and from the prototype foamy virus (PFV) exhibit more than 90% sequence homology at the protein level (79.5% identity; LALIGN, http://www.ch.embnet.org), some differences in their behavior have been reported. Bacterially expressed PFV PR-RT harbors many characteristics of orthoretroviral RTs; however, FV enzymes exhibit some peculiar features [10-16]. In comparison to human immunodeficiency virus type 1 (HIV-1) RT, PFV PR-RT appears to be a more processive polymerase [11]. This is probably due to differences in virus assembly. FV Pol packaging has been reported to require interactions of Pol with specific sequences in the RNA genome [17], and it has been suggested that there is a lower number of FV Pol molecules in the virus particle as compared to orthoretroviruses [11]. As a consequence, a highly processive polymerase is essential to enable synthesis of the complete double stranded genome.

* Correspondence: birgitta.woehrl@uni-bayreuth.de
[1]Universität Bayreuth, Lehrstuhl für Struktur und Chemie der Biopolymere & Research, Center for Biomacromolecules, 95440 Bayreuth, Germany

One antiretroviral drug that has been shown to inhibit FV replication is azidothymidine (AZT) [1,18,19]. In *in vivo* experiments SFVmac acquired high resistance to AZT by four mutations within the RT sequence [14,20]. PFV, however, did not develop resistance to AZT, and the introduction of the SFVmac mutations into the PFV RT gene did not result in viruses resistant to the nucleoside inhibitor [20]. Regarding the high amino acid homology of the two enzymes, this result was not to be expected. In SFVmac, the mechanism of resistance is due to the removal of already incorporated AZT-monophosphate (AZTMP) in the presence of ATP and thus resembles that of HIV-1 RT [14,21,22].

It has been shown previously that retroviral PRs are only active as homodimers. To create the active center, each subunit of the homodimer contributes catalytic residues located in the conserved motif DT/SG [23]. However, SFVmac PR-RT behaves as a monomer in solution, but nevertheless exhibits PR activity. Catalytic PR activity could only be observed at NaCl concentrations of 2-3 M [15], indicating that hydrophobic interactions might promote dimerization. Furthermore, by prevalent methods the separately expressed 12.6 kDa PR domain was also found to be monomeric but active [15]. Only further analyses using NMR paramagnetic relaxation enhancement proved that transient, lowly populated dimers are being formed (Hartl MJ, Schweimer K, Reger MH, Schwarzinger S, Bodem J, Rösch P, Wöhrl BM: Formation of transient dimers by a retroviral protease, submitted). Contradicting results were obtained by gel filtration analysis with a purified C-terminally extended 18 kDa PR domain of PFV, which indicated that PFV PR might be dimeric [6].

To clarify these issues and to shed more light on the properties of SFVmac and PFV PR-RT, we set out to purify both enzymes from bacterial lysates and directly compare their secondary structure, oligomerization state, and activities.

Results and Discussion

Protein purification

Overexpression of PFV PR-RT in *E. coli* resulted in partial degradation by cellular proteases. Thus, we could not adopt the purification protocol established for SFVmac PR-RT [14]. Instead, we had to set up a new purification procedure for PFV PR-RT which includes Ni-affinity followed by hydrophobic interaction chromatography to remove the PR-RT degradation products. The yields were much lower than for SFVmac PR-RT. Nevertheless, pure soluble protein (> 95% purity, as judged from SDS-polyacrylamide gels) could be obtained.

Biophysical properties

To exclude that the purified PR-RTs are partially or completely unfolded, we analyzed the secondary structure of PFV and SFVmac PR-RT by circular dichroism (CD) spectroscopy. The shape of the CD spectra obtained for the two enzymes was highly similar, implying comparable ratios of α-helices and β-strands (Fig. 1A). In both cases, the curves showed a broad minimum between 205 nm and 222 nm, characteristic for a mixture of α-helical and β-strand structures, and high ellipticity near 200 nm. Thus, the spectra are indicative of predominantly folded proteins. Although the spectrum obtained for SFVmac PR-RT deviates slightly from that of PFV PR-RT, the calculated values (Table 1) confirm the accordance in the secondary structure contents of PFV and SFVmac PR-RT. However, crystal structure analyses will be necessary to obtain more information on the structural similarities and differences of the two enzymes. The three-dimensional structure will probably also shed more light on the differences between PFV and SFVmac PR-RT in developing AZT-resistance.

Contradicting data have been published on the monomer/dimer status of FV PRs. PFV PR expressed separately was suggested to be dimeric [6], whereas we have shown by various analyses, like size exclusion chromatography and analytical ultracentrifugation that the full length PR-RT protein as well as the separate PR domain of SFVmac are monomeric, and only transient PR dimers are being formed [15] (Hartl MJ, Schweimer K, Reger MH, Schwarzinger S, Bodem J, Rösch P, Wöhrl BM: Formation of transient dimers by a retroviral protease, submitted).

Previous results obtained by sucrose density gradient analyses with PR-RT purified from SFVmac particles also indicated that the protein is monomeric [24]. To clarify the monomer/dimer status of PFV PR-RT, we performed size exclusion chromatography (Fig. 1B). Our data revealed a single peak, which corresponded to a molecular mass of 85.4 kDa. This is in good agreement with the theoretical molecular mass of the monomeric PFV PR-RT of 86.5 kDa. Moreover, no dimer peak

Table 1 CD values

enzyme	α-helix (%)	β-sheet (%)	β-turns (%)	random coil (%)	total (%)
PFV PR-RT	22	30	20	27	99
SFVmac PR-RT	22	29	20	28	99

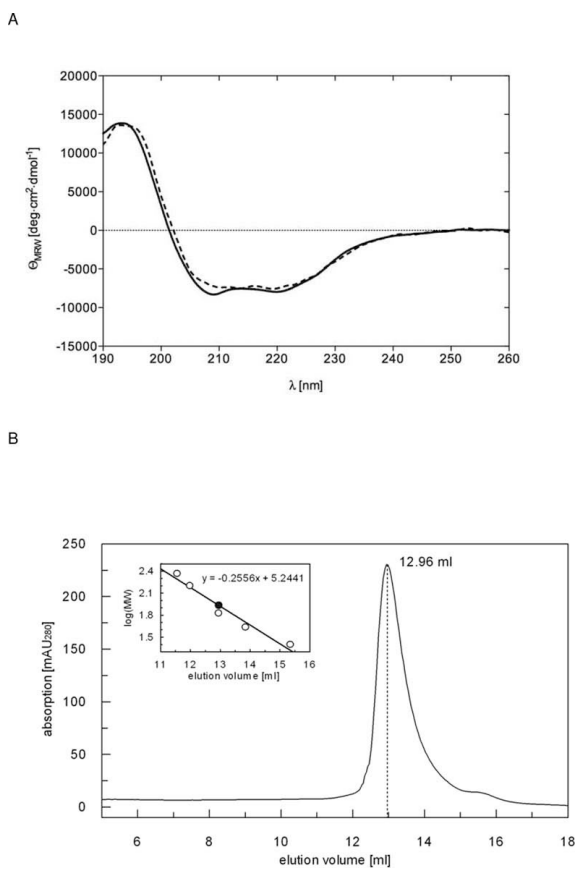

Figure 1 Biophysical properties of PFV and SFVmac PR-RT. **(A)** Far UV circular dichroism (CD) spectra of wild-type SFVmac (continuous line) and PFV PR-RT (dotted line) were acquired at 20°C using a band width of 1 nm, a sensitivity of 100 mdeg and a data density of 5 points/nm in a 0.1 cm cell with 0.5 μM of each enzyme in 25 mM Na_2HPO_4/NaH_2PO_4 pH 7.4, and 5 mM NaCl. **(B)** Size exclusion chromatography of PFV PR-RT using an S200 HR 10/30 column. The run was performed with 10 nmol PFV PR-RT in 50 mM Na_2HPO_4/NaH_2PO_4 pH 7.4, 300 mM NaCl and 0.5 mM DTT. The inset shows the fit to the data obtained for the molecular masses of the standard proteins (open circles), which was used for the determination of the molecular mass of PFV PR-RT (closed circle).

could be detected, indicating that under native conditions PFV PR-RT, like SFVmac PR-RT is monomeric to a great extent (> 95%).

PR activity

Activity of retroviral PRs is only achieved when a symmetric homodimer is formed, since each subunit provides a conserved aspartate residue to form the active center [23,25,26]. To detect residual PR activity we used a substrate, denoted GB1-GFP, that consists of a fusion protein between the immunoglobulin binding domain B1 of the streptococcal protein G (GB1) and the green fluorescent protein (GFP) enframing the natural SFVmac Pol cleavage site YVVH↓CNTT. Although in PFV Pol the His is exchanged by Asn, this substrate could also be used for PFV PR-RT, because retroviral PRs are able to recognize different cleavage sites.

A concentration of 3 M NaCl was used in the assay since under these conditions SFVmac PR-RT revealed the highest PR activity, and no activity was detected when low salt concentrations (ca. 0.2 - 0.4 M NaCl) were applied [15]. Fig. 2 illustrates that both proteins were capable of almost completely cleaving the provided substrate even though the offered sequence is different from the naturally occurring cleavage site in PFV Pol.

Size exclusion chromatography and PR activity assays revealed a new feature special to *spumaretrovirinae*. FVs appear to express a monomeric PR domain within the Pol polyprotein which is catalytically inactive. *In vitro* dimerization of the PR domain is inducible at high salt concentrations. This effect might be caused by a hydrophobic dimerization interface, which under high ionic strength disfavors the monomeric state.

Recently published results suggest that HIV-1 PR in the Gag-Pol precursor is only present as a transient dimer due to an inhibitory effect of the transframe region, which is located N-terminally of the PR domain [27]. Since there is no Gag-Pol fusion protein in FVs, an N-terminal extension of the PR does not exist. Thus, the regulation of the FV PR activity has to be different. We have shown recently, that SFVmac PR forms transient dimers at low salt concentrations. Obviously, *in vivo* PR activation cannot be achieved by increasing the NaCl concentration to 3 M, indicating that an additional cellular and/or viral factor must be involved in PR activation.

Characteristics of polymerization

A key step in the retroviral life cycle is the reverse transcription of the genomic RNA into double stranded (ds) DNA. For formation of dsDNA, the RT catalyzes RNA- and DNA-dependent DNA polymerization to synthesize the (-) and (+)-strand, respectively.

To further characterize the PR-RT enzymes, we performed polymerization assays on the homopolymeric poly(rA)/oligo$(dT)_{15}$ substrate and on heteropolymeric single-stranded M13 DNA. The incorporation of ^{3}H-TTP was used to determine Michaelis-Menten parameters. Comparison with values already published for SFVmac PR-RT for homopolymeric substrates revealed fairly similar K_M- and k_{cat}-values for the two enzymes. Moreover, the K_M-values for homo- and heteropolymeric substrates are comparable (Table 2) [14].

The K_M values determined here for FV PR-RTs are ca. 5-30 fold higher than those published for HIV-1 RT [28-30]. A recent publication compares the pre-steady-state kinetics of PFV PR-RT with those of HIV-1 and

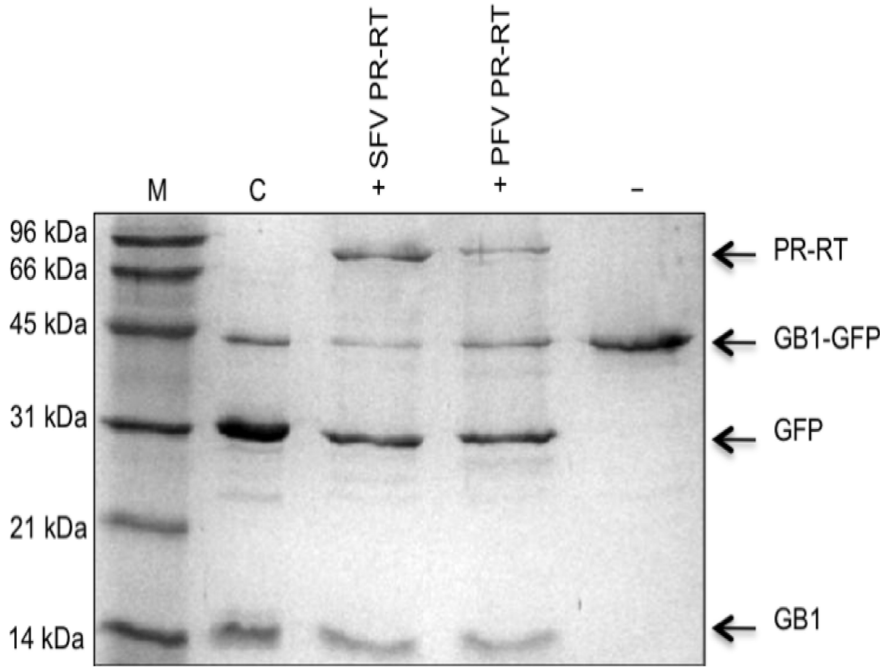

Figure 2 PR activity assay. Reaction products were analyzed by 19% SDS-PAGE. 10 μM GB1-GFP substrate harboring a FV PR cleavage site between GB1 and GFP was incubated with 10 μM SFVmac PR-RT or PFV PR-RT, respectively, at 37°C for 16 h in reaction buffer (50 mM Na_2HPO_4/NaH_2PO_4 pH 7.4, 0.5 mM DTT, 3 M NaCl). C, control, substrate cleavage with TEV protease; (-), uncleaved substrate; M, molecular weight standard. The sizes of the standard proteins are indicated on the left.

murine leukemia virus (MuLV) RT [31]. Although the k_{pol} values of the three enzymes are similar, the dissociation constants (K_D) for dNTP binding are about 10 - 80 fold higher with PFV PR-RT as compared to HIV-1 RT, but are comparable to the affinities obtained for MuLV RT [31]. These kinetic data together with our results reveal different polymerization properties of HIV-1 RT and FV PR-RTs. The data imply that DNA polymerization of FV PR-RTs is poor at low dNTP concentrations. One reason for the differences observed might be the fact that in contrast to FV, HIV-1 can replicate in non-dividing cells, where dNTP concentrations are low. In such an environment, polymerization efficiency can be improved by RTs with high affinities for dNTPs [31].

A qualitative analysis of DNA polymerization was performed by using a heteropolymeric single stranded M13 DNA as a template together with a radioactively 5' end labeled primer and saturating dNTP concentrations of 150 μM. The polymerization products were compared on a denaturing polyacrylamide/urea gel (Fig. 3). The results confirmed the kinetic data foreshadowed in Table 2, revealing a somewhat higher polymerization efficiency of PFV-PR-RT.

Since polymerization activities are also dependent on nucleic acid substrate affinities, we determined K_D-values of the two FV PR-RTs for DNA/RNA and DNA/DNA by fluorescence anisotropy. In each of these experiments a 24/40 mer primer/template (P/T) substrate was used containing a fluorescent dye

Table 2 Kinetic parameters of the polymerization activities of SFVmac and PFV PR-RT

enzyme	K_D DNA/RNA (nM)	K_D DNA/DNA (nM)	K_M [1)] (TTP/rAdT) (μM)	k_{cat} [1)] (TTP/rAdT) (s^{-1})	K_M [2)] (dNTPs/M13) (μM)	k_{cat} [2)] (dNTPs/M13) (s^{-1})
PFV PR-RT	9.9 (± 1.6)	44.4 (± 3.0)	45 (± 12)	7.1 (± 0.9)	46 (± 9)	3 (± 0.3)
SFVmac PR-RT	32.4 (± 4.2)[3)]	36.4 (± 2.4)[3)]	40.1 (± 4.0)[3)]	5.5 (± 0.3)[4)]	45 (± 3)	4 (± 0.1)

[1)] K_M and k_{cat}-values, respectively, determined for TTP on the homopolymeric substrate poly(rA)/oligo(dT).
[2)] K_M and k_{cat}-values, respectively, determined for dNTPs on a heteropolymeric single stranded M13 substrate
[3)] Data adopted from [14]
[4)] v_{max}-value used for k_{cat} calculation derived from [14].

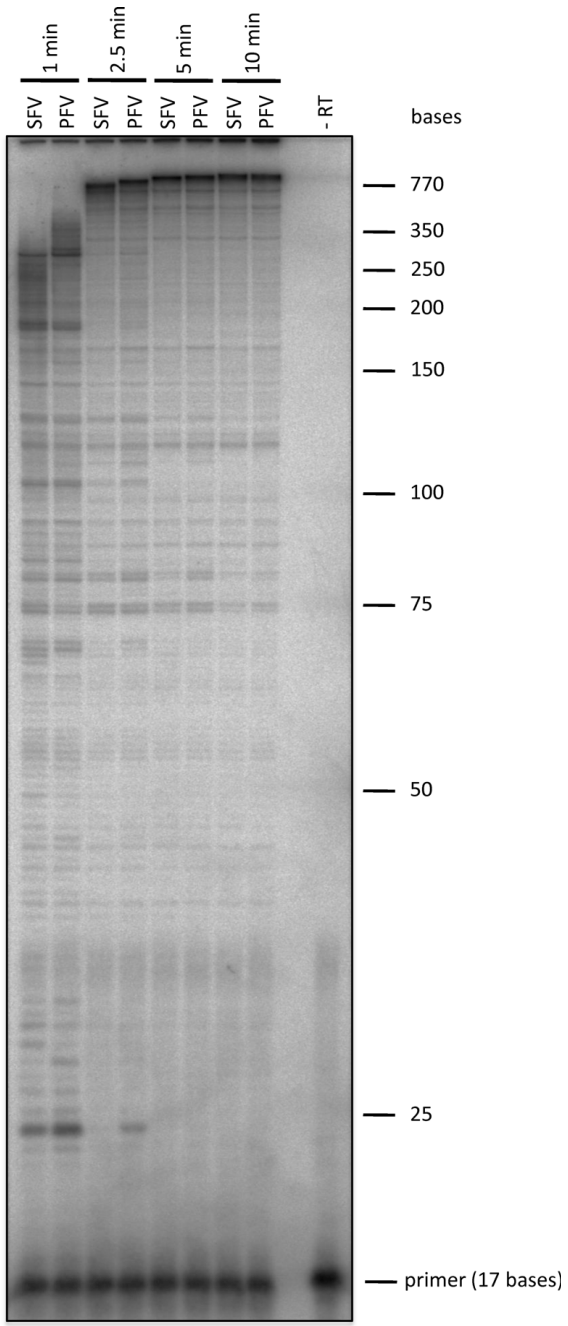

Figure 3 DNA-dependent DNA polymerase activity on a heteropolymeric substrate. Reactions were carried out at 37°C for the times indicated on top with 6 nM of the M13 P/T substrate, 85 nM of PFV or SFV PR-RT and 150 μM of each dNTP, analyzed by denaturing gel electrophoresis on a 10% sequencing gel and visualized by phosphoimaging. DNA size markers are marked on the right. - RT, assay without enzyme;

(Dy-647) at the 5' end of the template strand (Table 2, Fig. 4). For both enzymes, the affinity for the DNA/RNA P/T appeared to be higher than for DNA/DNA. This effect was far more pronounced for PFV PR-RT with a 4-fold lower K_D-value for the DNA/RNA substrate. Comparison with HIV-1 RT shows an unexpected difference, i.e. the affinities of HIV-1 RT for nucleic acid substrates are much higher. For DNA/DNA or DNA/RNA substrates K_D-values of approximately 2 nM have been determined [32-34].

RNase H activity

The third enzymatic activity associated with PR-RT is its RNase H activity, which is responsible for degradation of the RNA strand of an RNA/DNA hybrid and is indispensable in the reverse transcription process.

Polymerization-independent RNase H activity was tested on two different substrates. First, Michaelis-Menten-parameters were determined on a blunt-ended RNA/DNA substrate containing a fluorescent dye on the 3' end of the RNA and a quencher on the 5' end of the DNA. Upon cleavage of the RNA the fluorescent dye is released from the quencher resulting in an increase in fluorescence intensity. By varying substrate concentrations, K_M- and k_{cat}-values for RNase H activities were calculated (Table 3). SFVmac and PFV PR-RT showed K_M-values of 18.1 nM and 17.1 nM, respectively. These are in the range of HIV-1 RT (25 nM) [35]

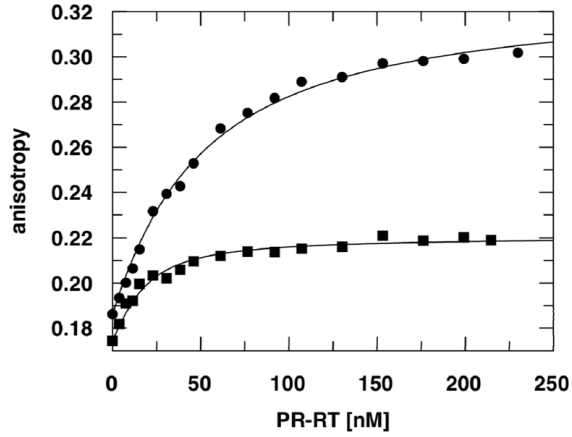

Figure 4 Determination of K_D-values by fluorescence anisotropy measurements. 15 nM of a fluorescently labeled DNA/DNA (black circle) or DNA/RNA (black square) P/T substrate was titrated with PFV PR-RT at 25°C. The curves show the best fit to a two component binding equation [14] describing the binding equilibrium with K_D-values shown in Table 2.

Table 3 Kinetic parameters of the RNase H activities of SFVmac and PFV PR-RT

enzyme	K_M RNase H (nM)	k_{cat} (s^{-1})
PFV PR-RT	17.1 (± 1.2)	0.017 (± 0.0003)
SFVmac PR-RT	18.1 (± 0.6)	0.020 (± 0.0003)

and *E. coli* RNase H (16 - 130 nM, depending on the substrate) [36]. Provided that indeed FV PR-RTs are less abundant in the virus particle, it is remarkable that the FV RNase H activities were not higher than those of HIV-1 RT.

To determine the endonucleolytic RNase H cleavage sites of the two PR-RTs qualitatively, a 40 mer RNA hybridized to a 24 mer DNA was used (Fig. 5). A fluorescent dye at the 5' end of the RNA allowed visualization of the cleavage products after separation on 15% sequencing gels. Our time course experiments indicated that with both enzymes a primary endonucleolytic cleavage at position -19 was followed by a 3' > 5' directed processing reaction leading to shorter RNA products (Fig. 5). Primary RNase H cleavage sites in the RNA at positions 15 -20 nucleotides away from the primer terminus of the hybrid were also detected for the RTs of *orthoretrovirinae* like HIV-1 and RSV [37-42]. They are directed by the 3'-end of the DNA-primer which binds to the active site of the polymerase [43,44]. While RSV RT appears to lack a 3' > 5' directed processing activity [37], SFVmac and PFV PR-RTs (Figure 5B) as well as HIV-1 and MoMLV RTs degrade the RNA to 8 mers or smaller products [41,45].

Conclusions

Our data reveal small differences of FV PR-RTs in their catalytic activities and biophysical properties. The K_M-values determined for HIV-1 RT are 5-30 fold lower than those for FV PR-RTs. These deviations in kinetic behavior might be based on the fact that HIV-1 can replicate in non-dividing cells. Remarkably, both FV PR-RTs are monomeric in solution, implying that transient dimers need to be formed in order to obtain PR activity. Transient dimerization has been demonstrated recently for SFVmac PR and was suggested to play a role in the regulation of a timely activation of PR activity (Hartl MJ, Schweimer K, Reger MH, Schwarzinger S, Bodem J, Rösch P, Wöhrl BM: Formation of transient dimers by a retroviral protease, submitted). Small structural and consequently catalytic variations between the two FV PR-RTs might account for the differences observed (e.g. in the resistance to the nucleoside inhibitor AZT.) Further structural and functional analyses will be necessary to elucidate these findings.

Methods

Plasmid construction and protein purification

For SFVmac PR-RT, gene expression and protein purification were performed as described previously [14]. The plasmid pET101TOPO-PFV-PR-RT-6His was constructed using the Champion™ pET Directional TOPO® Expression kit (Invitrogen, Darmstadt, Germany). The N-terminus of the PFV PR-RT starts with the amino acids MNPLQLLQPL corresponding to the N-terminus of the PR gene. The C-terminus contains a 6 × His tag and exhibits the following amino acid sequence: ATQG-SYVVNA-6His. The plasmid was transformed into the *Escherichia coli* (*E. coli*) strain BL21 (DE3) pREP4: GroESL [46], expressing *E. coli* chaperone proteins to facilitate folding of heterologous proteins. Cells were grown at 37°C in LB medium supplemented with 100 μg/ml ampicillin and 34 μg/ml kanamycin to an optical density of 600 nm (OD_{600}) of ca. 0.8. The temperature was reduced to 16°C until an $OD_{600}$of ca. 1.0 was reached. Expression of the recombinant PFV PR-RT-6His gene was then induced by the addition of 0.2 mM isopropyl-thiogalactoside (IPTG) at 16°C over night. Cells were harvested by centrifugation at 5000 g for 20 min at 4°C.

Purification of SFVmac and PFV PR-RT

SFVmac PR-RT was purified as described previously [14]. PFV PR-RT was purified as follows by a combination of Ni-affinity and hydrophobic interaction chromatography:

Ni-NTA affinity chromatography

Cells were resuspended in 50 mM Na-phosphate pH 7.4, 300 mM NaCl, 10 mM imidazole, 0.5 mM dithiothreitol (DTT). After addition of lysozyme, DNase I and one protease inhibitor cocktail tablet (Complete, EDTA-free, Roche Diagnostics GmbH, Mannheim) the suspension was stirred on ice for 30 min. After cell lysis using a microfluidizer (Microfluidics, Newton, MA, USA) the suspension was centrifuged at 19100 g for 30 min at 4° C. Purification of the protein was performed by a step gradient applying increasing concentrations of up to 500 mM imidazole on a HisTrap column (HisTrap, GE Healthcare, München, Germany).

Hydrophobic interaction chromatography

Fractions containing PFV PR-RT were pooled and dialyzed (Spectra/Por, MWCO 50 000 Da) twice for at least 2 h against 50 mM Na-phosphate pH 7.4, 300 mM NaCl, 1 M $(NH_4)_2SO_4$ and 0.5 mM DTT and then loaded onto a 5 ml butyl column (ButylFF, GE Healthcare, München, Germany). The protein was eluted by applying a step gradient from 1 M $(NH_4)_2SO_4$ and 300 mM NaCl to 0 M $(NH_4)_2SO_4$ and 0 M NaCl. After electrophoresis of the fractions on 10% SDS-polyacrylamide gels the relevant fractions were concentrated with

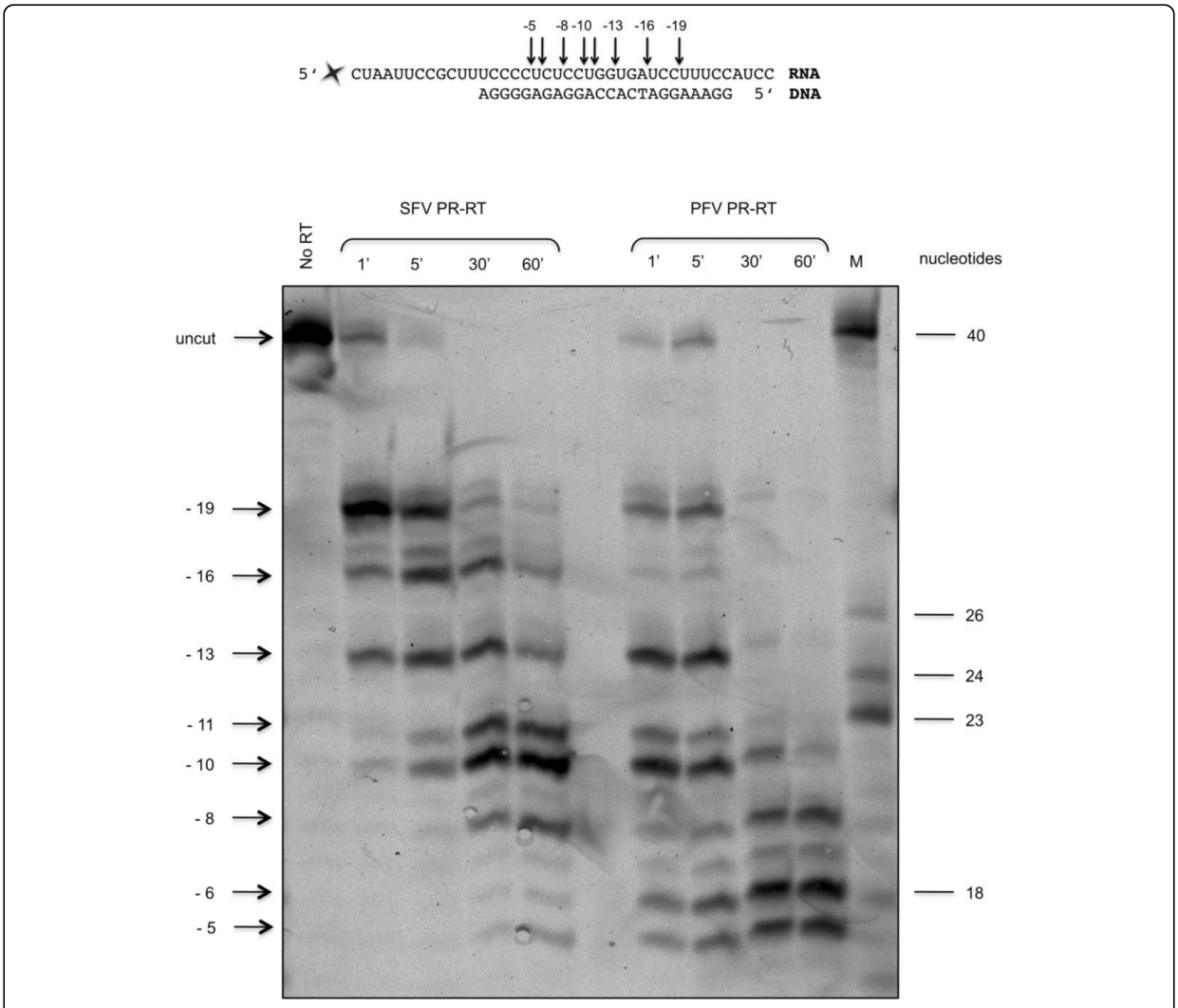

Figure 5 Qualitative RNase H assay. The DNA/RNA P/T substrate is shown on top. The cleavage sites determined for SFV and PFV PR-RT are indicated by arrows. 320 nM of DY-647 labeled P/T substrate was incubated with 50 nM of SFVmac or PFV PR-RT in 50 mM Tris/HCl, pH8.0, 80 mM KCl, 6 mM $MgCl_2$ for the times indicated on top of the gel. Reaction products were analyzed on a 15% polyacrylamide sequencing gel and visualized by detection of the fluorescence emission of the RNA template strand at 670 nm upon excitation at 633 nm. The cleavage sites are indicated on the left. The first nucleotide of the RNA hybridized to the 3'-OH nucleotide of the DNA primer is denoted -1. The partially hydrolyzed RNA on the right was used for the determination of the cleavage sites. Numbers on the right indicate the length of the RNA in nucleotides.

Vivaspin concentrators (MWCO 10 000 Da) to a volume of 200 μl and dialyzed against 50 mM Na-phosphate pH 7.4, 100 mM NaCl 0.5 mM DTT.

Analyses using circular dichroism (CD) spectra and size exclusion chromatography were performed with freshly purified SFVmac and PFV PR-RT. For PR, polymerization and RNase H measurements the PFV PR-RT was dialyzed (Spectra/Por, MWCO 50 000 Da) against 50 mM Na-phosphate pH 7.4, 100 mM NaCl, 0.5 mM DTT and 15% glycerol over night, the glycerol concentration was then increased to 50% and the protein stored at -20°C.

Peptide mass fingerprint (PMF) analysis

Protein bands of ca. 1 mm × 3 mm were excised from 10% SDS-polyacrylamide gels and the integrity and identity of PFV PR-RT was confirmed by peptide mass fingerprinting (ZMMK Köln, Zentrale Bioanalytik, Germany).

Circular dichroism

Far UV circular dichroism (CD) spectra of wild-type SFVmac and PFV PR-RT were acquired at 20°C using a Jasco J-810 spectropolarimeter (Japan Spectroscopic, Gross-Umstadt, Germany) at a band width of 1 nm, a sensitivity of 100 mdeg and a data density of 5 points/

nm in a 0.1 cm cell. 0.5 μM of each enzyme was measured in 25 mM Na-phosphate pH 7.4 and 5 mM NaCl. At least 12 scans in the range between 260 and 190 nm were averaged for each measurement, and the resulting spectrum was smoothed and normalized to a mean residual weight ellipticity [Θ_{MRW}] (deg·cm^2·dmol^{-1}) using Jasco Spectra Manager Software. For secondary structure predictions based on the CD data the program CDSSTR (Dichroweb) [14,27] was used.

Size exclusion chromatography

For analytical gel filtration of PFV PR-RT a Superdex 200 HR 10/30 column (GE Healthcare, Munich, Germany) calibrated with catalase (232 kDa), aldolase (158 kDa), ovalbumine (43 kDa) and chymotrypsinogen (25 kDa) (GE Healthcare, Munich, Germany) was used at a flow rate of 0.5 ml/min. The column was loaded with 10 nmol PFV PR-RT in 50 mM Na_2HPO_4/NaH_2PO_4 pH 7.4, 300 mM NaCl and 0.5 mM DTT.

PR activity assay

PR activity was measured as described before using a substrate which contained the SFVmac Pol cleavage site ATQGSYVVH↓CNTTP that can also be used by PFV PR-RT. Control digests with TEV protease were performed with the same substrate since it harbors a TEV cleavage site adjacent to the FV PR cleavage site [15].

Polymerization assays

RNA-dependent DNA polymerase activity was quantitated on a poly(rA)/oligo(dT)15 substrate (0.2 U/ml) (Roche Diagnostics GmbH, Mannheim, Germany) in a standard assay (30 μl reaction volume) as described previously [14]. For the determination of K_M, v_{max} and k_{cat} values, reactions were performed with increasing concentrations of TTP of 25, 50, 75,125 or 250 μM. For the determination of kinetic parameters on a heteropolymeric substrate 100 nM of single stranded M13mp18 DNA and 15 nM of PR-RT was used. dNTP concentrations of 25, 50, 75, 125 and 250 μM were added, using [3H]-TTP (3000 Ci/mmol, Hartmann Analytic GmbH, Braunschweig, Germany) as a tracer. K_M-values were calculated by linear regression using Eadie-Hofstee plots. k_{cat} is defined as v_{max}/enzyme concentration. Qualitative DNA polymerization assays on denaturing polyacrylamide/urea gels using single stranded M13mp18 DNA as a substrate were performed as described previously [14].

Fluorescence anisotropy measurements

Fluorescence equilibrium titrations were performed to determine the dissociation constants (K_D) for nucleic acid binding with a 24/40 mer DNA/DNA or DNA/RNA primer/template (P/T). Experiments and data fitting were carried out as described [14] with15 nM fluorescently labeled P/T at 25°C.

RNase H activity assays

Substrate preparation

The RNA-strand 5'-CCG AUG GCU CUC CUG GUG AUC CUU UCC-6-FAM (6-carboxy-fluorescein) and the DNA-strand 5'-Dabcyl-GGA AAG GAT CAC CAG GAG AG were synthesized by biomers.net (Ulm, Germany). The hybrid was formed by mixing the two oligonucleotides at a ratio of 1:1.2 respectively in 20 mM Tris/HCl pH 8.0 and 20 mM NaCl, followed by heating at 95°C for 2 min and cooling down to room temperature over a time period of 2 h. The resulting substrate was stored in aliquots at -20°C.

RNase H enzyme kinetics

Steady-state fluorescence measurements were performed at 25°C on a Fluorolog-Tau-3 spetrofluorometer (HORIBA Jobin Yvon GmbH, Unterhaching, Germany). The assay was carried out in a total volume of 1.2 ml containing 50 mM Tris/HCl pH 8.0, 80 mM KCl, 6 mM $MgCl_2$ and a final concentration of 1 nM PR-RT. To determine the Michaelis-Menten kinetic parameters the DNA-dabcyl/RNA-6-FAM P/T concentration was varied from 10 to 200 nM. Cleavage of the RNA in the hybrid leads to dissociation of a fluorescein labeled RNA fragment from the dabcyl quencher and thus to a fluorescence increase. Upon excitation of the substrate at 495 nm an increase in fluorescence emission can be detected at 520 nm. The maximum change in fluorescence intensity and thus complete substrate cleavage was determined by incubating the hybrid with a large excess of PR-RT (250 nM). Initial rates were calculated using the linear slope of the reaction progress curve where less than 5% of substrate was cleaved. Values for kinetic parameters (K_M and v_{max}) were obtained by linear Eadie-Hofstee regression of the Michaelis-Menten equation $V_0 = V_{max}\cdot[S_0]/(K_m + [S_0])$. k_{cat} is defined as v_{max}/enzyme concentration.

Qualitative RNase H assay

The gelelectrophoretic assay used a 5' fluorescently labeled RNA-oligonucleotide (5'- [DY-647]-CUA AUU CCG CUU UCC CCU CUC CUG GUG AUC CUU UCC AUC C; biomers.net, Ulm, Germany), which was purified on a 20% denaturing polyacrylamide gel and then annealed to the unlabeled DNA-oligonucleotide 5'-GGA AAG GAT CAC CAG GAG AGG GGA (biomers.net, Ulm, Germany). The hybrid was formed by mixing 2 μM Dye647-RNA with 2.4 μM DNA primer in 20 mM Tris/HCl pH 8.0 and 20 mM NaCl, followed by heating at 95°C for 2 min and cooling at room temperature over a time period of 2 h. The RNase H reaction was performed at 37°C in a total volume of 30 μl in 50 mM Tris/HCl pH 8.0, 80 mM KCl and 6 mM $MgCl_2$ with 320 nM P/T substrate. The reaction was initiated by

the addition of 50 nM PR-RT. Aliquots were removed at different time points and analyzed by electrophoresis on a 15% polyacrylamide sequencing gel. Products were visualized by fluorescence emission at 670 nm upon excitation at 633 nm using a fluorescence laser scanner (FLA 3000, raytest, Straubenhardt, Germany).

Abbreviations

CD: circular dichroism; *E. coli*: *Escherichia coli*; 6-FAM: 6-carboxy-fluorescein; GB1: immunoglobulin binding domain B1 of streptococcal protein G; GFP: green fluorescent protein; HIV-1: human immunodeficiency virus type 1; IPTG: isopropyl-thiogalactoside; LTR: long terminal repeat; MuLV: murine leukemia virus; PMF: peptide mass fingerprint; PFV: prototype foamy virus; SFVmac: simian foamy virus from macaques.

Acknowledgements

The project was funded by the Deutsche Forschungsgemeinschaft DFG (Re627/8-1, SFB 479, Wo630/7-3), the Graduate School in the Elite Network of Bavaria "Lead Structures of Cell Functions" and the University of Bayreuth.

Author details

[1]Universität Bayreuth, Lehrstuhl für Struktur und Chemie der Biopolymere & Research, Center for Biomacromolecules, 95440 Bayreuth, Germany. [2]Universität Würzburg, Institut für Virologie und Immunbiologie, 97078 Würzburg, Germany.

Authors' contributions

BMW conceived and coordinated the study. MJH and FM performed the experiments, AR provided reagents and participated in designing the experiments. BMW and MJH wrote the paper. All authors read and approved the manuscript.

Competing interests

The authors declare that they have no competing interests.

Received: 30 September 2009
Accepted: 29 January 2010 Published: 29 January 2010

References

1. Moebes A, Enssle J, Bieniasz PD, Heinkelein M, Lindemann D, Bock M, McClure MO, Rethwilm A: **Human foamy virus reverse transcription that occurs late in the viral replication cycle.** *J Virol* 1997, **71**:7305-7311.
2. Yu SF, Sullivan MD, Linial ML: **Evidence that the human foamy virus genome is DNA.** *J Virol* 1999, **73**:1565-1572.
3. Enssle J, Jordan I, Mauer B, Rethwilm A: **Foamy virus reverse transcriptase is expressed independently from the gag protein.** *Proc Natl Acad Sci USA* 1996, **93**:4137-4141.
4. Jordan I, Enssle J, Guttler E, Mauer B, Rethwilm A: **Expression of human foamy virus reverse transcriptase involves a spliced pol mRNA.** *Virology* 1996, **224**:314-319.
5. Löchelt M, Flügel RM: **The human foamy virus pol gene is expressed as a pro-pol polyprotein and not as a gag-pol fusion protein.** *J Virol* 1996, **70**:1033-1040.
6. Pfrepper KI, Rackwitz HR, Schnölzer M, Heid H, Löchelt M, Flügel RM: **Molecular characterization of proteolytic processing of the pol proteins of human foamy virus reveals novel features of the viral protease.** *J Virol* 1998, **72**:7648-7652.
7. Roy J, Linial ML: **Role of the foamy virus pol cleavage site in viral replication.** *J Virol* 2007, **81**:4956-4962.
8. Linial M: **Foamy viruses.** *Fields Virology* Lippincott Williams & Wilkins, PhiladelphiaKnipe DM, Howley PM 2007, 2245-2262.
9. Rethwilm A: **Foamy viruses.** *Topley & Wilson's Microbiology and Microbial Infections - Virology* London:Hodder Arnoldter Meulen V, Mahy BWJ 2005, 1304-1321.
10. Boyer PL, Stenbak CR, Clark PK, Linial ML, Hughes SH: **Characterization of the polymerase and RNase H activities of human foamy virus reverse transcriptase.** *J Virol* 2004, **78**:6112-6121.
11. Rinke CS, Boyer PL, Sullivan MD, Hughes SH, Linial ML: **Mutation of the catalytic domain of the foamy virus reverse transcriptase leads to loss of processivity and infectivity.** *J Virol* 2002, **76**:7560-7570.
12. Kögel D, Aboud M, Flügel RM: **Molecular biological characterization of the human foamy virus reverse transcriptase and ribonuclease H domains.** *Virology* 1995, **213**:97-108.
13. Kögel D, Aboud M, Flügel RM: **Mutational analysis of the reverse transcriptase and ribonuclease H domains of the human foamy virus.** *Nucleic Acids Res* 1995, **23**:2621-2625.
14. Hartl MJ, Kretzschmar B, Frohn A, Nowrouzi A, Rethwilm A, Wöhrl BM: **AZT resistance of simian foamy virus reverse transcriptase is based on the excision of AZTMP in the presence of ATP.** *Nucleic Acids Res* 2008, **36**:1009-1016.
15. Hartl MJ, Wöhrl BM, Rösch P, Schweimer K: **The solution structure of the simian foamy virus protease reveals a monomeric protein.** *J Mol Biol* 2008, **381**:141-149.
16. Boyer PL, Stenbak CR, Hoberman D, Linial ML, Hughes SH: **In vitro fidelity of the prototype primate foamy virus (PFV) RT compared to HIV-1 RT.** *Virology* 2007, **367**:253-264.
17. Peters K, Wiktorowicz T, Heinkelein M, Rethwilm A: **RNA and protein requirements for incorporation of the pol protein into foamy virus particles.** *J Virol* 2005, **79**:7005-7013.
18. Rosenblum LL, Patton G, Grigg AR, Frater AJ, Cain D, Erlwein O, Hill CL, Clarke JR, McClure MO: **Differential susceptibility of retroviruses to nucleoside analogues.** *Antivir Chem Chemother* 2001, **12**:91-97.
19. Lee CC, Ye F, Tarantal AF: **Comparison of growth and differentiation of fetal and adult rhesus monkey mesenchymal stem cells.** *Stem Cells Dev* 2006, **15**:209-220.
20. Kretzschmar B, Nowrouzi A, Hartl MJ, Gartner K, Wiktorowicz T, Herchenröder O, Kanzler S, Rudolph W, Mergia A, Wöhrl B, Rethwilm A: **AZT-resistant foamy virus.** *Virology* 2008, **370**:151-157.
21. Meyer PR, Matsuura SE, Mian AM, So AG, Scott WA: **A mechanism of AZT resistance: An increase in nucleotide-dependent primer unblocking by mutant HIV-1 reverse transcriptase.** *Mol Cell* 1999, **4**:35-43.
22. Meyer PR, Matsuura SE, So AG, Scott WA: **Unblocking of chain-terminated primer by HIV-1 reverse transcriptase through a nucleotide-dependent mechanism.** *Proc Natl Acad Sci USA* 1998, **95**:13471-13476.
23. Dunn BM, Goodenow MM, Gustchina A, Wlodawer A: **Retroviral proteases.** *Genome Biol* 2002, **3**:1465-6914.
24. Benzair AB, Rhodes-Feuillette A, Emanoil-Ravicovitch R, Peries J: **Reverse transcriptase from simian foamy virus serotype 1: Purification and characterization.** *J Virol* 1982, **44**:720-724.
25. Wlodawer A, Gustchina A: **Structural and biochemical studies of retroviral proteases.** *Biochim Biophys Acta* 2000, **1477**:16-34.
26. Wlodawer A, Miller M, Jaskolski M, Sathyanarayana BK, Baldwin E, Weber IT, Selk LM, Clawson L, Schneider J, Kent SB: **Conserved folding in retroviral proteases: Crystal structure of a synthetic HIV-1 protease.** *Science* 1989, **245**:616-621.
27. Tang C, Louis JM, Aniana A, Suh JY, Clore GM: **Visualizing transient events in amino-terminal autoprocessing of HIV-1 protease.** *Nature* 2008, **455**:693-696.
28. Martin JL, Wilson JE, Haynes RL, Furman PA: **Mechanism of resistance of human immunodeficiency virus type 1 to 2',3'-dideoxyinosine.** *Proc Natl Acad Sci USA* 1993, **90**:6135-6139.
29. Ueno T, Shirasaka T, Mitsuya H: **Enzymatic characterization of human immunodeficiency virus type 1 reverse transcriptase resistant to multiple 2',3'-dideoxynucleoside 5'-triphosphates.** *J Biol Chem* 1995, **270**:23605-23611.
30. Wilson JE, Aulabaugh A, Caligan B, McPherson S, Wakefield JK, Jablonski S, Morrow CD, Reardon JE, Furman PA: **Human immunodeficiency virus type-1 reverse transcriptase. contribution of met-184 to binding of nucleoside 5'-triphosphate.** *J Biol Chem* 1996, **271**:13656-13662.
31. Santos-Velazquez J, Kim B: **Deoxynucleoside triphosphate incorporation mechanism of foamy virus (FV) reverse transcriptase: Implications for cell tropism of FV.** *J Virol* 2008, **82**:8235-8238.
32. Krebs R, Immendörfer U, Thrall S, Wöhrl BM, Goody RS: **Single-step kinetics of HIV-reverse transcriptase mutants responsible for virus resistance to nucleoside inhibitors zidovudine and 3TC.** *Biochemistry (N Y)* 1997, **36**:10292-10300.
33. Wöhrl BM, Krebs R, Thrall SH, Le Grice SFJ, Scheidig AJ, Goody RS: **Kinetic analysis of four HIV-1 reverse transcriptase enzymes mutated in the**

primer grip region of p66. implications for DNA synthesis and dimerization. *J Biol Chem* 1997, **272**:17581-17587.
34. Gorshkova II, Rausch JW, Le Grice SF, Crouch RJ: **HIV-1 reverse transcriptase interaction with model RNA-DNA duplexes.** *Anal Biochem* 2001, **291**:198-206.
35. Parniak MA, Min KL, Budihas SR, Le Grice SF, Beutler JA: **A fluorescence-based high-throughput screening assay for inhibitors of human immunodeficiency virus-1 reverse transcriptase-associated ribonuclease H activity.** *Anal Biochem* 2003, **322**:33-39.
36. Rizzo J, Gifford LK, Zhang X, Gewirtz AM, Lu P: **Chimeric RNA-DNA molecular beacon assay for ribonuclease H activity.** *Mol Cell Probes* 2002, **16**:277-283.
37. Werner S, Wöhrl BM: **Soluble rous sarcoma virus reverse transcriptases α, αβ and β; purified from insect cells are processive DNA polymerases that lack an RNase H 3' > 5' directed processing activity.** *J Biol Chem* 1999, **274**:26329-26336.
38. Furfine ES, Reardon JE: **Reverse transcriptase.RNase H from the human immunodeficiency virus. relationship of the DNA polymerase and RNA hydrolysis activities.** *J Biol Chem* 1991, **266**:406-412.
39. Gopalakrishnan V, Peliska JA, Benkovic SJ: **Human immunodeficiency virus type 1 reverse transcriptase: Spatial and temporal relationship between the polymerase and RNase H activities.** *Proc Natl Acad Sci USA* 1992, **89**:10763-10767.
40. DeStefano JJ, Mallaber LM, Fay PJ, Bambara RA: **Quantitative analysis of RNA cleavage during RNA-directed DNA synthesis by human immunodeficiency and avian myeloblastosis virus reverse transcriptases.** *Nucleic Acids Res* 1994, **22**:3793-3800.
41. Schatz O, Mous J, Le Grice SFJ: **HIV-1 RT associated ribonuclease H displays both endonuclease and 3'-> 5' exonuclease activities.** *EMBO J* 1990, **9**:1171-1176.
42. Wöhrl BM, Moelling K: **Interaction of HIV-1 ribonuclease H with polypurine tract containing RNA-DNA hybrids.** *Biochemistry (N Y)* 1990, **29**:10141-10147.
43. Jacobo-Molina A, Ding J, Nanni RG, Clark AD Jr, Lu X, Tantillo C, Williams RL, Kamer G, Ferris AL, Clark P, Hizi A, Hughes SH, Arnold E: **Crystal structure of human immunodeficiency virus type 1 reverse transcriptase complexed with double-stranded DNA at 3.0 A resolution shows bent DNA.** *Proc Natl Acad Sci USA* 1993, **90**:6320-6324.
44. Jacobo-Molina A, Clark AD Jr, Williams RL, Nanni RG, Clark P, Ferris AL, Hughes SH, Arnold E: **Crystals of a ternary complex of human immunodeficiency virus type 1 reverse transcriptase with a monoclonal fab fragment and double stranded DNA diffract to 3.5 Å resolution.** *Proc Natl Acad Sci USA* 1992, **88**:10895-10899.
45. Boyer PL, Stenbak CR, Clark PK, Linial ML, Hughes SH: **Characterization of the polymerase and RNase H activities of human foamy virus reverse transcriptase.** *J Virol* 2004, **78**:6112-6121.
46. Cole PA: **Chaperone-assisted protein expression.** *Structure* 1996, **4**:239-242.

doi:10.1186/1742-4690-7-5
Cite this article as: Hartl *et al.*: Biophysical and enzymatic properties of the simian and prototype foamy virus reverse transcriptases. *Retrovirology* 2010 **7**:5.

8 Publication B

Benedikt Kretzschmar*, Ali Nowrouzi*, Maximilian J. Hartl, Kathleen Gärtner, Tatiana Wiktorowicz, Ottmar Herchenröder, Sylvia Kanzler, Wolfram Rudolph, Ayalew Mergia, Birgitta M. Wöhrl and Axel Rethwilm (2007): AZT-resistant foamy virus. *Virology* **370**, 151-157.

* both authors contributed equally to this study

Available online at www.sciencedirect.com
ScienceDirect
Virology 370 (2008) 151–157
VIROLOGY
www.elsevier.com/locate/yviro

AZT-resistant foamy virus

Benedikt Kretzschmar [a,2], Ali Nowrouzi [a,2], Maximilian J. Hartl [b], Kathleen Gärtner [a], Tatiana Wiktorowicz [a], Ottmar Herchenröder [c,1], Sylvia Kanzler [c], Wolfram Rudolph [c], Ayalew Mergia [d], Birgitta Wöhrl [b], Axel Rethwilm [a,*]

[a] *Universität Würzburg, Institut für Virologie und Immunbiologie, Versbacher Str. 7, 97078 Würzburg, Germany*
[b] *Universität Bayreuth, Lehrstuhl Biopolymere, Bayreuth, Germany*
[c] *Technische Universität Dresden, Medizinische Fakultät "Carl Gustav Carus," Institut für Virologie, Dresden, Germany*
[d] *Department of Infectious Disease and Pathology, College of Veterinary Medicine, University of Florida, Gainesville, FL, USA*

Received 27 June 2007; returned to author for revision 25 July 2007; accepted 21 August 2007
Available online 27 September 2007

Abstract

Azidothymidine (AZT) is a reverse transcriptase (RT) inhibitor that efficiently blocks the replication of spumaretroviruses or foamy viruses (FVs). To more precisely elucidate the mechanism of action of the FV RT enzyme, we generated an AZT-resistant FV in cell culture. Biologically resistant virus was obtained for simian foamy virus from macaque (SFVmac), which was insensitive to AZT concentrations of 1 mM, but not for FVs derived from chimpanzees. Nucleotide sequencing revealed four non-silent mutations in the *pol* gene. Introduction of these mutations into an infectious molecular clone identified all changes to be required for the fully AZT-resistant phenotype of SFVmac. The alteration of individual sites showed that AZT resistance in SFVmac was likely acquired by consecutive acquisition of *pol* mutations in a defined order, because some alterations on their own did not result in an efficiently replicating virus, neither in the presence nor in the absence of AZT. The introduction of the mutations into the RT of the closely related prototypic FV (PFV) did not yield an AZT-resistant virus, instead they significantly impaired the viral fitness.

Keywords: Foamy virus; Reverse transcriptase; AZT resistance

Introduction

Foamy viruses (FVs) constitute one of two subfamilies of retroviruses and follow a unique replication pathway (for reviews, see Linial, 2007; Rethwilm, 2003, 2005). Aside from early studies the comparative analysis of the replication strategy between spuma- and orthoretroviruses has only recently focused on the biochemistry of the RT enzyme (Benzair et al., 1982, 1983; Boyer et al., in press, 2004; Kögel et al., 1995a,b; Liu et al., 1977; Rinke et al., 2002). Although the characterization of bacterially expressed PFV RT revealed many features common to all retroviruses (Boyer et al., in press, 2004; Kögel et al., 1995a,b), it was also shown that PFV RT is much more processive than orthoretroviral enzymes (Rinke et al., 2002). Furthermore, mutation of the active center of the PFV RT from YVDD to YMDD did not result in sensitivity to the antiretroviral drug 3TC, as in human immunodeficiency virus (HIV), but rendered the virus replication-deficient (Rinke et al., 2002). These studies indicated that there are similarities and differences in the biochemistry of the RT enzymes between orthoretroviruses and foamy viruses.

A major difference between ortho- and spumaretroviral RT enzymes consists in the nature of the precursor and the definite cleavage products of the Pol protein. While in orthoretroviruses, the enzymatic proteins are cleaved from a Gag-protease (PR)-Pol precursor into PR, RT/RNaseH, and integrase (IN), FV Pol cleavage products are processed from an authentic PR-Pol precursor and cleavage between the PR and RT/RNaseH subunits does not occur (for a review, see Linial and Eastman, 2003). Thus, the only observed end products of FV Pol precursor cleavage are the 85-kDa PR-RT/RNaseH and the 40-kDa IN

* Corresponding author. Fax: +49 931 201 49553.
E-mail address: virologie@mail.uni-wuerzburg.de (A. Rethwilm).
[1] Present address: Universität Rostock, Institut für Virologie, Rostock, Germany.
[2] B.K. and A.N. contributed equally to this study.

0042-6822/$ - see front matter © 2007 Elsevier Inc. All rights reserved.
doi:10.1016/j.virol.2007.08.025

Table 1
Comparison of biologically selected AZT-resistant virus with molecularly cloned derivatives*

Virus	D3	D6	D9	D12	D15	D18
SK29-KISE −AZT	+	+++	++++	c.d.	n.d.	n.d.
SFVAZTres −AZT	+	+++	++++	c.d.	n.d.	n.d.
BK03QR-ITTK −AZT	+	+++	++++	c.d.	n.d.	n.d.
BK04RG-ITTK −AZT	+	+++	++++	c.d.	n.d.	n.d.
SK29-KISE +AZT	(+)	(+)	(+)	–	–	–
SFVAZTres +AZT	+	+	+	++	+++	++++
BK03QR-ITTK +AZT	+	+	+	++	+++	++++
BK04RG-ITTK +AZT	+	+	+	++	+++	++++

*10^5 BHK/LTR(SFVmac)lacZ cells were infected at a multiplicity of infection (MOI) of 0.001 with the respective viruses either in the absence (−AZT) or presence (+AZT) of 50 μM AZT. The cultures were stained for blue cells at the indicated days after infection and the replication of virus was monitored. (+), <1% infected cells; +, 1–10% infected cells; ++, 10–25% of cells were infected; +++, 25–50% infected cells; ++++, more than 50% of the cell culture was infected; c.d., cell culture was destroyed; n.d., not done. SK29-KISE is the wild-type molecular clone-derived virus, SFVAZTres is the biologically selected AZT-resistant virus, BK03QR-ITTK and BK04RG-ITTK are viruses derived from molecular clones containing the two *gag* and four *pol* or only the four *pol* gene mutations, respectively.

(Flügel and Pfrepper, 2003). This structural feature of FV RT enzymes probably has an impact on the function that has not been elucidated in detail yet.

In addition to tenofovir, AZT (zidovudine) is the only RT-inhibiting drug, which is active against FVs and completely inhibits PFV replication in cell culture at a concentration as low as 5 μM (Lee et al., 2006; Moebes et al., 1997; Rosenblum et al., 2001). Since the understanding of the biochemistry of the FV RT would greatly profit from the characterization of an AZT-resistant variant and the understanding of the mechanism of AZT resistance in orthoretroviruses, namely, human immunodeficiency virus (HIV), would mutually profit from studying a distantly related virus, we attempted to generate and characterize AZT-resistant FVs.

Furthermore, based on homology predictions of the PFV and HIV RT enzyme structures, AZT resistance in PFV has been suggested to occur by alteration of certain residues that are known to confer AZT resistance to HIV-1 (Yvon-Groussin et al., 2001). We also wanted to investigate this possibility because experimental evidence for this theory does not exist.

Results

Generation of biologically AZT-resistant FV

To obtain AZT-resistant viruses we cultivated plasmid-derived PFV, the chimpanzee FV isolate (SFVcpz), and SFVmac virus stocks on the appropriate indicator cells and gradually raised the AZT concentration. Although we were successful in obtaining an SFVmac variant (SFVAZTres) that was able to replicate in medium containing 1 mM AZT, several attempts to similarly generate PFV or SFVcpz variants failed (data not shown).

Genotypic analysis of AZT-resistant SFVmac

The *gag* and *pol* genes of SFVAZTres were amplified by PCR and subjected to nucleotide sequence analysis. In comparison with the full-length SFVmac sequence, which was assembled from subgenomic SFVmac molecular clones (Genbank accession numbers: X58484 and M33561; see Mergia et al., 1990a,b), six nucleotide alterations leading to amino acid changes were found. Two of the changes were located in the *gag* open reading frame (ORF) and involved $R535^{gag}$ and $G596^{gag}$, which were changed to Q and R, respectively. The presence of these *gag* mutations in the parental infectious SFVmac clone together with the *pol* mutations (as in pBK03QR-ITTK) did not influence the AZT susceptibility compared with an SFVmac clone having only the *pol* residues mutated (as in pBK04RG-ITTK) (Table 1). We therefore regarded the Gag ORF alterations as irrelevant for conferring AZT resistance and did not analyze them further.

Four point mutations involving residues 211 (K211I), 224 (I224T), 345 (S345T), and 350 (E350K) were detected in *pol* (Fig. 1). On the nucleic acid level, all alterations leading to these amino acid changes required only the mutation of single nucleotides. The mutations identified were at codon 211 from AAA to ATA, at codon 224 from ATT to ACT, at codon 345 from TCA to ACA, and at codon 350 from GAA to AAA. One published complete genomic sequence of SFVmac already harbors a threonine at position 224 of the Pol protein (Kupiec et al., 1991). 224T would be more consistent with the other primate FV Pol proteins, which all harbor a threonine in this position (Fig. 1).

```
            144      209                                312
SFVmac      QVG...DGKWRMVLDYREVNKIIPLIAA...YVDDIYISHDDPQEHLEQLEKIFSILLNAGYVVSLKKSEIAQREVEF
SFVres      QVG...DGIWRMVLDYREVNKTIPLIAA...YVDDIYISHDDPQEHLEQLEKIFSILLNAGYVVTLKKSKIAQREVEF
PFV         QVG...DGRWRHVLDYREVHKTIPLTAA...YVDDIYLSHDDPKEHVQQLEKVFQILLQAGYVVSLKKSETGQKTVEF
SFVcpz      QVG...DGRWKHVLDYREVHKTIPLTAA...YVDDIYLSHDNPHEHIQQLEKVFQILLQAGYVVSLKKSETGQKTVEF
SFVora      QVG...DGRWRMVLDYREVNKTIPLIAA...YVDDLYLSHDDPQEHLQVLQQVLHILHDAGYVVSLKKSAIAQKVVEF
SFVagm      QVG...DGKWRHVIDYREVHKTIPLIAA...YVDDIYISHDDPREHLEQLEKVFSLLLNAGYVVSLKKSEIAQHEVEF
FFV         QVG...HGRWRHVIDYRAVNKVTPLIAV...YVDDVYISHDSEKEHLEYLDILFNRLKEAFYIVSLKKSNIANSTVDF
BFV         QVG...DGRWRHVIDYREVHKVTPLVAT...YVDDVYVSSATEQEHLDILETIFNRLSTAGYIVSLKKSKLAKETVEF
EFV         QVG...DGRWRMVLDYRAVNKVTPAIAT...YVDDVYFSNDTEEEHLKTMDLLFQKLQTAGYIVSLKKSKLGQHTVDF
```

Fig. 1. Homology of Pol proteins of different FV and HIV-1. The RT regions of known FVs relevant to this study were aligned using the Genbank accession numbers for SFVmac (X58484 and M33561), PFV (Y07725), the chimpanzee isolate SFVcpz (U04327), orangutan FV (SFVora; AJ544579), African green monkey virus (SFVagm; M74895), FV from felines (FFV: AJ564746), bovines (BFV; U94514) and equines (EFV; AF20190).

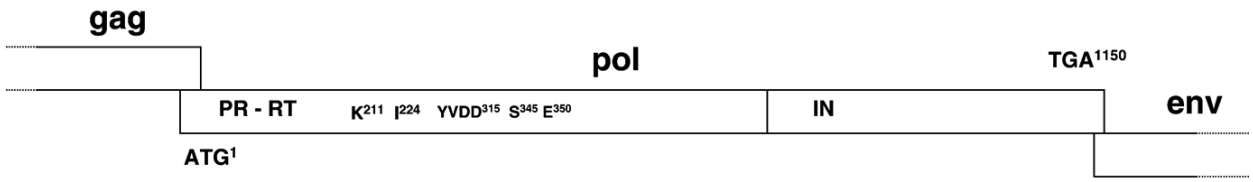

Virus	211pol	224pol	345pol	350pol	AZT-resistance
SK29-KISE	K	I	S	E	-
BK04-ITTK	I	T	T	K	++++
BK30-IISE	I	I	S	E	-
BK65-KTSE	K	T	S	E	(+)
SK50-KITE	K	I	T	E	+
SK51-KISK	K	I	S	K	(+)
BK81-ITSE	I	T	S	E	-
BK38-IITE	I	I	T	E	-
BK31-IISK	I	I	S	K	-
BK78-KTTE	K	T	T	T	++
BK76-KTSK	K	T	S	K	+
SK39-KITK	K	I	T	K	++
BK80-ITTE	I	T	T	E	+
BK77-ITSK	I	T	S	K	+
BK37-IITK	I	I	T	K	+
BK79-KTTK	K	T	T	K	+++
BK64-ITTK	I	T	T	K	++++

Fig. 2. Genome organization of the wild-type and mutant FV Pol open reading frames. The *pol* gene of SFVmac is shown in the upper panel with the relative location of the RT active center and the four amino acid residues associated with AZT resistance. The SFVmac mutants representing all possible combinations of the four mutations are shown in the lower panel together with the approximate levels of AZT resistance deduced from Table 2. The plasmids pBK04-ITTK and pBK64-ITTK are identical. Plasmid pBK04-ITTK was made by exchanging a *pol* gene fragment containing the four mutations and amplified from DNA of cell cultures infected with SFVAZTres for a corresponding fragment of pSK29-KISE and pBK64-ITTK was made by *in vitro* mutagenesis. M108 is a PFV mutant with the changed residues found in SFVAZTres.

However, the parental molecular clones pSFV-1 and pSK29-KISE code for an isoleucine at this position. Thus, the wild-type SFVmac may have a polymorphism at this site. Because we found I224T in SFVAZTres, we considered I224T as a mutation associated with AZT resistance.

Biologically selected SFVAZTres was compared with the parental virus and the virus derived from transfection of cells with molecular cloned variants bearing all four *pol* gene mutations. We observed only slight differences in the development of cell-free virus titers between the molecularly cloned and uncloned resistant viruses in the absence or presence of AZT (Table 1). This indicated that the four mutations identified in *pol* are sufficient to confer AZT resistance to SFVmac.

Analysis of reconstituted SFVmac molecular clones

To investigate which of the *pol* gene mutations was responsible for the resistant phenotype of SFVmac, we generated a series of full-length molecular clones in which all possible combinations of the four mutations found in SFVAZTres were represented (Fig. 2).

To analyze whether the introduced mutations affected the stability or other properties of SFVmac Pol protein, we first investigated the protein expression following transient transfection of 293T cells with the recombinant plasmids in cellular lysates. As shown in Fig. 3, all mutants were able to express Gag and Pol proteins to approximately the same level as non-mutant virus.

AZT resistance of SFVmac mutants

After demonstrating that the altered Pol proteins are efficiently expressed 293T cells were transfected with the parental molecular clone or the variants shown in Fig. 2 and analyzed on the appropriate indicator cells. Due to the peculiar replication strategy of FVs, namely, reverse transcription taking

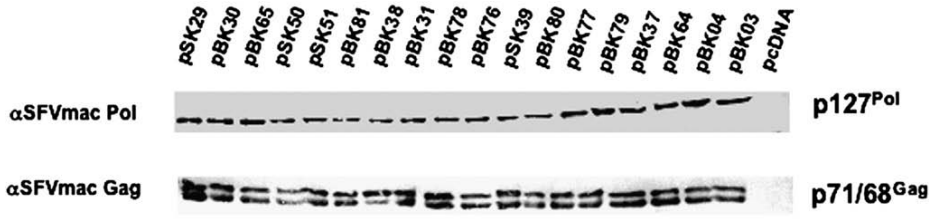

Fig. 3. SFVmac protein expression. The expression of Gag (pr71/p68) and Pol (pr127) proteins was analyzed by immunoblot with polyclonal rabbit antisera in lysates from cells transfected with the indicated plasmids.

Table 2
AZT-sensitivity of mutant viruses*

Virus	0.0 μM	0.5 μM	5.0 μM	50 μM
SK29-KISE	100%	0.7±0.5%	<0.1%	<0.1%
BK04-ITTK	117.0±18.4%	84.3±27.8%	71.0±12.7%	34.9±12.9%
BK30-IISE	1.2±1.2%	<0.1%	<0.1%	<0.1%
BK65KTSE	146.5±21.4%	1.2±0.9%	<0.1%	<0.1%
SK50-KITE	40.0±16.8%	5.6±3.2%	1.1±1.0%	<0.1%
SK51-KISK	31.7±8.8%	1.8±0.8%	<0.1%	<0.1%
BK81-ITSE	2.5±0.6%	<0.1%	<0.1%	<0.1%
BK38-IITE	<0.1%	<0.1%	<0.1%	<0.1%
BK31-IISK	23.0±7.9%	0.6±0.5%	<0.1%	<0.1%
BK78-KTTE	86.7±20.5%	18.7±12.9%	0.5±0.3%	<0.1%
BK76-KTSK	175.5±33.9%	8.1±4.5%	<0.1%	<0.1%
SK39-KITK	20.6±5.5%	10.8±7.5%	3.0±2.1%	1.0±0.6%
BK80-ITTE	7.3±3.6%	4.0±2.7%	1.0±0.8%	0.3±0.2%
BK77-ITSK	33.6±11.3%	3.8±3.0%	0.9±0.5%	<0.1%
BK37-IITK	8.6±2.7%	5.9±3.0%	2.8±1.3%	2.0±0.8%
BK79-KTTK	138.2±21.8%	86.9±11.5%	16.4±10.9%	1.4±0.4%
BK64-ITTK	113.0±19.2%	79.3±20.1%	68.8±18.8%	31.3±20.6%
HSRV2	100%	1.1±0.9%	0.4±0.1%	<0.1%
M108	1.3±0.1%	0.5±0.1%	0.4±0.1%	<0.1%

*293T cells were transiently transfected with 10 μg plasmid DNA either in the absence or presence of the concentrations of AZT indicated. The viral titers in the cell-free supernatants were determined on the appropriate indicator cells and are expressed as values relative to SK29-KISE (for SFVmac mutants) or HSRV2 (for the PFV mutant) in the absence of AZT and arbitrarily set to 100%. This corresponded to cell-free titers of 7×10^4 in the case of SFVmac and 6.3×10^4 for PFV.

place already in virus producing cells (Moebes et al., 1997; Yu et al., 1999), the production of virus after transfection of cells and the analysis of cell-free viral titers were performed in the absence or presence of AZT. As shown in Table 2, we observed pronounced differences in the replication competence of the various mutants that argue for a sequential acquisition of SFVmac *pol* gene mutations for replication in the presence of AZT.

The BK38-IITE virus, for instance, which bears the two mutations leading to K211I and S345T, did not replicate either in the absence or presence of AZT. Replication was also severely limited in the BK30-IISE, BK31-IITK, and BK81-ITSE viruses, whereas BK37-IISK, BK77-ITSK, BK80-ITTE, SK39-KITK, and SK51-KISK were moderately impaired to replicate irrespective of the AZT concentrations. All these mutants have K211 changed to isoleucine in various combinations (the BK viruses) or E350 modified to lysine (the SK viruses). It is therefore unlikely that either of these changes occurred first under drug selection. The only single mutation that was found to result in a moderate drug resistance was that leading to S345T (SK50-KITE). While conferring partial AZT resistance, this mutation weakened the virus to replicate in its absence (Table 2). Subsequent acquisition of I224T, in addition to S345T (BK78-KTTE), resulted in an enhancement of viral fitness and replication predominantly at low AZT concentration.

Alternatively, threonine may be the natural residue at position 224 in wild-type SFVmac (as discussed above), in which case the BK78-KTTE virus would be the first variant to emerge during AZT-induced selective pressure. Since the K211I variant greatly decreased replication, if it occurred before E350K (BK80-ITTE in Table 2), BK79-KTTK was probably the next virus to emerge. BK79-KTTK was able to replicate at 5 μM AZT and strongly enhanced replication without the drug. Finally, the resistant virus acquired the mutation leading to K211I in addition to I224T, S345T, and E350K (BK64-ITTK). Compared to BK79-KTTK the replication ability of BK64-ITTK in the absence of AZT was slightly reduced, however, it was greatly enhanced at higher drug concentrations (Table 2).

Attempts to create an AZT-resistant PFV

The introduction of the mutations leading to R211I, S345T, and E350K in M108 of PFV (residue 224 is already a threonine; see Fig. 1) did not lead to AZT resistance and, compared to the parental virus (HSRV2), severely reduced the viral fitness in the absence of AZT (Table 2). However, we cannot formally exclude the possibility that only one or two alterations of these residues might induce AZT resistance to PFV, although we regard this as very unlikely.

Discussion

The results shown here suggest that AZT resistance in SFVmac was acquired by sequential acquisition of mutations in the *pol* gene in the order: wild-type virus ->S345T ->I224T ->E350K ->K211I (Fig. 4). However, alternative scenarios are also possible, although less likely. In particular, the position in the order of events of the mutation leading to I224T appears variable (see above). The fully resistant virus was found to be able to replicate at 1 mM AZT. As shown in Table 2 the BK64-

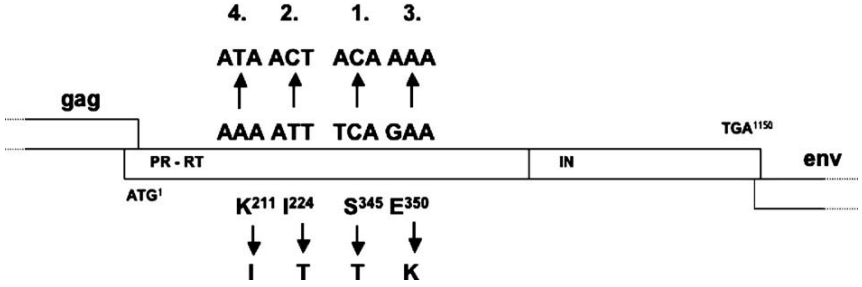

Fig. 4. Most likely order of mutagenic events resulting in AZT-resistant SFVmac.

ITTK virus replicated only to approximately one-third the level of wild-type virus. Thus, the acquisition of the mutations leading to drug resistance was accompanied by a moderate reduction of viral fitness.

The inability to obtain AZT-resistant PFV or chimpanzee foamy virus by gradually raising the drug concentration in the cell culture medium was surprising. Because SFVmac and PFV derived from our molecular clones replicate to approximately the same extracellular viral titers (Table 2), we regard it very unlikely that significant differences in the replication kinetics between the two parental viruses are responsible for our futile attempts in generating biologically drug-resistant PFV. Both viruses, SFVmac and PFV, have been amplified in cell culture for years. Although FVs are known to be genetically extremely stable (Switzer et al., 2005; Thümer et al., 2007), the cell culture-adapted virus does not necessarily reflect the wild-type situation. However, SFVcpz was molecular cloned approximately 1 month after virus isolation (Herchenröder et al., 1994, 1995). This questions significant changes in the FV RT sequence upon cell culture replication and points to differences between SFVmac and FVs of the higher primates in the ability to respond to AZT drug selection.

In addition, the introduction of the mutations conferring AZT resistance to SFVmac into the infectious PFV molecular clone also did not result in a drug-resistant virus. These mutations resulted in an approximately 70% reduction in viral fitness of SFVmac (Table 2). The reduction was much more substantial when the same mutations were introduced into PFV (Table 2). This may indicate that PFV is, *per se*, able to mutate into an AZT-resistant variant, but that the resistant virus lost the ability to replicate either in the presence or absence of AZT. The reason for this currently remains unknown. Answers may emerge when comparative biochemical analyses of PFV, SFVmac, and SFVAZTres RT enzymes and structural information become available.

In the HIV system, AZT resistance develops *in vivo* at least under the condition of monotherapy very quickly by consecutive mutations in the *pol* gene, while there exist only a few reports on cell culture selection of AZT-resistant HIV from wild-type virus (Dianzani et al., 1992; Gao et al., 1992; Kellam et al., 1994; Larder et al., 1991, 1989; Larder and Kemp, 1989; Smith et al., 1987). Nothing is known yet about the *in vivo* development of AZT resistance in FV infections. The biochemical and molecular bases of AZT resistance in HIV-1 and HIV-2 have been thoroughly studied. In each virus, a different mechanism dominates in the acquisition of AZT drug resistance (Boyer et al., 2006). Although HIV-1 preferentially excises AZT from the growing DNA chain, resistant HIV-2 was reported to discriminate between the inhibitor AZTTP and TTP during incorporation (Boyer et al., 2006). Thus, even closely related viruses can make use of different strategies to develop drug resistance. The homology between HIV-1 and HIV-2 RTs is around 60% (Boyer et al., 2006), while it is approximately 90% for PFV and SFVmac (Kupiec et al., 1991). Therefore, only subtle differences in the primary amino acid composition of SFVmac and PFV RT enzymes are responsible for the inability to generate an AZT-resistant PFV.

The analyses of FV RT enzymes revealed similarities with as well as differences to orthoretroviral RT enzymes. Our study shows that differences even exist within the rather homogenous FV subfamily of retroviruses. In this respect, it would be interesting to know whether the conversion of the active center of the FV RT enzyme from YVDD to YMDD, which led to a replication-deficient PFV (Rinke et al., 2002), would be tolerated by SFVmac.

Furthermore, our results do not indicate that the residues actually involved in FV AZT resistance, are those thought previously (Yvon-Groussin et al., 2001). In particular, the residues I182, D209, V343, and K347 were modelled to be involved in PFV AZT resistance. The results presented here do not support this view, since (i) the residues identified to confer AZT resistance to SFVmac are different and (ii) AZT-resistant PFV or SFVcpz could not be generated at all.

Materials and methods

Cells and viruses

BHK/LTR(SFVmac)lacZ (Roy et al., 2003), BHK/LTR (PFV)lacZ (Schmidt and Rethwilm, 1995) indicator cells, and 293T cells (DuBridge et al., 1987) were cultivated as described (DuBridge et al., 1987; Roy et al., 2003; Schmidt and Rethwilm, 1995). After transient transfection of cells with the proviral plasmids pSFV-1 (Mergia and Wu, 1998), pcHSRV2 (Moebes et al., 1997), or pSFVcpz (Herchenröder et al., 1995) viruses were cultivated on the appropriate indicator cells which were stained for β-Gal as reported (Schmidt and Rethwilm, 1995). AZT (Glaxo) was added to the culture medium at the concentrations indicated in the figures and tables.

To determine the susceptibility to AZT, virus was produced by transient transfection (48 h) of 293T cells using calcium phosphate coprecipitation with 10 μg of plasmid DNA in the absence or presence of the drug (Moebes et al., 1997). Gene expression was induced using Na-butyrate at a final concentration of 10 mM for 8 h (Heinkelein et al., 1998). The virus titer in the cell-free supernatant was determined on indicator cells in the absence or presence of AZT as described (Moebes et al., 1997). All virus titrations were performed at least three times. Virus stocks derived from molecular clones were abbreviated with the plasmid name lacking the “p” or “pc”.

Molecular cloning

The plasmid pSK29-KISE was obtained by treatment of partially *Kpn*I-digested pSFV-1 (Mergia and Wu, 1998) with T4 polymerase. This eliminated the *Kpn*I restriction site in the polylinker of the vector backbone.

After amplification and nucleotide sequencing of the complete *gag* and *pol* genes of the biological resistant SFVmac, a 3.4-kb *Xho*I/*Eco*RI fragment harboring the region with the identified mutations was amplified and inserted into the full-length proviral clone via a subclone containing a 8.2 kb *Xba*I/*Kpn*I fragment. Mutations were introduced into the *Xho*I/*Eco*RI subclone by recombinant PCR following the method of Higuchi

(1990) and then introduced back into the full-length clone as described above. To ease the identification of amino acid changes in Gag and Pol, relevant residues are indicated after the plasmid name.

Because PFV already bears a threonine at position 224 of its *pol* gene (see below), we constructed a triple mutant (M108) of pcHSRV2 (Moebes et al., 1997) that contains R211I, S345T, and E350K. PFV *pol* gene mutagenesis was carried out by recombinant PCR (Higuchi, 1990) on a subcloned 1.83-kb *Pac*I/*Swa*I fragment of pcHSRV2 before reinsertion into the full-length molecular clone.

For exclusion of inadvertent nucleotide exchanges all PCR-generated fragments were sequenced on the level of the full-length molecular clones. A detailed description of primers used for mutagenesis, amplification, and sequencing can be found online at http://viminfo.virologie.uni-wuerzburg.de/onlinematerial/Kretzschmar.pdf.

The complete *gag* and *pol* open reading frames (ORFs) of SFVmac were amplified separately and inserted into the vectors pRSET-A (Invitrogen) and pET28c (Novagen), respectively. The pET28c-SFVpol plasmid was used to delete the integrase gene via PCR in order to obtain a PR-RT subclone. A protease active site mutant (D24A) was created thereof by overlap PCR and transformed into the *E. coli* strain Rosetta DE3 (Novagen) for expression and purification of a PR (D24A)-RT fusion protein. Bacterial proteins were induced and purified via the C-terminal 6xHis-tag as described (Imrich et al., 2000) and used to generate polyclonal rabbit antisera at a commercial facility.

Immunoblotting

After transfection of 293T cells with proviral constructs, Gag and Pol protein expression in intracellular lysates was analyzed by immunoblotting with the rabbit Gag and Pol antisera as described previously (Heinkelein et al., 1998; Imrich et al., 2000).

Acknowledgments

We thank the DFG (Re 627/7-1, Re 627/8-1, Wo 630/7-1, and SFB479) for financial support.

References

Benzair, A.B., Rhodes-Feuillette, A., Emanoil-Ravicovitch, R., Peries, J., 1982. Reverse transcriptase from simian foamy virus serotype 1: purification and characterization. J. Virol. 44, 720–724.

Benzair, A.B., Rhodes-Feuillette, A., Emanoil-Ravicovitch, R., Peries, J., 1983. Characterization of RNase H activity associated with reverse transcriptase in simian foamy virus type 1. J. Virol. 47, 249–252.

Boyer, P.L., Stenbak, C.R., Clark, P.K., Linial, M.L., Hughes, S.H., 2004. Characterization of the polymerase and RNase H activities of human foamy virus reverse transcriptase. J. Virol. 78, 6112–6121.

Boyer, P.L., Srafianos, S.G., Clark, P.K., Arnold, E., Hughes, S.H., 2006. Why do HIV-1 and HIV-2 use different pathways to develop AZT resistance? PLoS Pathog. 2, e10.

Boyer, P.L., Stenbak, C., Hoberman, D., Linial, M., Hughes, S.H., in press. Fidelity of the prototype primate foamy virus (PFV) RT compared to HIV-1 RT. Virology.

Dianzani, F., Antonelli, G., Turriziani, O., Dong, G., Capobianchi, M.R., Riva, E., 1992. In vitro selection of human immunodeficiency virus type 1 resistant to 3′-azido-3′-deoxythymidine. Antivir. Res. 18, 39–52.

DuBridge, R.B., Tang, P., Hsia, H.C., Leong, P.-M., Miller, J.H., Calos, M.P., 1987. Analysis of mutation in human cells by using Epstein–Barr virus shuttle system. Mol. Cell. Biol. 7, 379–387.

Flügel, R.M., Pfrepper, K.I., 2003. Proteolytic processing of foamy virus gag and pol proteins. Curr. Top. Microbiol. Immunol. 277, 63–88.

Gao, Q., Gu, Z., Parniak, M.A., Li, Y., Wainberg, M.A., 1992. In vitro selection of variants of human immunodeficiency virus type 1 resistant to 3′-azido-3′-deoxythymidine and 2′,3′-dideoxyinosine. J. Virol. 66, 12–19.

Heinkelein, M., Schmidt, M., Fischer, N., Moebes, A., Lindemann, D., Enssle, J., Rethwilm, A., 1998. Characterization of a *cis*-acting sequence in the Pol region required to transfer human foamy virus vectors. J. Virol. 72, 6307–6314.

Herchenröder, O., Renne, R., Loncar, D., Cobb, E.K., Murthy, K.K., Schneider, J., Mergia, A., Luciw, P.A., 1994. Isolation, cloning, and sequencing of simian foamy viruses from chimpanzees (SFVcpz): high homology to human foamy virus (HFV). Virology 201, 187–199.

Herchenröder, O., Turek, R., Neumann-Haefelin, D., Rethwilm, A., Schneider, J., 1995. Infectious proviral clones of chimpanzee foamy virus (SFVcpz) generated by long PCR reveal close functional relatedness to human foamy virus. Virology 214, 685–689.

Higuchi, R., 1990. Recombinant PCR. In: Innis, M.A., Gelfand, D.H., White, T.J. (Eds.), PCR Protocols, A Guide to Methods and Applications. Academic Press, San Diego, CA, pp. 177–183.

Imrich, H., Heinkelein, M., Herchenröder, O., Rethwilm, A., 2000. Primate foamy virus Pol proteins are imported into the nucleus. J. Gen. Virol. 81, 2941–2947.

Kellam, P., Boucher, C.A.B., Tijnagel, J.M.G.H., Larder, B.A., 1994. Zidovudine treatment results in the selection of human immunodeficiency virus type 1 variants whose genotypes confer increasing levels of drug resistance. J. Gen. Virol. 75, 341–351.

Kögel, D., Aboud, M., Flügel, R.M., 1995a. Molecular biological characterization of the human foamy virus reverse transcriptase and ribonuclease H domains. Virology 213, 97–108.

Kögel, D., Aboud, M., Flügel, R.M., 1995b. Mutational analysis of the reverse transcriptase and ribonuclease H domains of the human foamy virus. Nucleic Acids Res. 23, 2621–2625.

Kupiec, J.J., Kay, A., Hayat, M., Ravier, R., Peries, J., Galibert, F., 1991. Sequence analysis of the simian foamy virus type 1 genome. Gene 101, 185–194.

Larder, B.A., Kemp, S.D., 1989. Multiple mutations in HIV-1 reverse transcriptase confer high-level resistance to zidovudine (AZT). Science 246, 1155–1158.

Larder, B.A., Darby, G., Richman, D.D., 1989. HIV with reduced sensitivity to zidovudine (AZT) isolated during prolonged therapy. Science 243, 1731–1734.

Larder, B.A., Coates, K.E., Kemp, S.D., 1991. Zidovudine-resistant human immunodeficiency virus selected by passage in cell culture. J. Virol. 65, 5232–5236.

Lee, C.C., Ye, F., Tarantal, A.F., 2006. Comparison of growth and differentiation of fetal and adult rhesus monkey mesenchymal stem cells. Stem Cells Dev. 15, 209–220.

Linial, M., 2007. Foamy viruses, In: Knipe, D.M., Howley, P.M. (Eds.), 5th ed. Fields Virology, vol. 2. Lippincott Williams & Wilkins, Philadelphia, pp. 2245–2262.

Linial, M.L., Eastman, S.W., 2003. Particle assembly and genome packaging. Curr. Top. Microbiol. Immunol. 277, 89–110.

Liu, W.T., Natori, T., Chang, K.S., Wu, A.M., 1977. Reverse transcriptase of foamy virus. Purification of the enzymes and immunological identification. Arch. Virol. 55, 187–200.

Mergia, A., Wu, M., 1998. Characterization of provirus clones of simian foamy virus type 1. J. Virol. 72, 817–822.

Mergia, A., Shaw, K.E.S., Lackner, E., Luciw, P.A., 1990a. Relationship of the env genes and the endonuclease domain of the pol genes of simian foamy virus type 1 in human foamy virus. J. Virol. 64, 406–410.

Mergia, A., Shaw, K.E.S., Pratt-Lowe, E., Barry, P.A., Luciw, P.A., 1990b.

Simian foamy virus type 1 is a retrovirus which encodes a transcriptional transactivator. J. Virol. 64, 3598–3604.
Moebes, A., Enssle, J., Bieniasz, P.D., Heinkelein, M., Lindemann, D., Bock, M., McClure, M.O., Rethwilm, A., 1997. Human foamy virus reverse transcription that occurs late in the viral replication cycle. J. Virol. 71, 7305–7311.
Rethwilm, A., 2003. The replication strategy of foamy viruses. Curr. Top. Microbiol. Immunol. 277, 1–26.
Rethwilm, A., 2005. Foamy viruses, In: Mahy, B.W.J., ter Meulen, V. (Eds.), 10th ed. Topley & Wilson's Microbiology and Microbial Infections—Virology, vol. 2. Hodder Arnold, London, pp. 1304–1321.
Rinke, C.S., Boyer, P.L., Sullivan, M.D., Hughes, S.H., Linial, M.L., 2002. Mutation of the catalytic domain of the foamy virus reverse transcriptase leads to loss of processivity and infectivity. J. Virol. 76, 7560–7570.
Rosenblum, L.L., Patton, G., Grigg, A.R., Frater, A.J., Cain, D., Erlwein, O., Hill, C.L., Clarke, J.R., McClure, M.O., 2001. Differential susceptibility of retroviruses to nucleoside analogues. Antivir. Chem. Chemother. 12, 91–97.
Roy, J., Rudolph, W., Juretzek, T., Gärtner, K., Bock, M., Herchenröder, O., Lindemann, D., Heinkelein, M., Rethwilm, A., 2003. Feline foamy virus genome and replication strategy. J. Virol. 77, 11324–11331.
Schmidt, M., Rethwilm, A., 1995. Replicating foamy virus-based vectors directing high level expression of foreign genes. Virology 210, 167–178.
Smith, M.S., Brian, E.L., Pagano, J.S., 1987. Resumption of virus production after human immunodeficiency virus infection of T lymphocytes in the presence of azidothymidine. J. Virol. 61, 3769–3773.
Switzer, W.M., Salemi, M., Shanmugan, V., Gao, F., Cong, M., Kulken, C., Bhullar, V., Beer, B.E., Vallet, D., Gautler-Hlon, A., Tooze, Z., Villinger, F., Holmes, E.C., Heneine, W., 2005. Ancient co-speciation of simian foamy viruses and primates. Nature 434, 376–380.
Thümer, L., Rethwilm, A., Holmes, E.C., Bodem, J., in press. The complete nucleotide sequence of a New World simian foamy virus. Virology.
Yu, S.F., Sullivan, M.D., Linial, M.L., 1999. Evidence that the human foamy virus genome is DNA. J. Virol. 73, 1565–1572.
Yvon-Groussin, A., Mugnier, P., Bertin, P., Grandadam, M., Agut, H., Huraux, J.M., Calvez, V., 2001. Efficacy of dideoxynucleosides against human foamy virus and relationship to its reverse transcriptase amino acid sequence and structure. J. Virol. 75, 7184–7187.

9 Publication C

Maximilian J. Hartl, Benedikt Kretzschmar, Anne Frohn, Ali Nowrouzi, Axel Rethwilm and Birgitta M. Wöhrl (2008): AZT resistance of simian foamy virus reverse transcriptase is based on the excision of AZTMP in the presence of ATP. *Nucleic Acids Research* **36**, 1009-1016.

Published online 20 December 2007

Nucleic Acids Research, 2008, Vol. 36, No. 3 ***1009–1016***
doi:10.1093/nar/gkm1087

AZT resistance of simian foamy virus reverse transcriptase is based on the excision of AZTMP in the presence of ATP

Maximilian J. Hartl[1], Benedikt Kretzschmar[2], Anne Frohn[1], Ali Nowrouzi[2], Axel Rethwilm[2] and Birgitta M. Wöhrl[1,*]

[1]Universität Bayreuth, Lehrstuhl für Struktur und Chemie der Biopolymere & Research Center for Biomacromolecules, 95440 Bayreuth and [2]Universität Würzburg, Institut für Virologie und Immunbiologie, Würzburg, Germany

Received September 25, 2007; Revised November 17, 2007; Accepted November 19, 2007

ABSTRACT

Azidothymidine (AZT, zidovudine) is one of the few nucleoside inhibitors known to inhibit foamy virus replication. We have shown previously that up to four mutations in the reverse transcriptase gene of simian foamy virus from macaque (SFVmac) are necessary to confer high resistance against AZT. To characterize the mechanism of AZT resistance we expressed two recombinant reverse transcriptases of highly AZT-resistant SFVmac in *Escherichia coli* harboring three (*K211I, S345T, E350K*) or four mutations (*K211I, I224T, S345T, E350K*) in the reverse transcriptase gene. Our analyses show that the polymerization activity of these mutants is impaired. In contrast to the AZT-resistant reverse transcriptase of HIV-1, the AZT resistant enzymes of SFVmac reveal differences in their kinetic properties. The SFVmac enzymes exhibit lower specific activities on poly(rA)/oligo(dT) and higher K_M-values for polymerization but no change in K_D-values for DNA/DNA or RNA/DNA substrates. The AZT resistance of the mutant enzymes is based on the excision of the incorporated inhibitor in the presence of ATP. The additional amino acid change of the quadruple mutant appears to be important for regaining polymerization efficiency.

INTRODUCTION

Foamy viruses belong to the retroviridae but follow a replication pattern unique among retroviruses: (i) reverse transcription occurs before the virus leaves the host cell, (ii) the *pol*-gene is expressed from an separate mRNA and (iii) the viral protease is not cleaved off the Pol-polyprotein (1,2). Only the integrase is removed from Pol (3). Thus, the FV reverse transcriptase (PR–RT) harbors a protease, polymerase and RNase H domain.

Apart form the nucleoside inhibitor tenofovir, only azidothymidine (AZT, zidovudine) is known to inhibit FV reverse transcriptase *in vivo* in cell culture assays at concentrations as low as 5 μM (4–6). We have shown recently that four point mutations involving the amino acids 211 (*K211I*), 224 (*I224T*) 345 (*S345T*) and 350 (*E350K*) located in the PR–RT gene are involved in AZT resistance of SFVmac. The fully resistant SFVmac virus harboring all four mutations was able to replicate in the presence of 1 mM AZT (7). While AZT resistance in HIV-1 is based on the excision of incorporated AZT-monophosphate (AZTMP), AZT-resistant HIV-2 can distinguish between AZT-triphosphate (AZTTP) and TTP during incorporation (8–11).

For FVs, the resistance mechanism is not known. To elucidate the mechanism of AZT resistance we set out to express partially and fully AZT-resistant SFVmac PR–RTs harboring either three or all four AZT resistance mutations in *Escherichia coli*. We were able to show that the mechanism of AZT resistance in SFVmac PR–RTs is based on AZTMP excision from a terminated primer in the presence of ATP. Although the resistant PR–RTs are impaired in their polymerase activities, the faster excision of AZTMP in the presence of ATP confers high resistance against AZT. The I224 mutation appears to be primarily important for regaining polymerization activities for efficient viral replication.

MATERIALS AND METHODS

Cloning, expression and purification of PR–RTs

The wild-type PR–RT gene was cloned into the vector pET28c (Novagen, Germany) via PCR amplification and by using the restriction sites XhoI and NcoI.

*To whom correspondence should be addressed. Tel: +49 921 55 3542; Fax: +49 921 55 3544; Email: birgitta.woehrl@uni-bayreuth.de
Present address:
Anne Frohn, Max Planck Institut für Biochemie, Martinsried, Germany

The expressed proteins contain a 6× His tag at the C-terminus. To avoid degradation of the PR–RT by autocatalytic activity of the PR, a mutant enzyme was constructed harboring an active site mutation in the PR region (*D24A*), which leads to an inactive PR. Thus the AZT-resistant mutants also contain the *D24A* mutation in the PR. The AZT-resistance mutations were created by site-directed mutagenesis according to the QuickChange kit from Stratagene (Heidelberg, Germany). The following potentially AZT-resistant PR–RT mutants were obtained:

mt3: *(D24A) K211I, S345T, E350K*

mt4: *(D24A) K211I, I224T, S345T, E350K*

The activities of the mutants were compared to wild-type PR–RT either without or with the PR *D24A* mutation (WT and WT*, respectively).

The corresponding plasmids were transformed into the *E. coli* strain Rosetta (DE3) (Novagen, Germany). Expression of the PR–RT genes was induced at an optical density of the culture of *ca.* 0.8–1.0 at 600 nm by the addition of 0.2 mM IPTG and incubated further over night at 25°C. The enzymes were purified via Ni-affinity chromatography (HisTrap, GE Healthcare, Munich, Germany), followed by chromatography over a heparin column (HiTrap heparin, GE Healthcare, Munich, Germany). The integrity of the proteins was verified by peptide mass fingerprints (Zentrale Bioanalytik, Zentrum für Molekulare Medizin, Köln, Germany). The purity of the proteins was >95% as judged by SDS–PAGE.

Quantitative polymerization assay

RNA-dependent DNA polymerase activity was quantitated on a poly(rA)/oligo(dT)$_{15}$ substrate (0.2 U/ml) (Roche Diagnostics GmbH, Mannheim, Germany) in a standard assay (30 µl reaction volume) as described previously (12,13) with 150 µM TTP and 41.7 Ci/ml [^{3}H]TTP (49.9 Ci/mmol; MP Biomedicals Inc., Irvine, CA, USA) in reaction buffer [50 mM Tris/HCl, pH 8.0, 80 mM KCl, 6 mM $MgCl_2$, 0.5 mM dithiothreitol (DTT), 0.05% Triton X-100]. Samples were pre-incubated for 2 min at 37°C. The reaction was started by the addition of 12 nM of PR–RT. After 10 min, 7.5 µl aliquots were taken out and spotted on DEAE filter paper and treated as described (12,13). Under these conditions 1 U of enzyme activity catalyzes the incorporation of 1 nmol of TTP into poly(rA)/oligo(dT)$_{15}$ in 10 min at 37°C. For the determination of K_M and v_{max} values, reactions were performed with increasing concentrations of TTP of 25, 50, 75 or 125 µM. K_M– and v_{max}–values were calculated by linear regression using Eadie–Hofstee plots.

5′-end labeling of primers

One hundred picomoles of M13 primer (5′-GTAAAA CGACGGCCAGT) or P_{30} primer (GCTCTAATGGCG TCCCTGTTCGGGCGCCTC) (IBA, Göttingen, Germany) was labeled with 60 µCi γ[^{32}P]-ATP with 2 U T4 polynucleotide kinase (New England Biolabs, Frankfurt, Germany) for 1 h at 37°C. After inactivation of the kinase for 20 min at 65°C the primer was purified via a MicroSpin column (GE Healthcare, Munich, Germany).

Chain termination assay

Chain termination assays were performed using single-stranded M13mp18 (Roche Diagnostics GmbH, Mannheim, Germany). The 5′ ^{32}P-labeled M13 primer was hybridized to a 1.2-fold molar excess of the M13 DNA in a buffer containing 50 mM Tris/HCl, pH 8.0 and 80 mM KCl by heating to 95°C for 2 min, followed by a transfer to a heating block at 70°C and slow cooling to room temperature. Reaction mixtures contained 6 nM of primer/template substrate (P/T), 85 nM of PR–RT, 150 µM of each dNTP and increasing concentrations of AZTTP (GeneCraft GmbH, Lüdinghausen, Germany) in a total volume of 10 µl. After a pre-incubation time of 5 min, reactions were carried out for 10 min at 37°C in reaction buffer (see above). Reactions were stopped by adding 10 µl of urea loading buffer [1 mM EDTA, 0.1% xylene cyanole, 0.1% bromophenol blue, 8 M urea in 1 × TBE (Tris/Borate/EDTA)] and analyzed by denaturing gel electrophoresis (10% polyacrylamide, 7 M urea). The reaction products were visualized by autoradiography or phosphoimaging and quantitated by densitometry using a phosphoimaging device (FLA 3000, raytest, Straubenhardt, Germany).

Fluorescence anisotropy measurements

Fluorescence equilibrium titrations were performed to determine the dissociation constants (K_D) for nucleic acid binding with a 24/40-mer DNA/DNA or DNA/RNA P/T substrate with the following sequences for the primer 5′-ATCACCAGGAGAGGGGAAAGCGGA and template 5′-DY647-CTAATTCCGCTTTCCCCTCTCCTG GTGATCCTTTCCATCC (biomers.net GmbH, Ulm, Germany). The RNA template sequence was identical, containing U instead of T. The templates harbored the fluorescent dye DY647 at their 5′ ends. Titrations were performed in fluorescence buffer (50 mM Tris/HCl, pH 8.0; 80 mM KCl, 10 mM EDTA, 0.5 mM DTT) in a total volume of 1 or 2 ml using a 10 × 4 mm quartz cuvette (Hellma GmbH, Mühlheim, Germany). The excitation wavelength was at 552 nm, and the emission intensity was measured at 573 nm. Slit widths were set at 4.9 and 5.0 nm for excitation and emission, respectively. All anisotropy measurements were performed at 25°C with 15 nM of fluorescently labeled P/T using an L-format Jobin-Yvon Horiba Fluoromax fluorimeter equipped with an automatic titration device (Hamilton). Following sample equilibration, at least six data points with an integration time of 1 s were collected for each titration point.

Data fitting. Data were fitted to a two-component binding equation to determine the equilibrium dissociation constant (K_D) using standard software. The anisotropy was calculated from:

$$A = f_{complex}\, A_{complex} + f_{RNA}\, A_{RNA} \quad \mathbf{1}$$

where A, $A_{complex}$ and A_{RNA} represent the anisotropy values and $f_{complex}$, f_{RNA} the fractional intensities. The change in fluorescence intensity has to be taken into account, so that the fraction bound is given by

$$\frac{[\text{complex}]}{[\text{RNA}]_0} = \frac{A - A_{\text{RNA}}}{(A - A_{\text{RNA}}) + R(A_{\text{complex}} - A)} \quad \mathbf{2}$$

with

$$[\text{complex}] = \left[\left(K_D + [P]_0 + [\text{RNA}]_0\right) - \sqrt{\left(K_D + [P]_0 + [\text{RNA}]_0\right)^2 - 4[P]_0[\text{RNA}]_0} \right] \times 2[\text{RNA}]_0 \quad \mathbf{3}$$

where A is the anisotropy, A_{RNA} is the initial free anisotropy, $A_{complex}$ is the anisotropy of the protein–RNA complex and P_0 and RNA_0 represent the total protein and RNA concentrations, respectively. R is the ratio of intensities of the bound and free forms.

Termination of the radioactively labeled P/T with AZTTP

The [^{32}P] end labeled P_{30} DNA primer was hybridized to a template deoxyoligonucleotide T_{50} (5′-GCTGTGGAAAA TCTCATGCAGAGGCGCCCGAACAGGGACGCCA TTACAGC) (IBA; Göttingen, Germany) as described for the M13 DNA and used for incorporation of AZTTP. P_{30}/T_{50} measuring 100 nM were mixed with 100 μM AZTTP and 150 nM WT PR–RT in reaction buffer and incubated for 2 h at 37° C. After phenol extraction and ethanol precipitation, the P/T substrate was purified over two MicroSpin columns (GE Healthcare, Munich, Germany) to eliminate protein and excess AZTTP.

Excision assay

Ten nanomolar of the [^{32}P] $P_{30\text{-AZTMP}}/T_{50}$ substrate were incubated with 20 nM PR–RT in a volume of 10 μl in reaction buffer for the times indicated. Either 150 μM of Na-pyrophosphate (PP_i) or 5 mM of ATP was present in the mixture. Reactions were started by the addition of enzyme. Where stated, the samples were pre-incubated for 5 min with 0.02 U of pyrophosphatase (Sigma–Aldrich Chemie GmbH, Taufkirchen, Germany). When different concentrations of PR–RTs were tested, the reactions were stopped after 20 min. An equal volume of urea loading buffer was added and the products were analyzed as stated above on denaturing polyacrylamide urea gels.

Primer rescue

One hundred micromolar of dCTP, dGTP, TTP and ddATP was added to the samples with 5 mM ATP described above to allow for elongation by 4 nt once the AZTMP is excised. Samples were pre-incubated for 5 min with 0.02 U of pyrophosphatase before the reaction was started with 40 nM of PR–RT. Reactions were stopped after 10 min and treated further as described above.

Table 1. Quantitative analysis of RNA-dependent DNA polymerase activities on a homopolymeric substrate

Enzyme	U/μg protein *10 min
WT	30.9 (± 0.9)
WT*	31.5 (± 0.1)
mt3	11.6 (± 0.2)
mt4	24.6 (± 0.7)

Activities are given in units per microgram of protein, where 1 U catalyzes the incorporation of 1 nmol TTP in poly(rA)/oligo(dT)$_{15}$ in 10 min at 37°C.

RESULTS

We have shown previously that it is possible to generate AZT-resistant SFVmac in cell culture which is able to replicate in medium containing 1 mM AZT (7). Four mutations were necessary to confer high resistance to the virus: *K211I*, *I224T*, *S345T* and *E350K*. Since one published genomic sequence of wild-type SFVmac already harbors a threonine at position 224 of Pol and since several other primate FV Pol proteins also possess a threonine at position 224, the wild-type SFVmac might have a polymorphism at this site. Thus, we decided to analyze a triple mutant PR–RT lacking the *I224T* mutation [*mt3*; (*D24A*), *K211I, S345T* and *E350K]* as well as the quadruple mutant harboring *I224T* [*mt4*; (*D24A*), *K211I, I224T, S345T* and *E350K*]. To avoid autoprocessing of the PR domain, the enzymes also contained a *D24A* amino acid exchange in the active site of the PR. Our data below indicate that this mutation does not influence the polymerization activities of the mutants. The purified enzymes were used to determine kinetic parameters of polymerization and to analyze the AZT resistance mechanism.

Polymerization activities

In order to characterize the AZT-resistant PR–RT enzymes we performed various polymerization assays. First, the specific activities of the enzymes were determined by observing the ^{3}H-TTP incorporation into poly(rA)/oligo(dT)$_{15}$ (Table 1). Our results indicate that the *D24A* mutation of the WT* does not interfere with polymerization activities. Furthermore, the activity of mt3 is reduced to ~38% of WT activity, whereas the additional mutation *I224T* of mt4 helps this enzyme to regain activity (80% of WT). These effects are even more pronounced regarding the replication activity of the corresponding mutant viruses (7): the virus replication activity of the virus containing mt3 was severely reduced (8.6% of WT) whereas the virus containing mt4 displayed a replication activity similar to the WT virus (113% of WT).

Dissociation constants

As shown above, polymerization activities of the two mutants are impaired. Since this might have an impact on AZT resistance, we wanted to analyze some kinetic parameters. To check if the reduced polymerization activity is due to changes in the affinity for nucleic acids,

Table 2. Parameters for P/T binding and the incorporation of dNTPs

Enzyme	K_D DNA/RNA (nM)	K_D DNA/DNA (nM)	K_M (μM)	V_{max} (pmol/min)
WT	32.4 (± 4.2)	36.4 (± 2.4)	40.1 (± 4.0)	29.6 (± 1.7)
WT*	30.4 (± 2.4)	44.0 (± 3.7)	40.3 (± 4.0)	29.6 (± 1.3)
mt3	28.3 (± 2.7)	39.5 (±3.0)	103.0 (± 16.0)	25.8 (± 2.5)
mt4	31.3 (± 3.2)	42.4 (± 3.0)	112.0 (± 4.0)	30.1 (± 3.3)

K_D-values were obtained by using Equation (3) to fit a curve to the titration data (see 'Materials and Methods section'). K_M- and v_{max}-values were determined by Eadie–Hofstee plots.

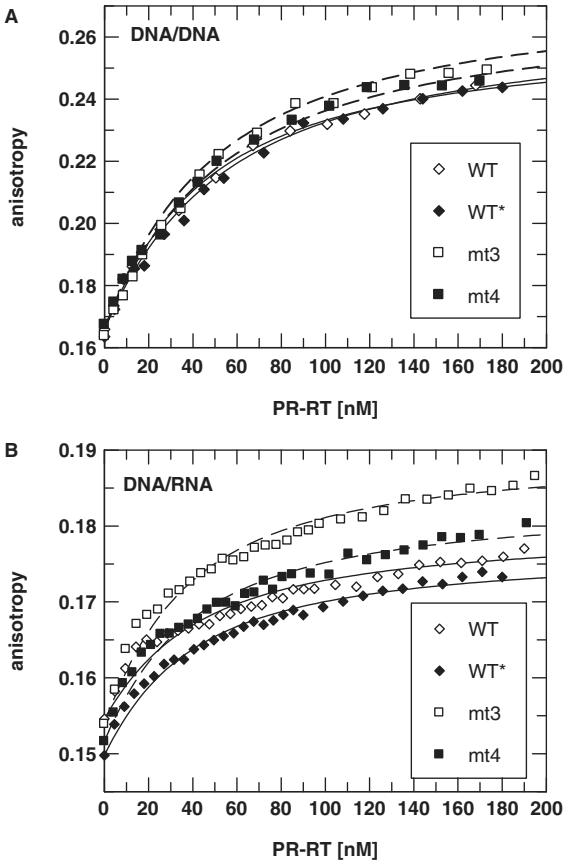

Figure 1. Determination of K_D-values by fluorescence anisotropy measurements. Fifteen nanomolar of a fluorescently labeled DNA/DNA (**A**) or DNA/RNA (**B**) P/T substrate was titrated with different PR–RTs at 25°C. The curves show the best fit to Equation (3) ('Materials and methods' section) describing the binding equilibrium with K_D-values shown in Table 2.

we determined the K_D-values for nucleic acid binding. Measurements were performed using fluorescence anisotropy titrations with 24/40mer DNA/RNA or DNA/DNA P/T substrates harboring a fluorescent dye (DY647) at the 5′ end of the template strand (Table 2, Figure 1). The K_D-values obtained show that there is no significant difference in substrate binding affinities of WT and mutant enzymes, implying that neither the *D24A* mutation nor the AZT-resistance mutations influence substrate binding. The affinity for the DNA/RNA substrate appears to be slightly higher than for DNA/DNA.

Determination of K_M and v_{max} values

This analysis was performed using poly(rA)/oligo(dT)$_{15}$ as a substrate (Table 2). Both AZT-resistant enzymes, mt3 and m4, reveal elevated K_M-values as compared to the two WT proteins. However, the v_{max} value of mt4 is higher than that of mt3 and comparable to the WT proteins, indicating that mt4 is able to exhibit similar polymerization activities like the WT at saturating dNTP concentrations. This might explain the high virus replication activities observed with mt4 containing virus in cell culture assays (7).

Polymerization in the presence of AZTTP

Two mechanisms for AZT resistance have been described. HIV-2 RT controls the incorporation of the inhibitor nucleotide AZTTP (11), whereas for HIV-1 RT excision of the incorporated AZTMP has been recognized as the mechanism of resistance (8–10). Thus, we first analyzed the polymerization behavior of the enzymes in the presence of AZTTP to check for incorporation control. We performed polymerization assays on poly(rA)/oligo(dT)$_{15}$ in the presence of increasing AZTTP concentrations up to 150 μM (Figure 2A). The TTP concentration was kept constant (150 μM) in all assays. Our data indicate that mt3 and mt4 do not exhibit AZT resistance in this assay.

We then used the heteropolymeric single-stranded M13 substrate with a ^{32}P-endlabeled DNA-primer for polymerization in the absence of inhibitor or in the presence of 5 and 50 μM AZTTP and analyzed the polymerization products on denaturing polyacrylamide gels (Figure 2B). As already described for the homopolymeric substrate, all enzymes are sensitive to AZTTP addition in the M13 assay. This result is reminiscent of HIV-1 RT (14), where the AZT resistance was also not visible in steady-state polymerization assays or during pre-steady-state analyses and could only be detected with an AZTMP-terminated P/T substrate (8–10). Our results indicate that the resistance mechanism of SFVmac PR–RTs is not comparable to HIV-2 RT where discrimination between the inhibitor and TTP takes place during incorporation (11).

AZTMP excision form a terminated primer

For HIV-1 RT, it has been shown previously that AZTMP can be excised from an AZTMP-terminated P/T substrate in the presence of PP_i or ATP (8–10). We thus tested these possibilities.

The ^{32}P-endlabeled and AZTMP-terminated substrate $P_{30\text{-AZTMP}}/T_{50}$ was incubated with 150 μM Na-PP_i or 5 mM ATP and PR–RT. Time course experiments were performed (Figures 3 and 4) and aliquots were analyzed on denaturing sequencing gels and quantified by densitometry. Our data indicate that in the presence of PP_i the WT* PR–RT can excise AZTMP from the terminated primer with similar efficiency as mt3 or mt4 (Figure 3B). Obviously, the ability to perform the reverse reaction of

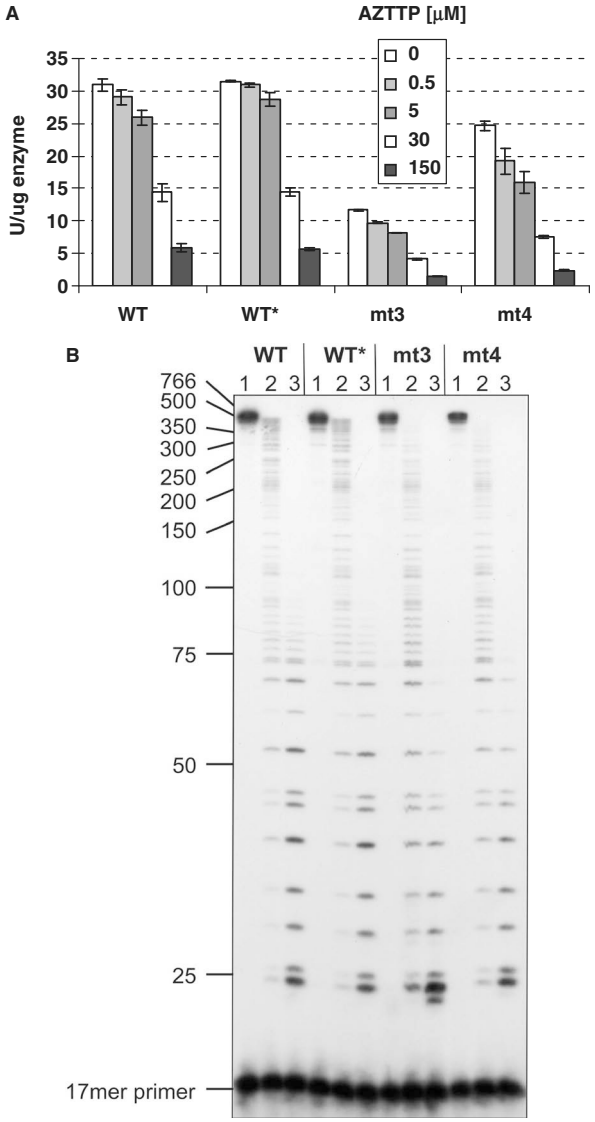

Figure 2. Polymerization activities in the presence of AZTTP. (**A**) Specific activities on 6 nM of poly(rA)/oligo(dT)$_{15}$ with 12 nM of the various SFVmac PR–RTs, 150 μM TTP and 0, 0.5, 5.0, 30.0 or 150 μM AZTTP. The reaction was stopped after 10 min at 37°C. (**B**) Chain termination by AZTMP incorporation during DNA polymerization with M13 ssDNA (for conditions and analysis see 'Materials and methods' section). Either no AZTTP (lane 1), 5 μM (lane 2) or 50 μM (lane 3) of AZTTP was added to the PR–RTs. DNA size markers are indicated on the left.

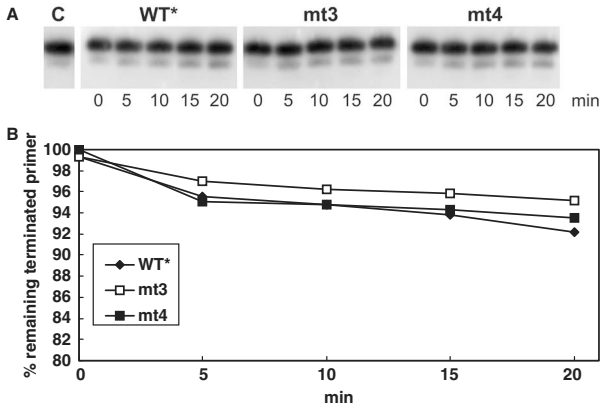

Figure 3. Time course of AZTMP removal in the presence of PP_i. (**A**) One hundred micro molar $NaPP_i$ was present in a mix containing 10 nM of an AZTMP-terminated P/T $P_{30\text{-}AZTMP}/T_{50}$ that was labeled with ^{32}P at the 5′ end of the primer. The reaction was started by the addition of 20 nM of the different PR–RTs and stopped at the time points indicated. Lane C, no enzyme added. (**B**) Quantification of pyrophosphorolytic removal of chain-terminating AZTMP was achieved by densitometry. The percentage of remaining terminated primer is shown.

nucleotide incorporation is an intrinsic property of RTs and might be used as a general proof reading function.

In contrast, when ATP is added (Figure 4), even after an incubation time of 20 min the WT* enzyme does not exhibit significant AZTMP removal activity, whereas mt3 and mt4 are able to excise AZTMP efficiently. To exclude an influence of PP_i in the excision reaction, an additional assay was performed after pre-incubating the reaction mix with pyrophosphatase (Figure 4B). The results shown in Figure 4A and B look very similar, indicating that only insignificant amounts of PP_i were present in the reactions. Quantification of the data of Figure 4B by densitometry (Figure 4C) demonstrates that the excision reactions of mt3 and mt4 are much faster than that of the WT*. However, they slow down when about 10% of the incorporated AZTMP is eliminated from the primer. This might be due to product inhibition by AZTp4A (15). These data clearly indicate that AZTMP excision in the presence of ATP is the valid mechanism for AZT resistance of SFVmac.

To substantiate our results, we performed the excision reactions with ATP using increasing concentrations of enzyme (Figure 5). The assays were also pre-incubated with pyrophosphatase. Again, our results demonstrate very clearly that in the presence of ATP the mutant enzymes are more efficient in AZTMP removal than the WT*. Furthermore, in the case of the mutants, large excess of enzyme leads to the excision of more than one nucleotide.

Primer rescue

The data delineated above are further confirmed by testing the enzymes in the presence of dNTPs to allow for extension of the primer after AZTMP removal (Figure 6). The assay was performed in the presence of ATP and pyrophosphatase. Due to the addition of ddATP, elongation of the primer comes to a halt after the incorporation of 4 nt. Figure 6 shows that only mt3 or mt4 can rescue DNA synthesis, whereas the WT* enzyme is not able to extend the primer.

We thus conclude that AZT resistance of SFVmac is due to AZTMP removal by ATP. Furthermore, the AZTMP excision activity obtained with the triple mutant is comparable to that of mt4. This data indicates that the

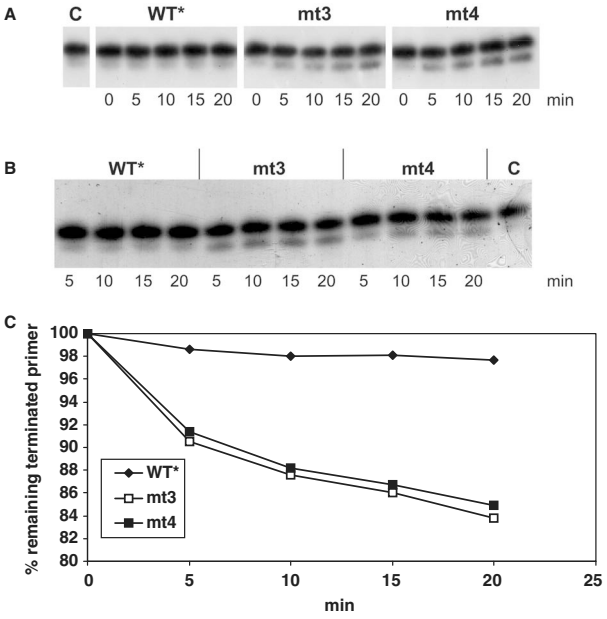

Figure 4. Time course of AZTMP removal in the presence of ATP. (**A**) Five millimolar ATP was present in a mix containing 10 nM of the AZTMP-terminated P/T $P_{30\text{-AZTMP}}/T_{50}$ that was labeled with ^{32}P at the 5′ end of the primer. The reaction was started by the addition of 20 nM of the different PR–RTs and stopped at the time points indicated. (**B**) Addition of 0.02 U pyrophosphatase to the mixture described in (A) 5 min before the PR–RT enzymes were added. Lane C, no enzyme added. (**C**) Quantification of (B) by densitometry. The percentage of remaining terminated primer is shown.

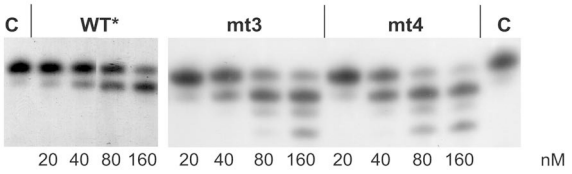

Figure 5. AZTMP removal by ATP in the presence of pyrophosphatase using increasing PR–RT concentrations. Five millimolar ATP and 10 nM of $P_{30\text{-AZTMP}}/T_{50}$ were pre-incubated for 5 min at 37°C in reaction mix. The reaction was started by the addition of different concentrations of the various PR–RTs as indicated and stopped after 20 min. Lane C, no enzyme added.

additional *I224T* change of mt4 is not important for the AZT-resistance mechanism but is necessary to improve the polymerization efficiency.

DISCUSSION

We have shown previously that SFVmac can gain resistance to the nucleoside inhibitor AZT (7). Here, we analyzed the corresponding mutated PR–RTs to elucidate the mechanism of AZT resistance. Our results obtained with purified SFVmac PR–RTs demonstrate that in the case of SFVmac the AZT-resistance mechanism is due to AZTMP removal in the presence of ATP. Remarkably, mt3 which exhibited severely impaired polymerization

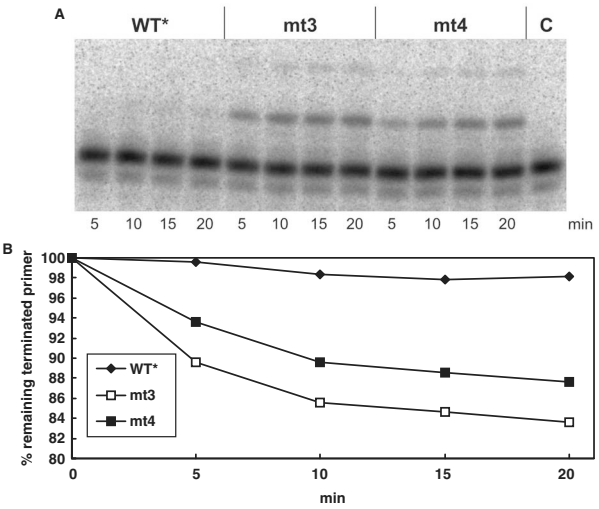

Figure 6. ATP-dependent rescue of AZTMP terminated DNA synthesis. (**A**) Primer rescue reactions using 10 nM $P_{30\text{-AZTMP}}/T_{50}$ were performed with 5 mM ATP, 0.02 U pyrophosphatase and 100 µM dCTP, dGTP, TTP and ddATP. Lane C, no enzyme added. (**B**) Quantification of (A) by densitometry. The percentage of the remaining unextended primer is shown.

activities on homo- and heteropolymeric substrates (Table 1 and Figure 2) also shows higher AZTMP excision activities than the WT* enzyme when ATP is present in the reaction (Figures 4–6). Although mt3 and mt4 are also able to excise AZTMP in the presence of PP_i (Figure 3) the WT* PR–RT exhibits similar efficiency in this reaction, indicating that this cannot be the mechanism of AZT resistance.

Interestingly, compared to the WT SFVmac PR–RTs, mt3 and mt4 exhibit differences in kinetic parameters. This is also noteworthy since the AZT-resistant HIV-1 RT did not differ from the WT HIV-1 RT in its kinetic parameters (14,16–18). The K_M values of the mutant SFVmac PR–RTs are about 2.5-fold higher than those of the WT PR–RTs. While mt3 also shows a reduced value for v_{max}, the *I224T* mutation of mt4 is obviously responsible for an increase of v_{max} similar to that of the WT levels (Table 2), implying that if saturating dNTP concentrations are present in infected cells, reverse transcription will not be greatly impaired in SFVmac viruses harboring mt4. This result indicates that the mutation *I224T* is important for viral fitness since it can reconstitute the polymerization activity of mt4 in SFVmac-infected cells (7).

It has been demonstrated previously that the RTs of HIV-1 and HIV-2 use different mechanisms for AZT resistance. HIV-2 can discriminate between AZTTP and TTP during nucleotide incorporation (11). In contrast, although certain HIV-1 RT mutations confer a 100-fold decrease in the sensitivity to AZT *in vivo* (19,20), this effect could not be demonstrated in *in vitro* assays (14,16–18), indicating that HIV-1 RT is not able to discriminate between AZTTP and TTP. In fact, the mechanism appears to be due to a removal of the chain terminating AZTMP residue after it has been incorporated in the DNA chain. The mutations involved in the enhanced excision of

Figure 7. Sequence alignment of the relevant regions from the HIV-1 and SFVmac RT domains. The amino acids conferring AZT resistance are indicated by filled gray boxes. The numbers represent the amino acid numbering in the HIV-1 RT and SFVmac PR–RT. Sequence alignment was performed with the program lalign (28).

AZTMP in HIV-1 RT are *M41L, D67N, K70R, T215Y/F* and *K219Q/E* (Figure 7) (8–10,21,22). Removal of the inhibitor was suggested to be accomplished by two mechanisms that use different substrates to carry out the reaction. AZTMP removal can take place either in the presence of PP_i or ATP. The chemistry involved in pyrophosphorolysis and the ribonucleotide-dependent phosphorolysis reaction is similar. Removal of the chain-terminating AZT results from nucleophilic attack of a polyphosphate in the phosphodiester bond between the last but one nucleotide and the AZTMP. In case of PP_i, this leads to removal of the 3′ AZTMP by creating AZTTP.

There is evidence that the phosphate donor in the excision reaction of AZT-resistant HIV-1 RT is ATP, leading to an ATP-AZTMP dinucleotide-tetraphosphate (adenosine-3′azido,3′deoxythymidine-5′-5′-tetraposphate, AZTp4A). For HIV-1 RT it was concluded from biochemical and structural data that the exchange of T215 to an aromatic residue (*T215F/Y*) enhances binding of ATP, but not PP_i, thus facilitating excision. The model suggests that in the AZT-resistant enzyme, the adenine moiety of the incoming ATP makes π–π interactions with the aromatic ring of the mutated amino acid (22–26).

Our results obtained with SFVmac PR–RT are especially interesting when comparing the AZT-resistance mutations of HIV-1 RT and SFVmac PR–RT since in the latter enzyme no mutation leading to an aromatic side chain is present. In addition, sequence alignments of the polymerase domains of HIV-1 and SFVmac reveal that the amino acid exchanges obtained with SFVmac are not the ones corresponding to the exchanges in HIV-1 RT (Figure 7). Furthermore, although the homology between PFV and SFVmac is around 90%, introduction of the SFVmac RT mutations into PFV did not result in AZT-resistant viruses (7).

These findings might indicate structural differences between HIV-1 and SFVmac RTs. This appears to be plausible since the RT domains of HIV-1 and SFVmac are phylogenetically rather distantly related (27). Thus, the interpretation of alignment data is also rather difficult. In addition, differences in the mechanism of ATP binding and/or ATP-mediated excision are possible. Structural analysis of WT and AZT-resistant SFVmac PR–RT are under way and will help to elucidate the differences between WT and mutant PR–RTs and also between HIV-1 and SFVmac.

ACKNOWLEDGEMENTS

We thank Philipp Weiglmeier for help with protein purifications and Prof. Paul Rösch for continuous support. The project was funded by the Deutsche Forschungsgemeinschaft DFG (Re627/7-1, Re627/8-1, SFB 479, Wo630/7-1), the Bavarian International Graduate School of Science (BIGSS) and the University of Bayreuth. Funding to pay the Open Access publication charges for this article was provided by Deutsche Forschungsgemeinschaft DFG, grant Wo630/7-1.

Conflict of interest statement. None declared.

REFERENCES

1. Rethwilm,A. (2003) The replication strategy of foamy viruses. *Curr. Top. Microbiol. Immunol.*, **277**, 1–26.
2. Linial,M. (2007) Foamy viruses. In Knipe,D.M. and Howley,P.M. (eds), *Fields Virology*, Vol. 2, Lippincott Williams & Wilkins, Philadelphia, pp. 2245–2262.
3. Pfrepper,K.I., Rackwitz,H.R., Schnölzer,M., Heid,H., Löchelt,M. and Flügel,R.M. (1998) Molecular characterization of proteolytic processing of the Pol proteins of human foamy virus reveals novel features of the viral protease. *J. Virol.*, **72**, 7648–7652.
4. Moebes,A., Enssle,J., Bieniasz,P.D., Heinkelein,M., Lindemann,D., Bock,M., McClure,M.O. and Rethwilm,A. (1997) Human foamy virus reverse transcription that occurs late in the viral replication cycle. *J. Virol.*, **71**, 7305–7311.
5. Rosenblum,L.L., Patton,G., Grigg,A.R., Frater,A.J., Cain,D., Erlwein,O., Hill,C.L., Clarke,J.R. and McClure,M.O. (2001) Differential susceptibility of retroviruses to nucleoside analogues. *Antivir. Chem. Chemother.*, **12**, 91–97.
6. Lee,C.C., Ye,F. and Tarantal,A.F. (2006) Comparison of growth and differentiation of fetal and adult rhesus monkey mesenchymal stem cells. *Stem Cells Dev.*, **15**, 209–220.
7. Kretzschmar,B., Nowrouzi,A., Hartl,M.J., Gärtner,K., Wiktorowicz,T., Herchenröder,O., Kanzler,S., Rudolph,W., Mergia,A. *et al.* (2008) AZT-resistant Foamy Virus. *Virology*, **370**, 151–157.
8. Arion,D., Kaushik,N., McCormick,S., Borkow,G. and Parniak,M.A. (1998) Phenotypic mechanism of HIV-1 resistance to 3′-azido-3′-deoxythymidine (AZT): increased polymerization processivity and enhanced sensitivity to pyrophosphate of the mutant viral reverse transcriptase. *Biochemistry*, **37**, 15908–15917.
9. Meyer,P.R., Matsuura,S.E., So,A.G. and Scott,W.A. (1998) Unblocking of chain-terminated primer by HIV-1 reverse transcriptase through a nucleotide-dependent mechanism. *Proc. Natl Acad. Sci. USA*, **95**, 13471–13476.
10. Meyer,P.R., Matsuura,S.E., Mian,A.M., So,A.G. and Scott,W.A. (1999) A mechanism of AZT resistance: an increase in nucleotide-dependent primer unblocking by mutant HIV-1 reverse transcriptase. *Mol. Cell*, **4**, 35–43.
11. Boyer,P.L., Sarafianos,S.G., Clark,P.K., Arnold,E. and Hughes,S.H. (2006) Why do HIV-1 and HIV-2 use different pathways to develop AZT resistance? *PLoS. Pathog.*, **2**, e10.
12. Jacques,P.S., Wöhrl,B.M., Ottmann,M., Darlix,J.-L. and Le Grice,S.F.J. (1994) Mutating the "primer grip" of p66 HIV-1 reverse transcriptase implicates tryptophan-229 in template-primer utilization. *J. Biol. Chem.*, **269**, 26472–26478.

13. Werner,S. and Wöhrl,B.M. (1999) Soluble Rous Sarcoma Virus reverse transcriptases α, αβ and β purified from insect cells are processive DNA polymerases that lack an RNase H 3′ > 5′ directed processing activity. *J. Biol. Chem.*, **274**, 26329–26336.
14. Krebs,R., Immendörfer,U., Thrall,S., Wöhrl,B.M. and Goody,R.S. (1997) Single-step kinetics of HIV-reverse transcriptase mutants responsible for virus resistance to nucleoside inhibitors zidovudine and 3TC. *Biochemistry*, **36**, 10292–10300.
15. Dharmasena,S., Pongracz,Z., Arnold,E., Sarafianos,S.G. and Parniak,M.A. (2007) 3′-Azido-3′-deoxythymidine-(5′)-tetraphospho-(5′)-adenosine, the product of ATP-mediated excision of chain-terminating AZTMP, is a potent chain-terminating substrate for HIV-1 reverse transcriptase. *Biochemistry*, **46**, 828–836.
16. Carroll,S.S., Geib,J., Olsen,D.B., Stahlhut,M., Shafer,J.A. and Kuo,L.C. (1994) Sensitivity of HIV-1 reverse transcriptase and its mutants to inhibition by azidothymidine triphosphate. *Biochemistry*, **33**, 2113–2120.
17. Lacey,S.F., Reardon,J.E., Furfine,E.S., Kunkel,T.A., Bebenek,K., Eckert,K.A., Kemp,S.D. and Larder,B.A. (1992) Biochemical studies on the reverse transcriptase and RNase H activities from human immunodeficiency virus strains resistant to 3′-azido-3′-deoxythymidine. *J. Biol. Chem.*, **267**, 15789–15794.
18. Kerr,S.G. and Anderson,K.S. (1997) RNA dependent DNA replication fidelity of HIV-1 reverse transcriptase: evidence of discrimination between DNA and RNA substrates. *Biochemistry*, **36**, 14056–14063.
19. Larder,B.A. and Kemp,S.D. (1989) Multiple mutations in HIV-1 reverse transcriptase confer high- level resistance to zidovudine (AZT). *Science*, **246**, 1155–1158.
20. Larder,B.A., Kellam,P. and Kemp,S.D. (1991) Zidovudine resistance predicted by direct detection of mutations in DNA from HIV-infected lymphocytes. *AIDS*, **5**, 137–144.
21. Meyer,P.R., Matsuura,S.E., Schinazi,R.F., So,A.G. and Scott,W.A. (2000) Differential removal of thymidine nucleotide analogues from blocked DNA chains by human immunodeficiency virus reverse transcriptase in the presence of physiological concentrations of 2′-deoxynucleoside triphosphates. *Antimicrob. Agents Chemother.*, **44**, 3465–3472.
22. Boyer,P.L., Sarafianos,S.G., Arnold,E. and Hughes,S.H. (2001) Selective excision of AZTMP by drug-resistant human immunodeficiency virus reverse transcriptase. *J. Virol.*, **75**, 4832–4842.
23. Boyer,P.L., Sarafianos,S.G., Arnold,E. and Hughes,S.H. (2002) The M184V mutation reduces the selective excision of zidovudine 5′-monophosphate (AZTMP) by the reverse transcriptase of human immunodeficiency virus type 1. *J. Virol.*, **76**, 3248–3256.
24. Boyer,P.L., Sarafianos,S.G., Arnold,E. and Hughes,S.H. (2002) Nucleoside analog resistance caused by insertions in the fingers of human immunodeficiency virus type 1 reverse transcriptase involves ATP-mediated excision. *J. Virol.*, **76**, 9143–9151.
25. Sarafianos,S.G., Clark,A.D.Jr, Das,K., Tuske,S., Birktoft,J.J., Ilankumaran,P., Ramesha,A.R., Sayer,J.M., Jerina,D.M. *et al.* (2002) Structures of HIV-1 reverse transcriptase with pre- and post-translocation AZTMP-terminated DNA. *EMBO J.*, **21**, 6614–6624.
26. Smith,A.J., Meyer,P.R., Asthana,D., Ashman,M.R. and Scott,W.A. (2005) Intracellular substrates for the primer-unblocking reaction by human immunodeficiency virus type 1 reverse transcriptase: detection and quantitation in extracts from quiescent- and activated-lymphocyte subpopulations. *Antimicrob. Agents Chemother.*, **49**, 1761–1769.
27. Vogt,V.M. (1997) Retroviral virions and genomes. In Coffin,J., Hughes,S.H. and Varmus,H. (eds), *Retroviruses*, Cold Spring Harbor Laboratory Press, New York, pp. 27–69.
28. Huang,X. and Miller,W. (1991) A time-efficient, linear-space local similarity algorithm. *Adv. Appl. Math*, **12**, 337–357.

10 Publication D

Maximilian J. Hartl, Birgitta M. Wöhrl and Kristian Schweimer (2007): Sequence-specific ^{1}H, ^{13}C and ^{15}N resonance assignments and secondary structure of a truncated protease from simian foamy virus. *Biomolecular NMR Assignment* **1**, 175-177.

Biomol NMR Assign (2007) 1:175–177
DOI 10.1007/s12104-007-9048-6

ARTICLE

Sequence-specific ^{1}H, ^{13}C and ^{15}N resonance assignments and secondary structure of a truncated protease from Simian Foamy Virus

Maximilian J. Hartl · Birgitta M. Wöhrl · Kristian Schweimer

Received: 31 July 2007 / Accepted: 27 August 2007 / Published online: 18 September 2007

Abstract The backbone and side chain assignments of the retroviral aspartate protease from Simian Foamy Virus from macaques (SFVmac) have been determined by triple resonance NMR techniques.

Keywords SFVmac · Retroviral protease · Heteronuclear NMR · Sequence-specific assignment

Biological context

Spumaviruses, or Foamy Viruses (FV), belong to the retroviridae and follow a replication pattern unique among retroviruses: (a) reverse transcription occurs before the virus leaves the host cell, (b) the *pol*-gene is expressed from a separate mRNA and (c) the viral protease is not cleaved off the Pol polyprotein (Linial 2007; Rethwilm 2003). Thus, the reverse transcriptase (PR-RT) harbors a protease, polymerase and RNase H domain. Genetic analysis has shown that the FV protease (PR) is absolutely required for infectivity and processing (Konvalinka et al. 1995).

Retroviral proteases belong to the family of aspartic acid proteases and have been shown to be active as homodimers. The active site amino acid residues Asp-Thr/Ser-Gly from each chain contribute to the symmetric active site of the enzyme (Pearl and Taylor 1987). A second sequence motif Gly-Arg-Asp/Asn that can be found in most retroviral PRs corresponds to Gly-Arg-Lys in FV PRs (Pearl and Taylor 1987). However, apart from these two motifs, FV PRs show very little sequence homology to other retroviral PRs. Moreover, the molecular weight of monomeric FV PRs is around 18 kDa whereas other retroviral PR monomers possess a molecular weight of ca. 10 kDa. For further analysis of FV PRs we used the PR domain of Simian Foamy Virus from macaque (SFVmac). Sequence comparisons of human immunodeficiency virus type 1 (HIV-1) PR (96 residues) and SFVmac PR (143 residues) showed that the two enzymes exhibit about 30% sequence similarity only in the N-terminal part of the SFVmac protein. The extended C-terminus which cannot be found in other retroviral PRs does not show any similarity, indicating that it might not be necessary for activity. Furthermore, gel filtrations experiments with the purified PR-RT of our group (data not shown) indicate that PR-RT is monomeric, raising the interesting question, how and when in the viral life cycle SFVmac PR dimerizes and functions. To further address this question, a high-resolution structure of SFVmac PR is desirable. As an initial step we cloned and expressed a recombinant SFVmac PR, called SFVmac PRshort (aa1-102), lacking the C-terminal region. The purified protein also elutes as a monomer as shown by gel filtration experiments (data not shown). We virtually completely assigned the ^{1}H, ^{13}C and ^{15}N resonances of SFVmac PRshort with multidimensional heteronuclear NMR and determined the secondary structure by chemical shift analyses.

Methods and results

The DNA coding for SFVmac PRshort was cloned into pET28c (Novagen). The protein was expressed in the *Escherichia coli* strain Rosetta DE3 (Novagen) and contained a 6 × His tag at the C-terminus. Expression was induced by adding 0.2 mM IPTG at 16°C over night. The

M. J. Hartl · B. M. Wöhrl (✉) · K. Schweimer
Lehrstuhl Biopolymere, Universität Bayreuth, Universitätsstr. 30, 95447 Bayreuth, Germany
e-mail: birgitta.woehrl@uni-bayreuth.de

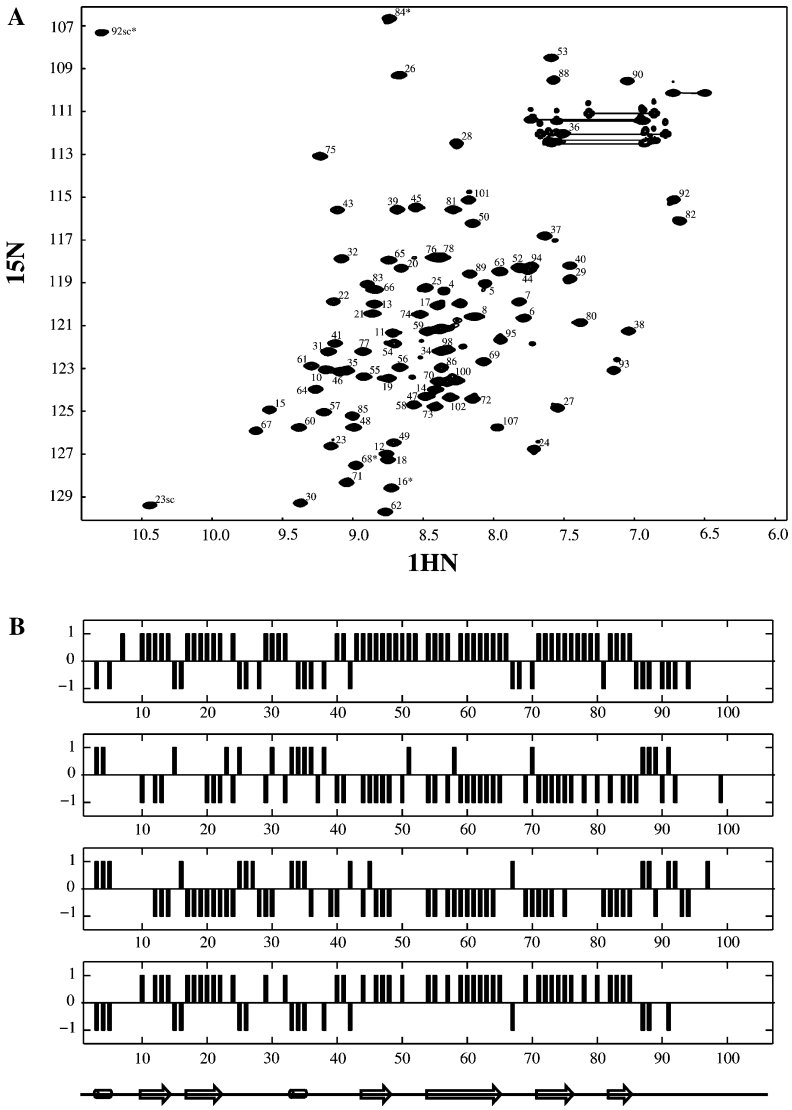

Fig. 1 (**A**) [^{1}H, ^{15}N] spectrum of the uniformly ^{15}N/^{13}C labeled SFVmac PRshort. NH_2 side chains are connected by lines, the arginine εNH, and the tryptophane NH are marked by 'sc'. (**B**) Secondary chemical shift indices for H^{α}, C^{α}, CO nuclei, and the consensus of SFVmac PRshort. Deduced β strands are represented by arrows, and helical regions by cylinders

protein was purified by immobilized Ni^{2+} affinity chromatography under native conditions.

The enzymatic activity of the purified PRshort was tested using a synthetic peptide (TQGSYVVH↓CNTTP) harboring the natural cleavage site of the PR in the Pol-precursor protein which is located between the reverse transcriptase and integrase domains. PRshort proved to be active and was able to cleave the peptide at the predicted position, as indicated by the arrow. Cleavage products were detected by ESI mass spectrometry (data not shown).

For NMR studies SFVmac PRshort was dissolved at a concentration of 2 mM in 50 mM Na-phosphate pH 7.4, 100 mM NaCl, 0.5 mM DTT, and 10% (v/v) D_2O.

All NMR spectra were acquired at 25°C on a Bruker Avance 700 MHz spectrometer equipped with a cryogenically cooled probe. HNCO, HNCACB, CBCA(CO)NH, CCONH, HBHA(CO)NH, HC(C)H-TOCSY (Bax and Grzesiek 1993; Sattler et al. 1999) 3D NMR experiments were recorded for backbone and aliphatic side chain resonance assignment. Assignment of aromatic resonances was achieved with a [^{1}H, ^{13}C]-HSQC spectrum recorded in the aromatic region and 3D ^{13}C-edited NOESY experiments. The NMR data was processed using in-house written software and analyzed with the program package NMRview (B.A. Johnson, Merck, Whitehouse Station, NJ, USA).

Extent of assignment and data deposition

Analysis of triple resonance data allowed the assignment of backbone resonances for all residues except Met1-Asp2, Ile51 and the carboxyterminal region Leu98-His107 containing the hexa-His-Tag. Side chain ^{1}H and ^{13}C shifts are nearly complete for the sequence region Pro3-Pro97 with few exceptions of some longer side chains. An assigned [^{1}H, ^{15}N] HSQC spectrum is shown in Fig. 1.

The secondary chemical shifts of $^{1}H^{\alpha}$, $^{13}C^{\alpha}$ and ^{13}CO indicate a mainly β sheet protein. The location of the β strands along the primary sequence is similar to the HIV protease.

The SFVmac-PRshort assignments have been deposited in the BioMagResBank, accession code 15403.

Acknowledgements We thank the DFG (Wo630/7-1), the Bavarian International Graduate School of Science (BIGSS) and the University of Bayreuth for financial support.

References

Bax A, Grzesiek A (1993) Methodological advances in protein NMR. Acc Chem Res 26:131–138

Konvalinka J, Löchelt M, Zentgraf H, Flügel RM, Kräusslich H-G (1995) Active foamy virus proteinase is essential for virus infectivity but not for formation of a Pol polyprotein. J Virol 69:7264–7268

Linial M (2007) Foamy Viruses. In: Knipe DM, Howley PM (eds) Fields Virology. Lippincott Williams & Wilkins, Philadelphia, pp 2245–2262

Pearl LH, Taylor WR (1987) A structural model for the retroviral proteases. Nature 329:351–354

Rethwilm A (2003) The replication strategy of foamy viruses. Curr Top Microbiol Immunol 277:1–26

Sattler M, Schleucher J, Griesinger C (1999) Herteronuclear multidimensional NMR experiments for the structure determination of proteins in solution empolying pulsed field gradients. Prog NMR Spectrosc 34:93–158

11 Publication E

Maximilian J. Hartl, Birgitta M. Wöhrl, Paul Rösch and Kristian Schweimer (2008): The solution structure of the simian foamy virus protease reveals a monomeric protein. *Journal of Molecular Biology* **381**, 141-149.

doi:10.1016/j.jmb.2008.05.064 J. Mol. Biol. (2008) 381, 141–149

JMB

Available online at www.sciencedirect.com

ScienceDirect

ELSEVIER

The Solution Structure of the Simian Foamy Virus Protease Reveals a Monomeric Protein

Maximilian J. Hartl, Birgitta M. Wöhrl*, Paul Rösch and Kristian Schweimer

Lehrstuhl für Struktur und Chemie der Biopolymere, Universität Bayreuth, 95440 Bayreuth, Germany

Research Center for Biomacromolecules, Universität Bayreuth, 95440 Bayreuth, Germany

Received 17 April 2008; received in revised form 23 May 2008; accepted 27 May 2008
Available online 3 June 2008

In contrast to orthoretroviruses, foamy viruses (FVs) express their Pol polyprotein from a separate *pol*-specific transcript. Only the integrase domain is cleaved off, leading to a protease-reverse transcriptase (PR-RT) protein. We purified the separate PR domain (PRshort) of simian FV from macaques by expressing the recombinant gene in *Escherichia coli*. Sedimentation analyses and size exclusion chromatography indicate that PRshort is a stable monomer in solution. This allowed us to determine the structure of the PRshort monomer using 1426 experimental restraints derived from NMR spectroscopy. The superposition of 20 conformers resulted in a backbone atom rmsd of 0.55 Å for residues Gln8–Leu93. Although the overall folds are similar, the macaque simian FV PRshort reveals significant differences in the dimerization interface relative to other retroviral PRs, such as HIV-1 (human immunodeficiency virus type 1) PR, which appear to be rather stable dimers. Especially the flap region and the N- and C-termini of PRshort are highly flexible. Neglecting these regions, the backbone atom rmsd drops to 0.32 Å, highlighting the good definition of the central part of the protein. To exclude that the monomeric state of PRshort is due to cleaving off the RT, we purified the complete PR-RT and performed size exclusion chromatography. Our data show that PR-RT is also monomeric. We thus conclude adoption of a monomeric state of PR-RT to be a regulatory mechanism to inhibit PR activity before virus assembly in order to reduce packaging problems. Dimerization might therefore be triggered by additional viral or cellular factors.

Keywords: retroviral protease; foamy virus; NMR spectroscopy; monomer; protein structure

Edited by M. F. Summers

Introduction

Spumaviruses or foamy viruses (FVs) possess a genomic organization typical for retroviruses, harboring the genes *gag*, *pol* and *env*. Furthermore, similar to HIV-1 (human immunodeficiency virus type 1), they express additional so-called accessory genes, which are important for regulatory processes. However, the replication of FVs differs from that of orthoretroviruses in some aspects.[1] Reverse transcription takes place to a large extent before the progeny virus leaves the cell, resulting in a double-stranded DNA genome.[2–4] Furthermore, the properties of the Pol protein and the reverse transcriptase (RT) are different.[5] In typical retroviruses, Pol and thus protease (PR) are part of the Gag–Pol precursor protein. FVs synthesize Pol from a separate mRNA, and the N-terminal PR of the Pol precursor is not cleaved off the RT. Thus, the mature RT found in virions is actually PR-RT.[6,7] Genetic analyses have shown that PR activity is absolutely required for FV infectivity and processing.[8] The activity of the FV PR must be highly regulated to avoid premature processing of Gag and Pol prior to virus assembly.

Retroviral PRs are aspartyl PRs and have been shown to be only active as symmetric homodimers with a single active site formed by the residues DS/

*Corresponding author. E-mail address: birgitta.woehrl@uni-bayreuth.de.

Abbreviations used: FV, foamy virus; GFP, green fluorescent protein; HIV-1, human immunodeficiency virus type 1; NOE, nuclear Overhauser enhancement; NOESY, nuclear Overhauser enhancement spectroscopy; PFV, prototype FV; PR, protease; RT, reverse transcriptase; SFVmac, simian foamy virus from macaques.

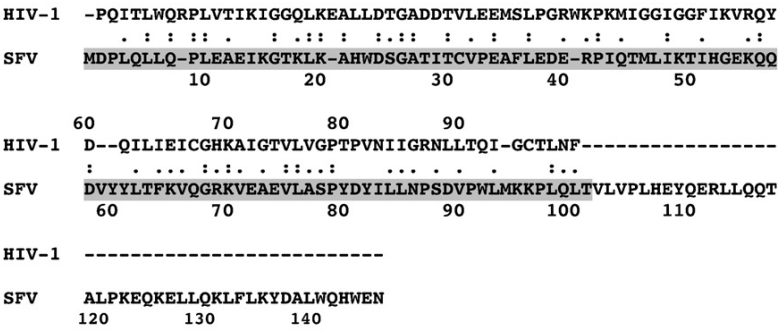

Fig. 1. Sequence comparison of HIV-1 and SFVmac PRs. The amino acid sequence of SFVmac PRshort is highlighted in gray.

TG originating from each monomer.[9–11] Three-dimensional structure analyses of several retroviral PRs by either NMR or X-ray crystallography show that despite large differences in the amino acid sequences, the global folds of these PRs are rather similar.[10–13] Retroviral PRs consist mainly of β-strands and a few short α-helical regions. The number and lengths of these elements vary depending on the PR species. In general, the PR monomer exhibits four characteristic structural elements: (1) a hairpin containing the A1 loop; (2) a large B1 loop, or "fireman's grip," containing the conserved DS/TG motif forming the active site; (3) an α-helix; and (4) a second large loop D1, which is also called the "flap" region. The fireman's grip, the flap region and the N- and C-terminal regions, which form a four-stranded β-sheet, are essential for PR dimerization.

Here, we present the structure of the PR domain (PRshort) from simian FV from macaques (SFVmac). Our results show that PRshort is a stable monomer but that, under certain conditions using high NaCl concentrations of 2–3 M, PR activity can be observed. Since the PR of FVs is not cleaved off the RT during virus maturation, we also analyzed the monomer/dimer state of recombinant PR-RT from SFVmac. Gel filtration analyses indicate that PR-RT is also monomeric. Our results have implications on the regulation of PR activity during virus assembly and maturation.

Results

Analytical ultracentrifugation and size exclusion chromatography

Experiments using prototype FV (PFV, formerly HFV) PR implied that a potential cleavage site between the PR and RT domains is located after residue Asn143 of the Pol protein.[14] Since PFV and SFV exhibit high sequence homology and possess the same putative cleavage site between PR and RT,[14] we expressed the corresponding 143-amino-acid-long SFVmac PR. The 18-kDa PR domain of SFVmac PR-RT exhibits proteolytic activity at NaCl concentrations of 2 M and higher when expressed separately. At low NaCl concentrations, no activity can be detected (data not shown). Gel filtration experiments indicated a high tendency of the protein to aggregate.

Sequence comparisons of HIV-1 PR (99 residues) with the 18-kDa SFVmac PR (143 residues) revealed a sequence similarity of about 29%, albeit only in the N-terminal part of the SFVmac protein. The C-terminal region of SFVmac PR does not show any homology (Fig. 1). Possibly, the non-homologous region serves only as a flexible linker between the PR and polymerase domains. We thus decided to construct an SFVmac PR that is similar in size to HIV-1 PR. SFVmac PRshort spans the region homologous to HIV-1 PR and has a molecular mass of approximately 12.6 kDa, including a C-terminal 6× His tag.

Analysis of the protein by size exclusion chromatography indicated that SFVmac PRshort is a monomer. Tests were done in a buffer containing either 300 mM (data not shown) or 2 M NaCl, since we could detect proteolytic activity of SFVmac PRshort at the latter concentration. However, even at 2 M NaCl, no dimer is detectable (Fig. 2a). This was surprising since retroviral PRs are only active as homodimers.[10,11] To confirm our results, we determined the molecular mass of PRshort by analytical ultracentrifugation (Fig. 2b). Sedimentation analysis resulted in a molecular mass of 11.6 kDa, proving the protein to be monomeric.

To exclude the possibility that the monomeric state of SFVmac PRshort is an artifact due to expression of the separate PR domain, we also performed size exclusion chromatography of recombinant SFVmac PR-RT, which represents the mature polymerase in FV virions. Analyses were done at 300 mM (data not shown) and 2 M NaCl (Fig. 3). The results of the two experiments were comparable, and our data indicate clearly that PR-RT is also monomeric.

PR activity

Activity of retroviral PRs is exhibited only by the PR dimer.[10,11] We thus determined whether PRshort and PR-RT do possess PR activity. A GB1–green fluorescent protein (GFP) fusion protein harboring the natural Pol cleavage site between GB1 and GFP was used as a substrate. Since it was shown previously that PFV PR is only active at high salt concentrations,[15,16] PR activities were analyzed at 0.1, 2 and 3 M NaCl. Our data show clearly that at 0.1 M NaCl, no cleavage product can be detected

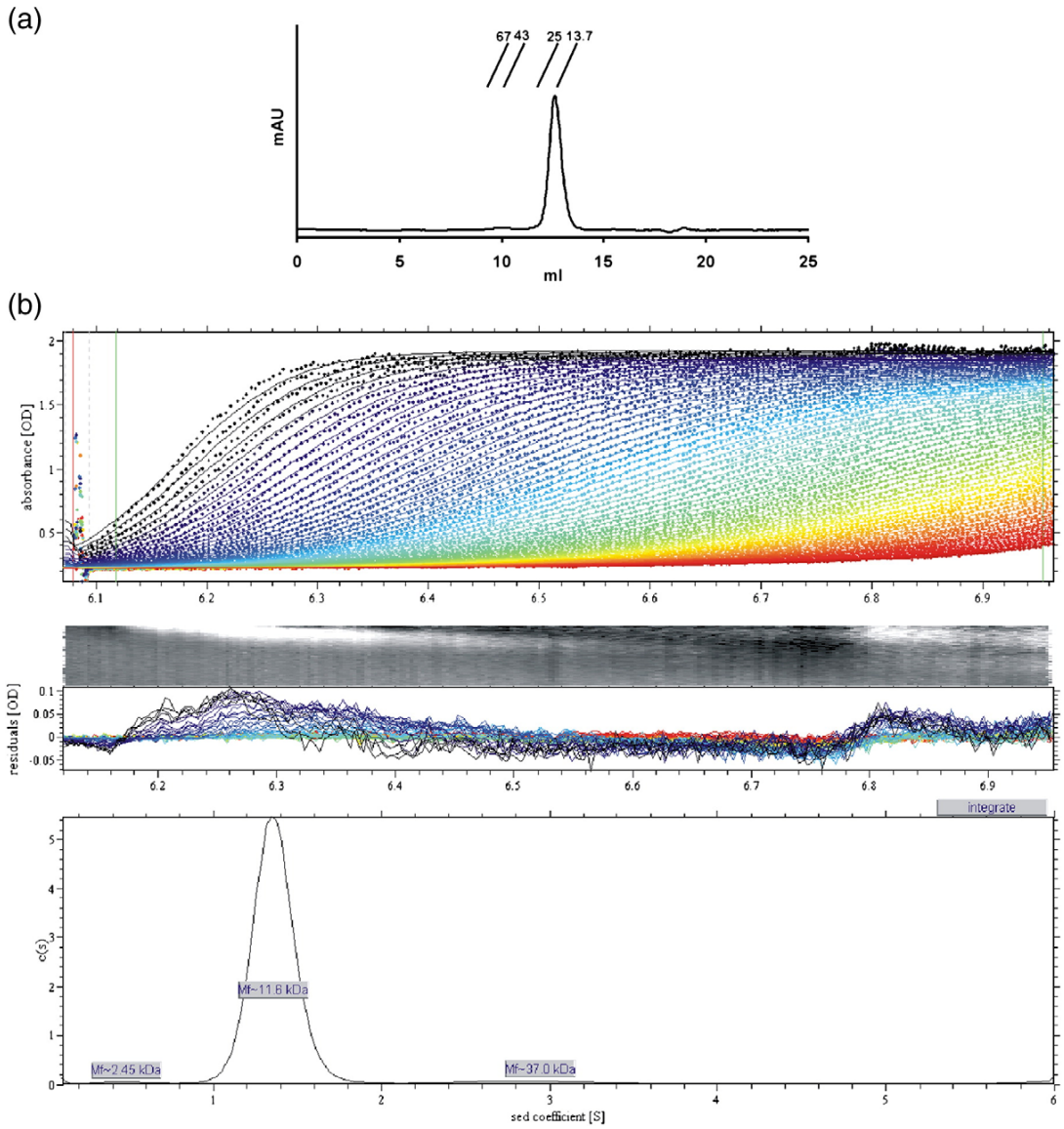

Fig. 2. Size exclusion chromatography and analytical ultracentrifugation of PRshort. (a) Chromatogram of SFVmac PRshort using an S75 HR 10/30 column. The run was performed in 100 mM Na–phosphate buffer, pH 7.4, 2 M NaCl and 0.5 mM DTT. The positions of the standard proteins used for column calibration are indicated. (b) Sedimentation velocity analysis of SFVmac PRshort at 60,000 rpm in 50 mM Na–phosphate buffer, pH 7.4, and 100 mM NaCl. The sedimentation profiles (top) were monitored at a wavelength of 280 nm and fitted as described in Materials and Methods. The symbols represent the raw sedimentation data; the lines, theoretical fitted data. The fitting residuals are shown underneath (middle). The *S* value, normalized for water at 20 °C [$S_w(20,w)$], was 1.4415. The bottom panel shows the continuous sedimentation coefficient distribution of SFVmac PRshort. The calculated molecular mass for SFVmac PRshort is 11,613 Da with a best-fit friction ratio of 1.283. The peak represents 93.488% of the total peak areas.

even after an incubation time of 16 h at 37 °C (Fig. 4). However, cleavage can be observed at 2 M and is even more pronounced at 3 M NaCl, indicating that dimerization is facilitated at higher NaCl concentrations. Furthermore, although we were able to detect cleavage of the GB1–GFP substrate, we did not observe any cleavage of the PR-RT due to autoprocessing. This is an additional confirmation that cleavage between PR and RT does not take place in the FV life cycle.

Additionally, we analyzed by NMR spectroscopy whether a peptide representing the cleavage site between the RNase H and IN domains could bind to SFVmac PRshort and initialize dimerization. Addition of a threefold excess of peptide to 500 μM protein at a NaCl concentration of 100 mM did not lead to any signal changes in $^{1}H,^{15}N$ heteronuclear single quantum coherence spectra, indicating no binding under these conditions. High NaCl concentrations (2 M) led to insufficient quality of the spectra.

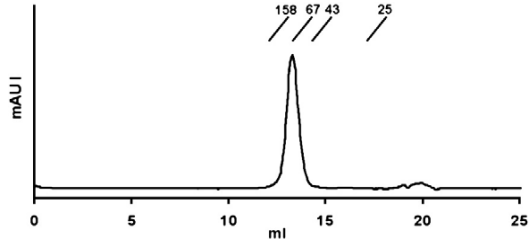

Fig. 3. Size exclusion chromatography SFVmac PR-RT. Chromatogram of SFVmac PR-RT using an S200 HR 10/30 column. The run was performed in 100 mM Na–phosphate buffer, pH 7.4, 2 M NaCl and 0.5 mM DTT. The positions of the standard proteins used for column calibration are indicated.

NMR structure and dynamics

NMR analyses were performed with ca 1 mM PRshort in 50 mM Na–phosphate buffer, pH 7.4, 0.5 mM DTT and 10% (v/v) D_2O, containing 100 mM NaCl, thus favoring the monomeric state of PRshort. From the multidimensional NMR experiments, 1426 restraints were derived (Table 1). The final structure calculation resulted in an ensemble with no distance restraint violation larger than 0.1 Å and no dihedral angle restraint violation larger than 3.1° together with good stereochemical properties displayed by 89% of the residues in the most favored regions of the Ramachandran map. The superposition of the 20 conformers results in a backbone atom rmsd of 0.55 Å for residues Gln8–Leu93, showing that the structure is well defined except for the unstructured N- and C-termini (Fig. 5). Neglecting the flap region (Pro42–Asp58), which shows significant flexibility on the picosecond-to-nanosecond timescale as determined from $\{^1H\}^{15}N$ heteronuclear nuclear Overhauser enhancement (NOE) measurements (Fig. 6), the backbone atom rmsd drops to 0.32 Å, highlighting the good definition of the central part of SFVmac PRshort.

The solution structure of PRshort (Fig. 5) consists of seven β-strands (β1 = Leu10–Ile14, β2 = Thr17–Trp23, β3 = Thr30–Pro33, β4 = Gln44–Lys49, β5 = Glu54–Val66, β6 = Lys70–Ser78, β7 = Ile83–Leu85) and a helical turn (Glu34–Leu37). The β-strands form a closed barrel-like β-sheet with the strand order β1–β2–β7–β3–β6–β5(Val59–Val66)–β1. The strands β2 and β7 are arranged in parallel, while all other strands are arranged in an anti-parallel manner. The amino-terminal halves (Glu54–Asp58) of β5 and β4 form a β-hairpin corresponding to the flap region of retroviral and non-viral aspartate PRs.[10] This β-hairpin is well defined locally by 92 inter-strand NOEs and backbone ϕ/φ angles, derived from secondary chemical shifts typical for an extended conformation for all residues except Ile51 and His52. Due to missing contacts of residues Gln44–Gln56 to the core of the protein, a defined orientation of the flap could not be determined.

The overall fold shows significant similarity with the monomeric HIV-1 PR (1–95),[18] which also resembles the structure of one subunit of the native dimeric HIV-1 PR. The backbone heavy atom rmsd between SFVmac PRshort and HIV-1 PR (1–95) is 1.6 Å, excluding the flap region. Superposition of 11 residues of the loop containing the active site (Lys20–Thr30) results in a backbone rmsd of 0.32 Å to the solution structure of the monomeric HIV-1 PR[18] and that of 0.64 Å to the crystal structure of the active dimeric HIV-1 PR (Protein Data Bank accession code 3HVP).[12] The necessary backbone conformation of the active site is therefore preformed in the monomeric structures. The side chains do not show a defined conformation (e.g., Ser25 of the "fireman's grip"). Due to their solvent accessibility, high mobility is expected.

^{15}N relaxation NMR experiments (Fig. 6) were performed to characterize the dynamics of SFVmac PRshort. From ^{15}N longitudinal relaxation (1.28± 0.07 s^{-1} for residues with $\{^1H\}^{15}N$ NOE >0.65) and ^{15}N transverse relaxation (12.99±1.20 s^{-1} for residues with $\{^1H\}^{15}N$ NOE >0.65) rates, a rotational correlation time τ_c of 9.5 ns at a temperature of 298 K for isotropic rotational diffusion can be derived. Taking temperature and temperature-dependent solvent viscosity into account, the expected correlation time of SFVmac PRshort at 293 K would be 10.9 ns, which is comparable with the relaxation data of HIV-1 PR at 293 K.[19–21] This is roughly the average of the τ_c values determined for the HIV-1 PR dimer (12.8 ns at 293 K)[20] and the HIV-1 PR monomer (8.6 ns at 293 K).[21] However, direct comparison is difficult, as

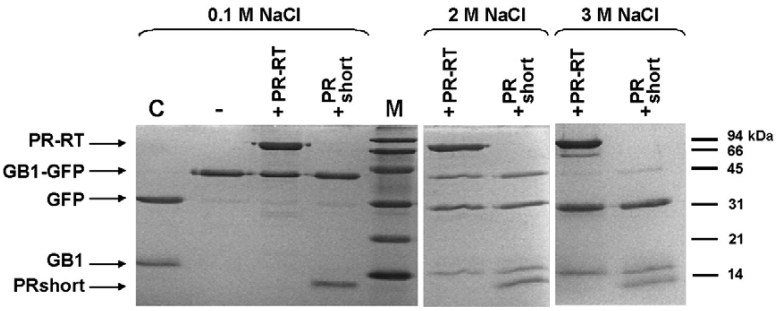

Fig. 4. PR activity assay. The reaction products were analyzed by 19% SDS-PAGE. A total of 10 μM GB1–GFP substrate was incubated with 10 μM SFVmac PR-RT or 10 μM PRshort at 37 °C for 16 h in a reaction buffer (50 mM Na–phosphate buffer, pH 7.4, and 0.5 mM DTT) with increasing NaCl concentrations as indicated. C, control, substrate cleavage with Tev PR; (−), uncleaved substrate; and M, molecular weight standard, with the sizes of the standard proteins indicated on the right.

Table 1. Structural statistics

Experimentally derived restraints	
Distance restraints	
NOE	1338
Intra-residual	205
Sequential	350
Medium range	227
Long range	556
Hydrogen bonds	17
Dihedral restraints	57
Restraint violation	
Average distance	0.0037±0.0005 Å
Maximum distance	<0.1 Å
Average dihedral	0.21±0.11
Maximum dihedral	3.2°
Deviation from ideal geometry	
Bond length	0.00072±0.00004 Å
Bond angle	0.14°±0.008°
Coordinate precision[a] *(Å)*	
Gln8–Leu93	
Backbone heavy atoms	0.55
All heavy atoms	1.05
Gln8–Arg41; Val59–Leu93	
Backbone heavy atoms	0.30
All heavy atoms	0.89
Ramachandran plot statistics[b] *(%)*	
Most favored	89.3
Additionally allowed	10.5
Generously allowed	0.1
Disallowed	0.1

[a] The precision of the coordinates is defined as the average atomic rmsd between the accepted simulated annealing structures and the corresponding mean structure calculated for the given sequence regions.
[b] Ramachandran plot statistics were determined using PROCHECK.

SFVmac PRshort contains a C-terminal His tag, adding 13 amino acids, which will lead to an increased correlation time.[22]

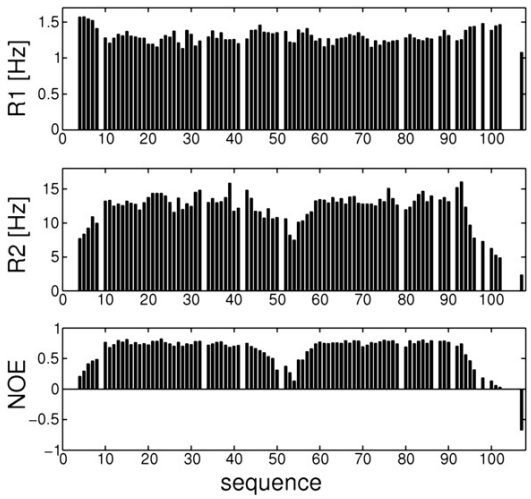

Fig. 6. ^{15}N relaxation data of SFVmac PRshort. Longitudinal (R_1, top) and transverse (R_2, middle) ^{15}N relaxation rates and steady-state heteronuclear $\{^1H\}^{15}N$ NOE at 14.1 T of SFVmac PRshort at 298 K as a function of the sequence position.

SFVmac PRshort, accidentally truncated by proteolytic cleavage at sequence position Gln99–Leu100, showed a ^{15}N transverse relaxation rate of $10\pm1\ s^{-1}$ and an average longitudinal relaxation rate of $1.5\pm0.1\ s^{-1}$, which in turn yielded a rotational correlation time of 7.3 ns, corresponding to 8.3 ns at 293 K. This value is very close to that for the HIV-1 PR monomer, suggesting that SFVmac PRshort is monomeric to a very high extent at concentrations of 1–2 mM. Furthermore, these data imply that the His tag does not affect the oligomerization state of the PR.

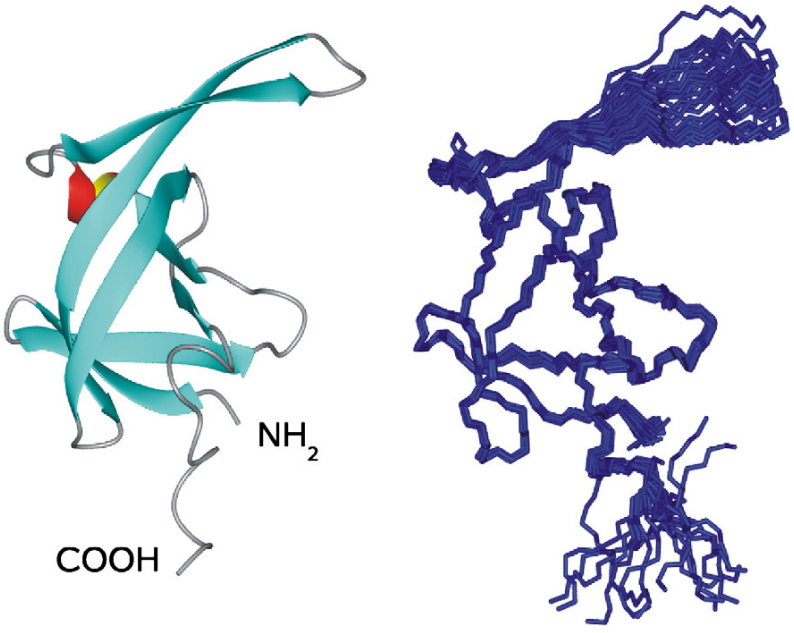

Fig. 5. Solution structure of the SFVmac PRshort monomer. A cartoon representation of the structure is shown on the left, whereas superposition of the 20 lowest energy structures is shown on the right. The residues of the flap region Pro42–Asp58 were not included in coordinate fitting. The figure was generated using MOLMOL.[17]

The presence of the long unstructured termini of SFVmac PRshort alters the rotational diffusion tensor on the timescale of the rotational correlation time, rendering the separation of overall tumbling and internal motion difficult and thus preventing more detailed analysis of the relaxation data. Therefore, the internal dynamics were characterized qualitatively using steady-state $\{^1H\}^{15}N$ heteronuclear NOE measurements (Fig. 6). The heteronuclear NOE shows values larger than 0.68 for residues Leu10–Gln44 and Val59–Trp92, indicating these residues to be highly restricted on the picosecond-to-nanosecond timescale, an observation characteristic for folded proteins.[23] The heteronuclear NOE decreases towards the amino- and carboxy-termini, reflecting their high level of flexibility. The residues of the flap region also show a decreased heteronuclear NOE towards the tip of the flap, indicating a high level of flexibility on the picosecond-to-nanosecond timescale for these residues.

Discussion

Retroviral PRs are only active as homodimers, with the catalytic site positioned between the two identical subunits.[10–12,24] Extensive studies with the HIV-1 PR revealed the regions and sequence positions important for dimer formation: the essential structural feature for dimerization is the inter-monomeric four-stranded β-sheet involving the amino- and carboxy-termini of retroviral PRs. Since the carboxy-termini of both monomers form the inner strands of this β-sheet, truncation of the carboxy-terminus results in loss of dimer formation. The amino-termini stabilize the structure. Additionally, Arg87 of HIV-1 PR forms an intra-monomer hydrogen bond with Asp29. This interaction was suggested to orient the carboxy-terminus to form the β-sheet,[19,25] and, together with the adjacent residues (the triad Gly86–Arg87–N/D88), it is highly conserved in retroviral PRs.[10]

In SFVmac PRshort, this conserved arginine is replaced by a proline; therefore, this intra-monomer hydrogen bond cannot be formed. Furthermore, the sequence region Asn86–Leu99 (SFVmac PRshort) contains three prolines (Pro87, Pro91 and Pro97) at positions where retroviral PRs harbor α-helix C2 (e.g., HIV-1 PR, Gly86–Gly94) and the terminal β-strand (HIV-1 PR, Thr96–Phe99). Additionally, a proline (Pro3) is located in the amino-terminal sequence region of SFVmac PRshort, corresponding to the outer strand of the inter-monomeric β-sheet of retroviral PRs. The steric requirements for a proline make a location inside a helix or a β-strand unfavorable. This might prohibit the formation of the essential inter-monomeric β-sheet in SFVmac PRshort that is important for dimerization of HIV-1 PR. Thus, SFVmac PR lacks several important structural features necessary for dimer formation as observed for other retroviral PRs.

Mason–Pfizer monkey virus PR also exists as a monomer in solution.[26,27] For this retroviral PR, the formation of an intra-molecular disulfide bridge between a cysteine near the N-terminus and a second one near the C-terminus is proposed to be the activating mechanism for dimerization.[27,28] SFVmac PRshort does not contain cysteines at the N- or C-terminus, rendering such a mechanism impossible.

Finally, SFVmac PR harbors a Ser in the conserved DT/SG motif of the fireman's grip. For HIV, a mutation resulting in an exchange of Thr to Ser resulted in destabilization of the native dimer.[29] Furthermore, it was suggested that the fireman's grip mediates the initial contact of the two monomers, which leads to the proper conformation and orientation of the two polypeptide chains in the dimer,[29] in accordance with a higher dimer instability of FV PRs.

The high level of flexibility observed for SFVmac PRshort was also found in the truncated monomer[19] as well as in the unligated dimer[20] of HIV-1 PR. The tip of the flap is glycine-rich in all retroviral PRs.[10] The sequence region Gly48–Phe53 of HIV-1 PR contains four glycines (Gly48, Gly49, Gly51 and Gly52). Except for Gly48, all glycines are conserved in retroviral PRs. PRs, such as feline immunodeficiency virus and Rous sarcoma virus PRs, where Gly48 is exchanged for another amino acid contain a glycine at sequence position 53 (numbering corresponding to HIV-1 PR). Molecular dynamics calculations suggest that the opening of the flap of the dimeric retroviral PRs is essential for substrate entry.[30–34] The high number of glycines introduces the required flexibility by occupying regions of the Ramachandran map unfavorable for other amino acids.[34] The flap region of HIV-1 PR is very intolerant against glycine exchange, highlighting the important role of this amino acid for activity.[35] In contrast to other retroviral PRs, SFVmac PR contains only a single glycine, Gly53 (corresponding to Gly52 in HIV-1 PR), in the flap region. Despite the lack of three glycines in the tip of the flap, a high level of flexibility on the picosecond-to-nanosecond timescale still persists as shown by the $\{^1H\}^{15}N$ NOE data. Gly51Asn substitution in HIV-1 PR *in silico* demonstrates a reduced flexibility during molecular dynamics simulations.[34] Our experimental data on SFVmac PRshort suggest that the glycines themselves are not responsible for increased flap dynamics *per se* but probably increase the population of conformations necessary for substrate binding as proposed by molecular dynamics simulations.[34]

The monomeric state of SFVmac PR may be key in the regulation of the viral life cycle. PR activity is highly undesirable before polyproteins are packaged as, otherwise, proteins such as the viral IN, which does not harbor a packaging signal, will not be taken up into the virus particle.[36] Thus, PR activity is relevant and tolerable only after complete assembly of the virus particle, a problem faced by all retroviruses. It has been suggested that activation of retroviral PRs is not solely due to mass action (i.e., increase of protein concentration in the virus).[37] Even at concentrations of 1 mM protein and in the presence of a peptide substrate, dimerization of SFVmac PRshort cannot be detected by NMR, suggesting that FV PR dimerization can only take

place under particular conditions that we can mimic using high NaCl concentrations. How SFVmac PR is activated is still an unresolved issue, and viral or even cellular factors may be necessary for PR dimerization and activation.

Materials and Methods

Protein expression and purification

The plasmid pET28c-SFVmacPRshort[38] harboring the N-terminal 101 amino acid residues of SFVmac PR was expressed in the *Escherichia coli* strain Rosetta DE3 (Novagen, Darmstadt, Germany) grown in M9 minimal medium[39] supplemented with trace element solution TS2[40] and with $(^{15}NH_4)_2SO_4$ and 0.4% uniformly labeled ^{13}C glucose as the only N and C sources, respectively. When an OD_{600} (optical density at 600 nm) of 0.8–1.0 was reached, expression was induced by adding 0.2 mM IPTG and the cells were incubated further at 16 °C overnight. After the addition of lysozyme, DNase I and one PR inhibitor cocktail tablet (ethylenediaminetetraacetic acid free; Complete, Roche Diagnostics GmbH, Mannheim, Germany), cells were lysed by sonication (3×60 s, pulse=1.0, 100% amplitude) in binding buffer (50 mM Na_2HPO_4/NaH_2PO_4, pH 7.4, 300 mM NaCl, 10 mM imidazole and 0.5 mM DTT) and then centrifuged at 19,000*g* for 30 min at 4 °C. The protein was purified from the supernatant via the C-terminal 6× His tag by immobilized Ni^{2+} affinity chromatography (1 ml of IMAC, BioRad, Munich, Germany) under native conditions using an imidazole step gradient and dialyzed against 50 mM Na_2HPO_4/NaH_2PO_4, pH 7.4, 100 mM NaCl and 0.5 mM DTT.

Purification of recombinant SFVmac PR-RT was performed as described previously.[41] As judged by SDS-PAGE, the purity of all proteins used was >95%.

PR activity assay

The SFVmac RT IN cleavage site of the Pol polyprotein (ATQGSYVVH↓CNTTP) was cloned into the vector pETGB1a (G. Stier, EMBL, Heidelberg, Germany) between the GB1 and GFP coding sequences downstream of the sequence coding for a Tev cleavage site via PCR amplification and by using the restriction sites NcoI and PstI in order to obtain a substrate for SFVmac PR. The plasmid was transformed into the *Escherichia coli* strain Rosetta (DE3) (Novagen). Gene expression was induced at an OD_{600} of ca 0.8–1.0 by addition of 0.2 mM IPTG to obtain the fusion protein. Cells were grown overnight at 25 °C. After cell lysis (as described above), purification of the protein was done via Ni affinity chromatography (His-Trap, GE Healthcare, Munich, Germany), followed by chromatography over a QXL column (HighTrap, GE Healthcare).

PR activity assays were carried out using 10 μM concentration of the purified GB1–GFP fusion protein. GB1–GFP was incubated with 10 μM SFVmac PRshort or PR-RT or 0.5 μM Tev PR (positive control) at 37 °C for 16 h in a total volume of 300 μl. The reactions were carried out in 50 mM Na_2HPO_4/NaH_2PO_4, pH 7.4, and 0.5 mM DTT with 100 mM, 2 M or 3 M NaCl. Reaction products were analyzed by 19% SDS-PAGE.

Size exclusion chromatography

For analytical gel filtration of SFVmac PRshort, a Superdex 75 HR 10/30 column (GE Healthcare) was used. The column was loaded with 140 nmol PRshort in 50 mM Na_2HPO_4/NaH_2PO_4, pH 7.4, 0.5 mM DTT and 300 mM or 2 M NaCl. Calibration was performed with albumin (67 kDa), ovalbumin (43 kDa), chymotrypsinogen (25 kDa) and RNase A (13.7 kDa; GE Healthcare) using the same buffer. In the same way, 13 nmol SFVmac PR-RT was analyzed on a Superdex 200 HR 10/30 column (GE Healthcare) calibrated with catalase (232 kDa), aldolase (158 kDa), ovalbumin (43 kDa) and chymotrypsinogen (25 kDa; GE Healthcare).

Analytical ultracentrifugation

Sedimentation velocity experiments were performed on an Optima XL-I analytical centrifuge (Beckman Inc., Palo Alto, CA) using an An60Ti rotor and double-sector 12-mm centerpieces. Measurements were performed with 0.73 mg/ml of SFVmac PRshort in 50 mM Na–phosphate buffer, pH 7.4, containing 100 mM NaCl. Buffer density was measured to 1.01024 kg/l using a DMA 5000 densitometer (Anton Paar, Graz, Austria). Protein concentration distribution was monitored at 280 nm and at 60,000 rpm. Time-derivative analysis was computed using the SEDFIT software package,[42] resulting in a $g(s^*)$ distribution and an estimate for the molecular weight (from the sedimentation and diffusion coefficients, inferred from the peak width).

NMR spectroscopy

All NMR experiments were conducted at 298 K on a Bruker Avance 600- or 700-MHz (equipped with a cryogenic probe) spectrometer. In addition to the previously described experiments for resonance assignment,[38] the experiments subsequently discussed were conducted to obtain structural and dynamic data.

HNHB, ^{13}CO and ^{15}N spin-echo difference experiments were performed for χ_1 restraints.[43] ^{15}N- and ^{13}C-edited NOE spectroscopy (NOESY) experiments (mixing time=120 ms) were acquired for obtaining distance restraints.

For the characterization of overall and internal motions, ^{15}N longitudinal (R_1) and transverse (R_2) relaxation rates, together with the steady-state $\{^1H\}^{15}N$ NOE, were recorded using standard methods at 600.2 MHz ^1H frequency at a calibrated temperature of 297.7 K. For ^{15}N R_1, the delays for the relaxation delay were 10.75 (3×), 268.17 (3×), 643.58 (3×), 1072.62 (3×), 1930.70 (3×) and 2258.42 (3×) ms. For ^{15}N R_2, delays of 7.82 (3×), 23.52 (3×), 39.20 (3×), 78.40 (3×), 117.60 (3×), 156.80 (3×) and 196.00 (3×) ms were used. The steady-state $\{^1H\}^{15}N$ NOE spectra were measured with a 6 s relaxation delay. For the saturated subspectrum, 120° pulses with 5 ms inter-pulse delay were applied during the final 3 s of the relaxation delay. Relaxation delays of R_1 and R_2 relaxation experiments were fitted to a mono-exponential decay using the program CURVEFIT (A.G. Palmer, Columbia University, USA). The correlation time was determined for an isotropic tumbling model using the TENSOR2 package.[44]

NMR titration experiments were carried out using a synthetic peptide (Thermo Electron, Dreieich, Germany) corresponding to the RT IN cleavage site (indicated by an arrow) in the Pol polyprotein (TQGSYVVH↓CNTTP).

Structure calculations

Distance restraints for structure calculation were derived from ^{15}N- and ^{13}C-edited NOESY spectra. NOESY cross-peaks were classified according to their relative intensities

and converted to distance restraints with upper limits of 3.0 Å (*strong*), 4.0 Å (*medium*), 5.0 Å (*weak*) and 6.0 Å (*very weak*). For ambiguous distance restraints, the r^{-6} summation over all assigned possibilities defined the upper limit. Experimental NOESY spectra were validated semi-quantitatively against back-calculated spectra to confirm the assignment and to avoid bias of upper distance restraints by spin diffusion.

Hydrogen bonds were included for backbone amide protons in a regular secondary structure, when the amide proton does not show a water exchange cross-peak in the ^{15}N-edited NOESY spectrum. Dihedral restraints for χ_1 angles based on $^3J(N,H^\beta)$, $^3J(N,CH_3)$ and $^3J(CO,CH_3)$ coupling constants were included as restraints for the most probable rotamer with 30° tolerance. Dihedral restraints for φ angles were obtained from secondary chemical shifts and were included as ($-120°\pm40°$) restraints for residues in β-strands or ($-60°\pm40°$) restraints for residues in helical regions.

The structure calculations were performed with the program Xplor-NIH 1.2.1[45] using a three-step simulated annealing protocol with floating assignment of prochiral groups including a conformational database potential. The 20 structures showing the lowest values of the target function excluding the database potential were further analyzed with Xplor,[45] MOLMOL[17] and PROCHECK 3.5.4.[46]

Accession codes

The structure coordinates were deposited in the Protein Data Bank under accession code 2JYS. Chemical shift assignments[38] were deposited in the BioMagResBank under accession code 15403.

Acknowledgements

This project was funded by the Deutsche Forschungsgemeinschaft through grant WO630/7-1 to B.M.W. and by the Elite Network of Bavaria. We thank Dr. Stephan Uebel (Max Planck Institut für Biochemie, Martinsried, Germany) for performing the analytical ultracentrifugation, Andreas Hofmann for his help in enzyme purification and analysis and Prof. Dr. Axel Rethwilm for helpful discussions.

References

1. Rethwilm, A. (2003). The replication strategy of foamy viruses. *Curr. Top. Microbiol. Immunol.* **277**, 1–26.
2. Moebes, A., Enssle, J., Bieniasz, P. D., Heinkelein, M., Lindemann, D., Bock, M. *et al.* (1997). Human foamy virus reverse transcription that occurs late in the viral replication cycle. *J. Virol.* **71**, 7305–7311.
3. Roy, J., Rudolph, W., Juretzek, T., Gartner, K., Bock, M., Herchenröder, O. *et al.* (2003). Feline foamy virus genome and replication strategy. *J. Virol.* **77**, 11324–11331.
4. Yu, S. F., Sullivan, M. D. & Linial, M. L. (1999). Evidence that the human foamy virus genome is DNA. *J. Virol.* **73**, 1565–1572.
5. Flügel, R. M. & Pfrepper, K. I. (2003). Proteolytic processing of foamy virus Gag and Pol proteins. *Curr. Top. Microbiol. Immunol.* **277**, 63–88.
6. Linial, M. (2007). Foamy viruses. In (Knipe, D. M. & Howley, P. M., eds), pp. 2245–2262, Lippincott Williams & Wilkins, Philadelphia, PA.
7. Rethwilm, A. (2005). Foamy viruses. In (ter Meulen, V. & Mahy, B. W. J., eds), pp. 1304–1321, Hodder Arnold, London, UK.
8. Konvalinka, J., Löchelt, M., Zentgraf, H., Flügel, R. M. & Kräusslich, H.-G. (1995). Active foamy virus proteinase is essential for virus infectivity but not for formation of a Pol polyprotein. *J. Virol.* **69**, 7264–7268.
9. Grant, S. K., Deckman, I. C., Culp, J. S., Minnich, M. D., Brooks, I. S., Hensley, P. *et al.* (1992). Use of protein unfolding studies to determine the conformational and dimeric stabilities of HIV-1 and SIV proteases. *Biochemistry*, **31**, 9491–9501.
10. Wlodawer, A. & Gustchina, A. (2000). Structural and biochemical studies of retroviral proteases. *Biochim. Biophys. Acta*, **1477**, 16–34.
11. Dunn, B. M., Goodenow, M. M., Gustchina, A. & Wlodawer, A. (2002). Retroviral proteases.*Genome Biol.* **3**, 3006; REVIEWS.
12. Wlodawer, A., Miller, M., Jaskolski, M., Sathyanarayana, B. K., Baldwin, E., Weber, I. T. *et al.* (1989). Conserved folding in retroviral proteases: crystal structure of a synthetic HIV-1 protease. *Science*, **245**, 616–621.
13. Jaskolski, M., Miller, M., Rao, J. K., Leis, J. & Wlodawer, A. (1990). Structure of the aspartic protease from Rous sarcoma retrovirus refined at 2-Å resolution. *Biochemistry*, **29**, 5889–5898.
14. Pfrepper, K. I., Rackwitz, H. R., Schnölzer, M., Heid, H., Löchelt, M. & Flügel, R. M. (1998). Molecular characterization of proteolytic processing of the Pol proteins of human foamy virus reveals novel features of the viral protease. *J. Virol.* **72**, 7648–7652.
15. Fenyöfalvi, G., Bagossi, P., Copeland, T. D., Oroszlan, S., Boross, P. & Tözsér, J. (1999). Expression and characterization of human foamy virus proteinase. *FEBS Lett.* **462**, 397–401.
16. Boross, P., Tözser, J. & Bagossi, P. (2006). Improved purification protocol for wild-type and mutant human foamy virus proteases. *Protein Expression Purif.* **46**, 343–347.
17. Koradi, R., Billeter, M. & Wüthrich, K. (1996). MOLMOL: a program for display and analysis of macromolecular structure. *J. Mol. Graphics*, **14**, 51–55.
18. Ishima, R., Torchia, D. A., Lynch, S. M., Gronenborn, A. M. & Louis, J. M. (2003). Solution structure of the mature HIV-1 protease monomer: insight into the tertiary fold and stability of a precursor. *J. Biol. Chem.* **278**, 43311–43319.
19. Ishima, R., Ghirlando, R., Tozser, J., Gronenborn, A. M., Torchia, D. A. & Louis, J. M. (2001). Folded monomer of HIV-1 protease. *J. Biol. Chem.* **276**, 49110–49116.
20. Freedberg, D. I., Ishima, R., Jacob, J., Wang, Y. X., Kustanovich, I., Louis, J. M. & Torchia, D. A. (2002). Rapid structural fluctuations of the free HIV protease flaps in solution: relationship to crystal structures and comparison with predictions of dynamics calculations. *Protein Sci.* **11**, 221–232.
21. Ishima, R. & Louis, J. M. (2007). A diverse view of protein dynamics from NMR studies of HIV-1 protease flaps. *Proteins*, **70**, 1408–1415.
22. Nicastro, G., Margiocco, P., Cardinali, B., Stagnaro, P., Cauglia, F., Cuniberti, C. *et al.* (2004). The role of unstructured extensions in the rotational diffusion properties of a globular protein: the example of the titin i27 module. *Biophys. J.* **87**, 1227–1240.
23. Kay, L. E., Torchia, D. A. & Bax, A. (1989). Backbone dynamics of proteins as studied by ^{15}N inverse

detected heteronuclear NMR spectroscopy: application to staphylococcal nuclease. *Biochemistry*, **28**, 8972–8979.
24. Katoh, I., Ikawa, Y. & Yoshinaka, Y. (1989). Retrovirus protease characterized as a dimeric aspartic proteinase. *J. Virol.* **63**, 2226–2232.
25. Louis, J. M., Ishima, R., Nesheiwat, I., Pannell, K. L., Lynch, S. M., Torchia, D. A. & Gronenborn, A. M. (2003). Revisiting monomeric HIV-1 protease. Characterization and redesign for improved properties. *J. Biol. Chem.* **278**, 6085–6092.
26. Veverka, V., Bauerova, H., Zabransky, A., Pichova, I. & Hrabal, R. (2001). Backbone resonance assignment of protease from Mason–Pfizer monkey virus. *J. Biomol. NMR*, **20**, 291–292.
27. Veverka, V., Bauerova, H., Zabransky, A., Lang, J., Ruml, T., Pichova, I. & Hrabal, R. (2003). Three-dimensional structure of a monomeric form of a retroviral protease. *J. Mol. Biol.* **333**, 771–780.
28. Zabranska, H., Tuma, R., Kluh, I., Svatos, A., Ruml, T., Hrabal, R. & Pichova, I. (2007). The role of the S–S bridge in retroviral protease function and virion maturation. *J. Mol. Biol.* **365**, 1493–1504.
29. Ingr, M., Uhlikova, T., Strisovsky, K., Majerova, E. & Konvalinka, J. (2003). Kinetics of the dimerization of retroviral proteases: the "fireman's grip" and dimerization. *Protein Sci.* **12**, 2173–2182.
30. Harte, W. E., Jr., Swaminathan, S., Mansuri, M. M., Martin, J. C., Rosenberg, I. E. & Beveridge, D. L. (1990). Domain communication in the dynamical structure of human immunodeficiency virus 1 protease. *Proc. Natl. Acad. Sci. USA*, **87**, 8864–8868.
31. York, D. M., Darden, T. A., Pedersen, L. G. & Anderson, M. W. (1993). Molecular dynamics simulation of HIV-1 protease in a crystalline environment and in solution. *Biochemistry*, **32**, 1443–1453.
32. Liu, H., Muller-Plathe, F. & van Gunsteren, W. F. (1996). A combined quantum/classical molecular dynamics study of the catalytic mechanism of HIV protease. *J. Mol. Biol.* **261**, 454–469.
33. Rick, S. W., Erickson, J. W. & Burt, S. K. (1998). Reaction path and free energy calculations of the transition between alternate conformations of HIV-1 protease. *Proteins*, **32**, 7–16.
34. Scott, W. R. & Schiffer, C. A. (2000). Curling of flap tips in HIV-1 protease as a mechanism for substrate entry and tolerance of drug resistance. *Structure*, **8**, 1259–1265.
35. Shao, W., Everitt, L., Manchester, M., Loeb, D. D., Hutchison, C. A., III & Swanstrom, R. (1997). Sequence requirements of the HIV-1 protease flap region determined by saturation mutagenesis and kinetic analysis of flap mutants. *Proc. Natl. Acad. Sci. USA*, **94**, 2243–2248.
36. Peters, K., Wiktorowicz, T., Heinkelein, M. & Rethwilm, A. (2005). RNA and protein requirements for incorporation of the Pol protein into foamy virus particles. *J. Virol.* **79**, 7005–7013.
37. Schatz, G. W., Reinking, J., Zippin, J., Nicholson, L. K. & Vogt, V. M. (2001). Importance of the N terminus of Rous sarcoma virus protease for structure and enzymatic function. *J. Virol.* **75**, 4761–4770.
38. Hartl, M. J., Wöhrl, B. M. & Schweimer, K. (2007). Sequence-specific ^{1}H, ^{13}C and ^{15}N resonance assignments and secondary structure of a truncated protease from simian foamy virus. *Biomol. NMR Assign.* **1**, 175–177.
39. Sambrook, J., Fritsch, E. F. & Maniatis, T. (1994). *Molecular Cloning—A Laboratory Manual.* Cold Spring Harbor Laboratory Press, Cold Spring Harbor, NY.
40. Meyer, O. & Schlegel, H. G. (1983). Biology of aerobic carbon-monoxide oxidizing bacteria. *Annu. Rev. Microbiol.* **37**, 277–310.
41. Hartl, M. J., Kretzschmar, B., Frohn, A., Nowrouzi, A., Rethwilm, A. & Wöhrl, B. M. (2008). AZT resistance of simian foamy virus reverse transcriptase is based on the excision of AZTMP in the presence of ATP. *Nucleic Acids Res.* **36**, 1009–1016.
42. Schuck, P. (2000). Size-distribution analysis of macromolecules by sedimentation velocity ultracentrifugation and Lamm equation modeling. *Biophys. J.* **78**, 1606–1619.
43. Bax, A., Vuister, G. W., Grzesiek, S., Delaglio, F., Wang, A. C., Tschudin, R. & Zhu, G. (1994). Measurement of homo- and heteronuclear J couplings from quantitative J correlation. *Methods Enzymol.* **239**, 79–105.
44. Dosset, P., Hus, J. C., Blackledge, M. & Marion, D. (2000). Efficient analysis of macromolecular rotational diffusion from heteronuclear relaxation data. *J. Biomol. NMR*, **16**, 23–28.
45. Schwieters, C. D., Kuszewski, J. J., Tjandra, N. & Clore, G. M. (2003). The Xplor-NIH NMR molecular structure determination package. *J. Magn. Reson.* **160**, 65–73.
46. Laskowski, R. A., MacArthur, M. W., Moss, D. S. & Thornton, J. M. (1993). PROCHECK: a program to check the stereochemical quality of protein structures. *J. Appl. Crystallogr.* **26**, 283–291.

12 Publication F

Maximilian J. Hartl, Kristian Schweimer, Martin H. Reger, Stephan Schwarzinger, Jochen Bodem, Paul Rösch and Birgitta M. Wöhrl (2010): Formation of transient dimers by a retroviral protease. *Biochemical Journal* **427**, 197-203.

BJ www.biochemj.org

BJ Structure

Biochem. J. (2010) **427**, 197–203 (Printed in Great Britain) doi:10.1042/BJ20091451

Formation of transient dimers by a retroviral protease

Maximilian J. HARTL*, Kristian SCHWEIMER*, Martin H. REGER*, Stephan SCHWARZINGER*, Jochen BODEM†, Paul RÖSCH* and Birgitta M. WÖHRL*[1]

*Universität Bayreuth, Lehrstuhl für Struktur und Chemie der Biopolymere and Research Centre for Biomacromolecules, Bayreuth 95440, Germany, and †Universität Würzburg, Institut für Virologie und Immunbiologie, Würzburg 97978, Germany

Retroviral proteases have been shown previously to be only active as homodimers. They are essential to form the separate and active proteins from the viral precursors. Spumaretroviruses produce separate precursors for Gag and Pol, rather than a Gag and a Gag–Pol precursor. Nevertheless, processing of Pol into a PR (protease)–RT (reverse transcriptase) and integrase is essential in order to obtain infectious viral particles. We showed recently that the PR–RT from a simian foamy virus, as well as the separate PRshort (protease) domain, exhibit proteolytic activities, although only monomeric forms could be detected. In the present study, we demonstrate that PRshort and PR–RT can be inhibited by the putative dimerization inhibitor cholic acid. Various other inhibitors, including darunavir and tipranavir, known to prevent HIV-1 PR dimerization in cells, had no effect on foamy virus protease *in vitro*. ^{1}H-^{15}N HSQC (heteronuclear single quantum coherence) NMR analysis of PRshort indicates that cholic acid binds in the proposed PRshort dimerization interface and appears to impair formation of the correct dimer. NMR analysis by paramagnetic relaxation enhancement resulted in elevated transverse relaxation rates of those amino acids predicted to participate in dimer formation. Our results suggest transient PRshort homodimers are formed under native conditions but are only present as a minor transient species, which is not detectable by traditional methods.

Key words: cholic acid, foamy virus, NMR, paramagnetic relaxation enhancement (PRE), protease, spin label, transient dimer.

INTRODUCTION

The virus family of *retroviridae* consists of the two subfamilies *orthoretrovirinae* and *spumaretrovirinae* or FVs (foamy viruses). Retroviruses create viral proteins by producing large polyprotein precursors, derived from the three genes *gag*, *pol* and *env*. *gag* encodes the structural proteins (e.g. capsid, matrix and nucleocapsid protein), *pol* harbours the ORFs (open reading frames) for the viral enzymes [PR (protease), RT (reverse transcriptase) and integrase] and *env* encodes for the surface and transmembrane proteins, which are localized in the viral lipid envelope and are essential for binding to the cellular receptors. The Gag and Pol polyprotein precursors are processed by the viral PR during virion maturation [1].

FVs differ in several aspects from *orthoretrovirinae*, e.g. FVs synthesize separate Gag and Pol precursors whereas in the case of *orthoretrovirinae* a Gag and a Gag–Pol precursor are formed. In FVs the PR domain, which is located at the N-terminus of the Pol precursor protein, is not cleaved off from the RT. Only the C-terminal integrase is removed from Pol, thus leading to a mature PR–RT enzyme [2–5]. In contrast, in *orthoretrovirinae* the PR is created by autoprocessing of the Gag–Pol precursor protein and is subsequently present as a separate enzyme [6,7].

PRs from retroviruses are members of the well-characterized family of aspartic PRs [8,9]. This group also includes cellular mammalian PRs such as chymosin and pepsin. In contrast with the cellular proteases, which are monomers with distinct N- and C-terminal domains, retroviral PRs are homodimers [10]. In order to create the active site of retroviral PRs each subunit of the homodimer contributes one catalytic aspartate residue located in the conserved motif Asp-Thr/Ser-Gly. Moreover, the flap and the C- and N-termini are important for formation of the active dimer [7].

In orthoretroviruses the viral genomic RNA and the precursor proteins are packaged to form the viral particles. Therefore regulation of the activity of retroviral PRs during the viral life cycle is absolutely required to avoid premature processing of the precursors. If untimely cleavage of the polyproteins happened before virus assembly, this would lead to incomplete uptake of various viral proteins as not all of them harbour independent packaging signals.

For HIV-1 it has been shown that regulation of PR activity in the Gag–Pol precursor protein is modulated by the N-terminal flanking transframe region sequence [11–16], whereas the C-terminal RT domain does not significantly influence the PR activity of the precursor [17,18]. The presence of the N-terminal extension leads to the formation of weak dimers with low PR activity. Once the N-terminal region is cleaved off, stable and active PR dimers can be formed [19]. This type of regulation cannot take place with the FV PR as there is no Gag–Pol precursor and thus no N-terminal extension of the PR. How FV PRs are activated is still unknown. Nevertheless, dimerization, in order to form the catalytic centre, also appears to be a prerequisite for FV PR activity.

We have demonstrated recently that PRshort (the separate PR domain) of SFVmac [SFV (simian foamy virus) from macaques], as well as the full length PR–RT, exhibit proteolytic activity. Nevertheless, both enzymes appear as monomeric protein species when analysed by size-exclusion chromatography or analytical ultracentrifugation [20]. Furthermore, determination of the solution structure of PRshort by NMR also corroborated the existence of a monomeric protein [20]. We thus postulated that

Abbreviations used: FV, foamy virus; GB1, immunoglobulin-binding domain B1 of streptococcal protein G; GFP, green fluorescent protein; HSQC, heteronuclear single quantum coherence; oxyl-1-NHS, 1-oxyl-2,2,5,5-tetramethylpyrroline-3-carboxylate *N*-hydroxysuccinimide ester; PR, protease; PRE, paramagnetic relaxation enhancement; PRshort, separate PR domain; RT, reverse transcriptase; SFV, simian foamy virus; SFVmac, SFV from macaques.

[1] To whom correspondence should be addressed (email birgitta.woehrl@uni-bayreuth.de).

PRshort, as well as the PR domain of PR–RT, have to form weak transient dimers that are only present under certain conditions and are only populated to a low fraction and are not detectable by the methods and/or conditions applied previously.

Thus we set out to analyse the monomer/dimer status of PRshort by PRE (paramagnetic relaxation enhancement) analysis, a NMR method exquisitely suited for detecting the presence of minor species, in our case the postulated transient dimer [21–23].

A transient state is characterized by an equilibrium between a lowly populated short-lived state in high-dynamic exchange with the ground state. The fast exchange of the different states causes an averaging of observable properties. If the lowly populated transient state does not contribute significantly to the observed parameters it remains undetected. This could be the reason why several techniques for apparent molecular mass determination of PRshort could not detect a dimer.

PRE relies on the fact that the nuclear spins can be influenced by an unpaired electron of a paramagnetic molecule in close proximity, i.e. less than approx. 20 Å (1 Å = 0.1 nm) away. Depending on the distance, the interaction of the nuclear spin with the unpaired electron can enhance transverse relaxation rates up to several decades; a paramagnetic centre of a nitroxyl group located approx. 8 Å from a given amide proton adds approx. 1800 Hz to the transverse relaxation rate, typically in the range 30–50 Hz in the diamagnetic state. Therefore even a low fraction of transient states contributes significantly to the observed population averaged rate and allows the detection of these states. In the case of transient interactions between different molecules (e.g. dimer formation) the interaction can be detected elegantly by placing the nuclear spins observed by NMR spectroscopy and the paramagnetic centres on different molecules [21–23].

In the present study, we show for the first time by biochemical and NMR analyses, using a PR inhibitor and PRE, that indeed a transient SFVmac PR homodimer is formed.

EXPERIMENTAL

Gene expression and protein purification

Expressions and purifications of ^{15}N-labelled and unlabelled SFVmac PRshort and PR–RT and the PR substrate GB1 (immunoglobulin-binding domain B1 of streptococcal protein G)–GFP (green fluorescent protein) were performed as described previously [20,24,25].

PR inhibition assay

The proteolytic activities of SFVmac PR–RT and PRshort were tested as described previously [20] in buffer [50 mM Na_2HPO_4/NaH_2PO_4, pH 6.4, containing 3 M NaCl and 0.5 mM DTT (dithiothreitol)] for 2 h at room temperature (20 °C) using substrate and enzyme concentrations of 10 and 5 μM respectively. The inhibitor tipranavir was dissolved in 5 % (v/v) ethyl acetate to a concentration of 500 μM. Darunavir and the peptidyl inhibitor indinavir sulfate were dissolved in water to concentrations of 250 and 500 μM respectively. These three reagents were obtained through the AIDS Research and Reference Reagent Program, Division of AIDS, National Institute of Allergy and Infectious Diseases (NIAID), National Institutes of Health. Cholic acid, betulinic acid (both Roth) and lithocholic acid (Sigma–Aldrich) were dissolved in 100 % DMSO at concentrations of 600, 530 and 130 mM respectively. The final DMSO or ethyl acetate concentration in the activity assays was 1 %.

The final concentrations of cholic acid in the assays are indicated in Figure 1. Reaction products were separated by electrophoresis on 10 % Bis-Tris gels (Invitrogen) in buffer (50 mM Mes, pH 7.3, containing 50 mM Tris base, 0.1 % SDS and 1 mM EDTA) and quantified by analysing the bands densitometrically using the software Quantity One on a Gel Doc 2000 device (Bio-Rad Laboratories). The concentration of inhibitor at which half of the PR activity was measured was defined as IC_{50}. To determine the IC_{50}, a curve was fitted to the data using a 4PL (four-parameter logistic model), also called Hill slope model [26], with the slope describing the steepness of the curve:

$$\%\ \text{activity} = \min + \frac{\max - \min}{1 + ([\text{inhibitor}]/IC_{50})^{\text{slope}}}$$

where min is the percentage minimal enzyme activity and max is percentage maximal enzyme activity.

Tissue culture assays

Antiviral activity of cholic acid was analysed essentially as described previously [27]. In brief, HEK-293T cells [HEK (human embryonic kidney)-293 cells expressing the large T-antigen of SV40 (simian virus 40)] were transfected with pcHSRV2, SFV-1 and NL4-3. The supernatants were removed 16 h after transfection and replaced by fresh pre-warmed medium containing cholic acid at final concentrations from 0.125 to 2 mM or a DMSO solvent control. All cholic acid titrations were performed in independent triplicate assays. Cells were harvested 48 h after infection [27], washed twice with PBS and lysed with 200 μl sample buffer [27], and Gag expression was analysed by Western blotting. Infectious viral titres were determined on indicator cells, which expressed the *LacZ* gene from an LTR (long terminal repeat) promoter responsive to the respective viral transactivator.

Spin labelling of PRshort

Spin labelling of the ε-amino groups of lysine residues was performed essentially as described previously [28,29]. Freeze-dried SFVmac PRshort was dissolved in 10 mM Na_2HCO_3, pH 9.2, to a final concentration of 9.4 mg/ml. Oxyl-1-NHS (1-oxyl-2,2,5,5-tetramethylpyrroline-3-carboxylate *N*-hydroxysuccinimide ester; Toronto Research Chemicals) was dissolved in 100 % DMSO and added to the PRshort solution at an approx. 5-fold molar excess over the basic ε-amino groups of PRshort. The solution was incubated using an end-over-end shaker at room temperature for 1 h followed by 1 h at 4 °C. Buffer exchange was performed by dialysing the solution against buffer (50 mM Na_2HPO_4/NaH_2PO_4, pH 7.4, containing 300 mM NaCl) using a Vivaspin concentrator with a molecular mass cut-off of 5000 (Sartorius). The efficiency of the labelling procedure was analysed by MALDI–TOF (matrix-assisted laser-desorption ionization–time-of-flight) at the Zentrale Bioanalytik, Universität Köln, Germany, and indicated a mixture of different PRshort species containing one to all nine labelled lysine residues (results not shown). The labelled species were almost equally distributed with a slightly increased peak for the doubly labelled species. Owing to the solvent-exposed position of all lysine residues in PRshort we assume a random distribution of the spin label in cases of incomplete labelling. The fractional presence of completely labelled PRshort in the mass spectrum showed that all lysine residues are accessible for labelling. The reaction was not driven further to completion in order to avoid large influences of the spin label on the PR structure or on dimer formation.

NMR measurements

NMR experiments were recorded on Bruker Avance 600 MHz, 700 MHz (equipped with a CryoProbe) and 800 MHz (equipped with a CryoProbe) spectrometers at a sample temperature of 298 K.

NMR samples contained 100–200 μM ^{15}N-labelled SFVmac PRshort in 50 mM Na_2HPO_4/NaH_2PO_4, pH 7.4, containing 100 mM NaCl and 1 mM DTT. Samples used for PRE measurements did not contain DTT to avoid reduction of the spin label. Cholic acid was added to the desired concentration from a stock solution in DMSO. Addition of the same amount of free DMSO to the PR solution did not result in any chemical shift changes. This verifies the absence of DMSO binding to PRshort. Resonance assignments were taken from the literature [20,24]. PREs of amide protons were determined using a two-point measurement with an HSQC (heteronuclear single quantum coherence)-based experiment [30]. The dissociation constant for cholic acid was determined by fitting the chemical shift changes to a two-state model during successive addition of cholic acid in a series of HSQC experiments.

RESULTS

In vitro inhibition of PR activity by cholic acid

We have shown previously by prevalent methods that FV PR behaves like a monomeric protein [20]. However, dimerization is a prerequisite for functional retroviral PRs. As we were able to detect proteolytic activities with FV PR, we postulated that a low population of the protein is present as a dimer. Thus potential protease dimerization inhibitors should be able to inhibit proteolytic activity.

For HIV-1, triterpenes and steroids have been shown to inhibit PR activity [31]. Molecular modelling studies with HIV-1 PR suggested that these substances work by inhibiting dimerization or formation of the correct, and thus active, dimer [32]. The structures of retroviral PRs are very similar, even if their primary sequences exhibit large differences [7,33]. The monomer structure of SFVmac PRshort reveals high structural homology with the HIV-1 PR monomer, as well as to the monomeric subunits of the homodimer, even though the similarity on the amino acid level is only approx. 29 % [20,34,35]. Therefore we tested whether the steroid inhibitors cholic acid, lithocholic acid and betulinic acid, which have been shown to inhibit HIV-1 PR activity [32], are also able to inhibit PR activity of SFVmac PRshort and of full length PR–RT. The IC_{50} values for *in vitro* HIV-1 PR inhibition by these substances were approx. 350 μM for cholic acid, 10 μM for lithocholic acid and 2.5 μM for betulinic acid [32].

The proteolytic activities of PRshort and the full length PR–RT were tested with a GB1–GFP fusion protein, a substrate used previously, harbouring the natural SFVmac PR cleavage site of the Pol precursor between the GB1 and GFP domains [20]. As we have shown previously that, similar to other FV PRs, SFVmac PRshort is only active at high salt concentrations, the pH optimum for PR activity was determined using NaCl concentrations of 3 M [20]. Our results indicated the highest cleavage activity at pH 6.4 (results not shown), thus these conditions were used for further analyses.

Our results using cholic acid (Figure 1) show that substrate cleavage can be inhibited *in vitro* at increasing cholic acid concentrations, implying that this HIV-1 PR inhibitor is functional with SFVmac PRshort as well as PR–RT. Quantification of the cleavage products yielded comparable IC_{50} values for cholic acid, approx. 0.6 mM for SFVmac PRshort and 0.75 mM for PR–RT.

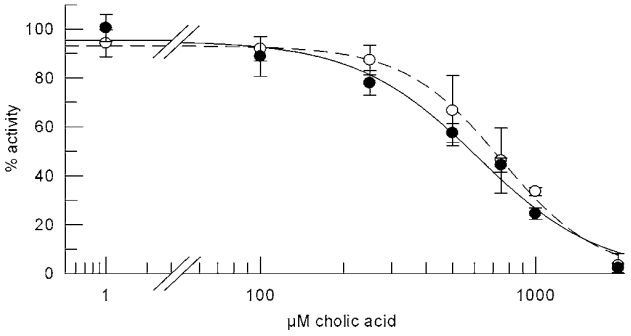

Figure 1 PRshort and PR–RT inhibition by cholic acid

Inhibition of 5 μM SFVmac PR–RT (○) or PRshort (●) by increasing concentrations of cholic acid. The IC_{50} values for PR–RT (749 $\pm$ 32 μM) and PRshort (615 $\pm$ 70 μM) were determined. The curves show the best fit to the data using the equation given in the Experimental section.

Testing the inhibitory effect of cholic acid against SFVmac in tissue culture assays was prevented by the toxicity of the substance for the cells at concentrations higher than 500 μM. The IC_{50} values for PR–RT using lithocholic acid was approx. 1 mM, whereas the IC_{50} of betulinic acid could not be determined due to enzyme precipitation upon addition (results not shown).

As the IC_{50} values obtained with the steroid derivatives are relatively high, we tested additional substances known to inhibit the PR activity of HIV-1 at much lower concentrations than cholic acid. Two non-peptidyl inhibitors, namely darunavir and tipranavir, are used for the treatment of HIV infections in patients. They have been shown to inhibit HIV-1 replication by blocking the formation of active PR dimers at the stage of PR maturation [36–38]. However, they fail to dissociate mature PR dimers [36]. These inhibitors prevent HIV-1 PR dimerization at concentrations as low as 0.01 μM [36]. As the largest portion of FV PR–RT is monomeric, these inhibitors appeared to be good candidates to prevent FV PR dimerization. However, neither of these substances was able to inhibit the proteolytic activity of PR–RT at concentrations up 100 μM in our assays (results not shown).

Furthermore, the peptidomimetic HIV-1 PR inhibitor indinavir, an active-site transition state analogue, was also not capable of inhibiting FV PR–RT at concentrations up to 100 μM. Thus we used cholic acid for further analysis.

Cholic acid binds in the putative dimerization interface of SFVmac PR

To determine the inhibitor-binding interface and to confirm the integrity of the three-dimensional structure of PRshort after inhibitor addition, we analysed PRshort in the absence and presence of increasing concentrations of cholic acid by observing chemical shift perturbations in ^{1}H-^{15}N HSQC experiments (Figure 2A). Addition of cholic acid to ^{15}N-labelled PRshort, up to a protein/inhibitor ratio of 1:150, led to gradual chemical shift changes in the ^{1}H-^{15}N HSQC spectra, characteristic for complex formation in the fast-exchange regime of the NMR time scale. Residues showing chemical shift perturbation upon addition of cholic acid were found in (or sequentially close to) the active-site loop (e.g. Trp^{23}, Ala^{27}, Thr^{28}, Thr^{30} and Val^{32}), the flap region (Ile^{43}, Thr^{45}, Met^{46}, Lys^{49}, Thr^{50}, His^{51} and Gln^{57}) and in the C-terminal region (Leu^{93}, Met^{94}, Lys^{96} and Leu^{100}). All of these regions contribute to the known dimer interface for retroviral PRs, e.g. the essential intermonomeric antiparallel β-sheet involving the N- and C-termini, as well as contacts close to the active site and the flap region [7,33,34] (Figures 2B–2D).

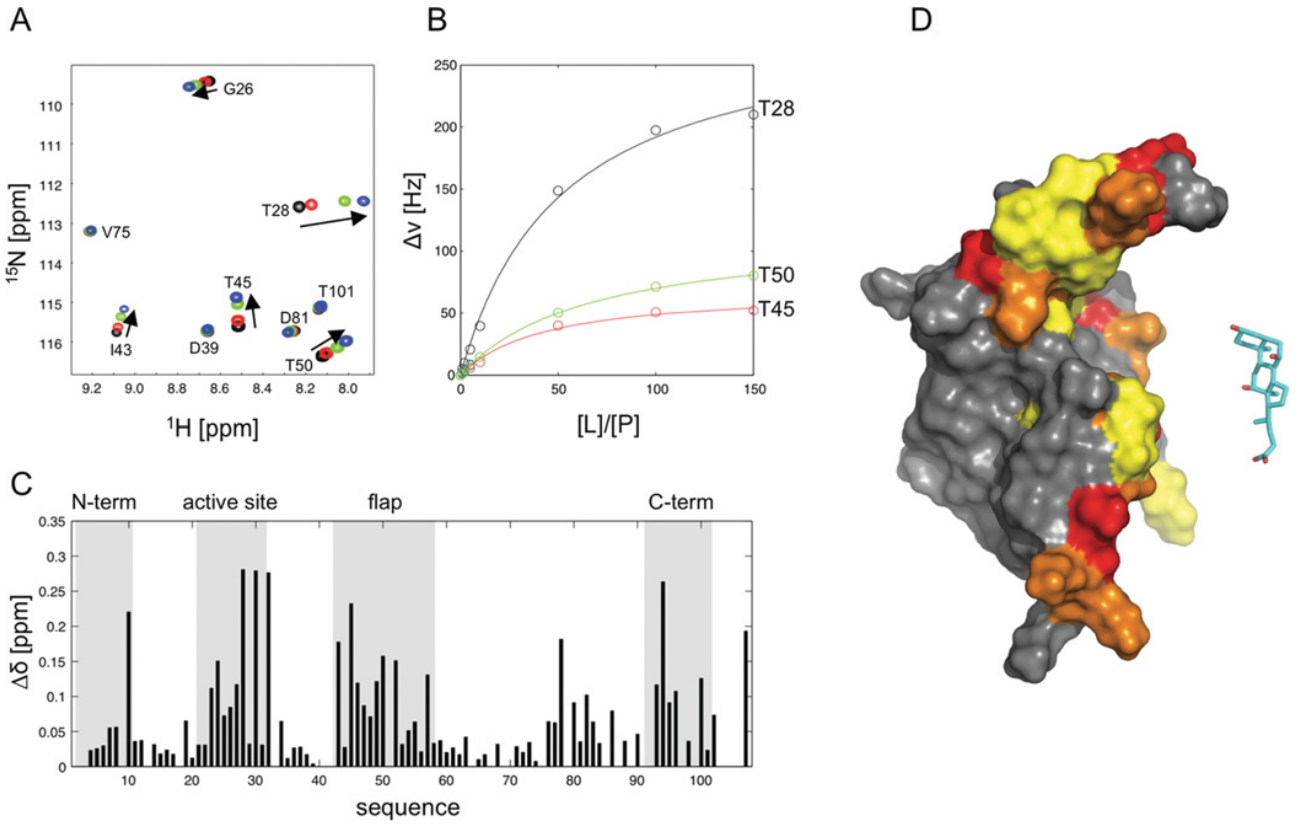

Figure 2 Determination of the inhibitor-binding interface

(**A**) Overlay of ^{1}H-^{15}N HSQC spectra recorded during titration with different protein (100 μM)/inhibitor ratios. Black 1:0; red 1:5; green 1:50; and blue 1:150. (**B**) Determination of the dissociation constant for cholic acid. Normalized chemical shift changes of residues Thr^{28} (K_d of 5.1 mM), Thr^{45} (K_d = 4.3 mM) and Thr^{50} (K_d of 6.6 mM) are shown exemplarily as a function of the cholic acid ([L])/PRshort ([P]) ratio. (**C**) Normalized chemical shift changes for PRshort upon cholic acid binding. Changes larger than 0.05 p.p.m. were considered significant. Changes from 0.05 to 0.15 p.p.m. were assigned as weak, >0.15–0.25 p.p.m. as medium, and >0.25 p.p.m. as strong. (**D**) Observed chemical shift changes colour coded on a ribbon diagram of the PRshort monomer (PDB code 2JYS). The amino acids showing significant chemical shift changes are indicated in yellow (weak), orange (medium) and red (strong). The structure and relative size of cholic acid is shown on the right-hand side.

From the chemical shift changes obtained upon addition of cholic acid, the dissociation constant (K_d) could be determined assuming a two-state binding model. Exemplified titration curves for some of these residues are shown in Figure 2(B). The K_d values determined for all of the amino acids analysed were in the range of 5.3 ± 0.9 mM. For residues spatially close to the N- and C-terminus (Leu^{10} and Met^{94}) slightly weaker affinities were observed (a K_d of 10 mM). Comparison of the dimensions of the interaction surface, defined by strongly shifting residues, with the size of cholic acid reveals a region significantly larger than cholic acid (Figure 2D). The chemical shift changes observed may arise from direct interaction of amino acid residues with cholic acid or by subtle structural changes (e.g. side chain rotations) transmitted to regions farther away from the exact binding site. Therefore determining a more detailed location of the binding site on SFVmac PRshort is difficult. Taken together, our results suggest that the inhibitor impairs the formation of an active PRshort dimer which in turn hinders the ability of PR to catalyse substrate cleavage.

Specific transient dimerization detected by PRE

Electron–nuclear spin interactions that result in a dramatic enhancement of transverse relaxation rates of protons close to a paramagnetic centre [22,23,40], could be assigned to residues from the N- and C-terminal regions (Figure 3A) (e.g. Leu^{7}, Leu^{8}, Lys^{96} and Leu^{98}), from the active-site loop (e.g. Trp^{23}, Asp^{24}, Ser^{25}, Thr^{28} and Ile^{29}) and from the flap region (e.g. Lys^{49} and Gln^{56}). All of these regions are known to contribute to the dimer formation of active retroviral PRs [7,41]. These results clearly demonstrate an interaction of spin-labelled with ^{15}N-labelled SFVmac PRshort. The transversal relaxation rates, Γ_2, after the addition of spin-labelled PRshort indicated that the residues affected are located in the putative dimerization region of the PRshort monomer (Figure 3B). Amide protons of residues far from the dimerization interface do not exhibit significant changes in the transversal relaxation rates, demonstrating that the transient dimerization of SFVmac PR is structure-specific (Figure 3C).

Despite the large distance between Gln^{67} and Lys^{70} and the dimerization interface, significant Γ_2 values were observed. These residues are located in the β-sheet strand 6 and the preceding loop. Inspection of the dimeric structure of HIV-1 PR reveals that this region is close to the intermonomeric β-sheet [34]. Therefore short distances to residues of the C-terminal region of the other monomer carrying spin-labelled lysine residues can be expected.

To support the hypothesis of the role of cholic acid as a dimerization inhibitor, the inhibitor was added to the mixture of ^{15}N- and spin-labelled PRshort (Figure 4). Chemical shift changes

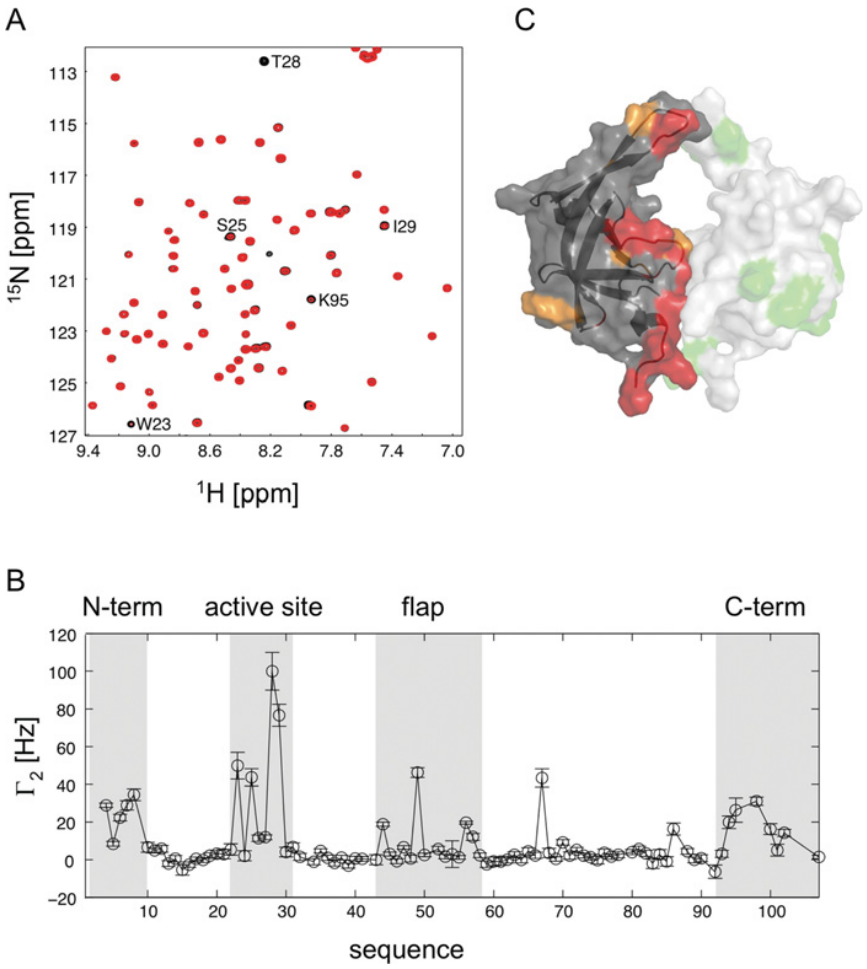

Figure 3 Determination of the dimer interface

(**A**) Overlay of ^{1}H-^{15}N HSQC spectra of ^{15}N-labelled PRshort recorded in the absence (black) or presence (red) of equimolar amounts of PRshort labelled at lysine residues with the paramagnetic spin label oxyl-1-NHS. (**B**) The PREs of ^{15}N-labelled PRshort after the addition of the spin-labelled PRshort. The relevant regions of the protein are indicated at the top of the Figure. (**C**) Three-dimensional structure representing the hypothetical SFVmac PR dimer. The structure is based on the crystal structure of HIV-1 PR (PDB code 3HVP). The left half of the molecule represents the ^{15}N-labelled monomer with colour coded PREs upon addition of spin-labelled PR. Residues with PREs >20 Hz are coloured red, with PREs >10 Hz are coloured orange. Spin-labelled lysine residues are highlighted in green on the right-hand monomer subunit.

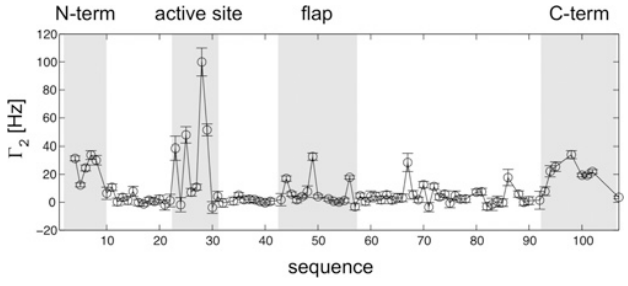

Figure 4 PREs in the presence of cholic acid

The PREs of ^{15}N-labelled PRshort after the addition of cholic acid to the mixture. Numbers indicate the sequence position and the relevant regions of the protein are labelled at the top of the figure.

observed for the ^{15}N-labelled PRshort are virtually identical with the values found in the previous titration experiments presented in Figure 2 where ^{15}N-labelled PRshort is titrated with cholic acid. These results confirm the binding of cholic acid. The titration curves reveal saturation with cholic acid to an extent of approx. 70 %. The PRE rates observed for the mixture of ^{15}N-labelled and spin-labelled PRshort in the presence of cholic acid (Figure 4) show slightly reduced values (approx. 80 % of the original values), but are still present for all regions, indicating that formation of the correct dimer is impaired, but not dimerization as such.

In summary the results of the present study reveal for the first time the transient nature of the SFVmac PRshort dimer.

DISCUSSION

The active site of retroviral PRs is composed of residues from two monomeric subunits. Therefore dimerization is a prerequisite for PR activity [7,33,34].

The NMR structure of the PR domain from SFVmac, as well as analytical ultracentrifugation and size-exclusion analyses, revealed previously that the protein is a monomer in solution

[20]. This is in strong contrast with HIV-1 PR, where several mutations were necessary to obtain the monomeric form [42–44]. Despite the exclusive detection of this apparent monomeric state for SFVmac PRshort under prevalent experimental conditions, proteolytic activity could be observed [20]. Thus a small fraction of an active dimeric species was hypothesized to exist. To test this hypothesis, we analysed SFVmac PR activity in the presence of several HIV-1 PR inhibitors, which had been suggested to impair PR dimerization. Indinavir, a peptidomimetic HIV-1 PR inhibitor, which binds to the active site, was also tested for comparison, but did not have any impact on FV PR activity. Tipranavir and darunavir, which inhibit HIV-1 PR at concentrations as low as 0.01 μM by preventing dimerization in cells, showed no inhibitory effect on SFVmac PR. This could be due to the assay conditions which included 3 M NaCl (the inhibitors might not be able to bind to the PR in high-salt buffers). Furthermore, deviations in the dimer interfaces of HIV-1 and FV PRs, which are based on low sequence homologies, obviously result in dissimilar monomer/dimer states of the two proteins, indicating that these differences are too large to allow for the inhibitors to bind to FV PR.

Of the steroid derivatives suggested to inhibit HIV-1 PR dimerization cholic acid and lithocholic acid were able to impair FV PR activity. However, as cholic acid showed lower IC_{50} values, of 0.6–0.75 mM, this inhibitor was used for further analyses. Our results have shown that SFVmac PR activity is reduced in the presence of cholic acid (Figure 1), and NMR titration experiments (Figure 2) revealed the interaction sites of cholic acid with SFVmac PRshort.

The mode of action of cholic acid as a dimerization inhibitor for HIV-1 PR was proposed by an *in silico* study that suggested a binding site of cholic acid between the active-site loop and the intermonomeric β-sheet of the PR [32]. This is consistent with the large number of chemical shift perturbations of SFVmac PRshort observed in our titration experiments for residues in the N- and C-terminal regions as well as for residues in the active-site loop. In addition, we observed strong chemical shift changes in the flap region, which is located at the opposite site of the protein (Figure 2). This region is flexible in solution and forms the gate for the substrate [7,41]. The chemical shift changes observed could be explained by large structural rearrangements throughout the protein should cholic acid bind between the intermonomeric β-sheet and the active-site loop.

Alternatively, a second independent binding site could exist between the active-site loop and the flap region, either close to or in the active-site cavity. However, we were unable to directly deduce whether there was a second binding site from the titration curves (Figure 2), as the K_d values for cholic acid were too weak and the inhibitor concentration could not be increased due to solubility problems. More than one binding site for an HIV-1 PR inhibitor has been detected previously by high-resolution crystallography [45].

Our PRE measurements using spin-labelled SFVmac PRshort clearly show the presence of intermonomeric contacts even in the presence of cholic acid (Figure 4). The reduction of the PREs after the addition of cholic acid is smaller than expected for the case of complete suppression of dimer formation, implying that cholic acid only hinders the concerted interaction of regions necessary to form the correct dimer interface. Thus the action of cholic acid should be better characterized as impairing the formation of the active dimer rather than completely preventing dimerization.

The existence of specific contacts between different monomers can be shown explicitly by the observation of PREs on the ^{15}N-labelled SFVmac PRshort after mixing with the spin-labelled PR species (Figure 3). The PREs were detected on HSQC signals corresponding to the monomeric protein, demonstrating that the interaction is in fast exchange and transient. This is in agreement with the recent observation of transient events during N-terminal autoprocessing of HIV-1 PR [19]. The observed monomer/dimer equilibrium probably regulates PR activity, as for retroviruses timely processing of the Gag–Pol or, in the case of FVs, the Pol precursor protein is essential for virus maturation. Premature autoprocessing of the precursors is deleterious for the virus, as uptake of all viral proteins necessary for formation of the infectious virus particle would be prevented.

For HIV-1 PR it has been shown that autoprocessing of the N-terminus of the PR at the Gag–PR junction is essential for the regulation of activity and occurs via an intramolecular first-order cleavage of the precursor, whereas processing at the C-terminus of the PR does not appear to be important [12,46,47]. However, this regulatory mechanism cannot be responsible for PR activation in FV, as no Gag–Pol precursor exists and FV PRs already comprise the N-terminus of the Pol precursor. Thus other, as yet unknown, regulatory mechanisms for the activation of the PR appear to be important during the life cycle of FVs.

AUTHOR CONTRIBUTION

Birgitta Wöhrl conceived and co-ordinated the study. Maximilian Hartl conducted the majority of the experiments together with Kristian Schweimer and Martin Reger. Jochen Bodem designed and performed the cell culture assays. Kristian Schweimer and Stephan Schwarzinger designed the NMR experiments. Kristian Schweimer, Maximilian Hartl, Martin Reger and Stephan Schwarzinger analysed the NMR data. Paul Rösch and Stephan Schwarzinger provided conceptual input and suggestions for the completion of the manuscript. Birgitta Wöhrl, Kristian Schweimer and Maximilian Hartl wrote the paper.

ACKNOWLEDGEMENTS

We thank Dr H. Schramm (Max Planck Institut für Biochmie, Martinsried, Germany) for helpful discussions and Claudia Breit (Lehrstuhl fur Struktur und Chemie der Biopolymere, Universität Bayreuth, Germany) for initial PR cleavage experiments.

FUNDING

This work was supported by the Deutsche Forschungsgemeinschaft (DFG) [grant numbers Re627/7-1, Re627/8-1, SFB 479, Wo630/7-3]; and by the Graduate School in the Elite Network of Bavaria 'Lead Structures of Cell Functions'.

REFERENCES

1 Linial, M. L. (1999) Foamy viruses are unconventional retroviruses. J. Virol. **73**, 1747–1755
2 Enssle, J., Jordan, I., Mauer, B. and Rethwilm, A. (1996) Foamy virus reverse transcriptase is expressed independently from the gag protein. Proc. Natl. Acad. Sci. U.S.A. **93**, 4137–4141
3 Löchelt, M. and Flügel, R. M. (1996) The human foamy virus pol gene is expressed as a pro-pol polyprotein and not as a gag-pol fusion protein. J. Virol. **70**, 1033–1040
4 Rethwilm, A. (2003) The replication strategy of foamy viruses. Curr. Top. Microbiol. Immunol. **277**, 1–26
5 Rethwilm, A. (2005) Foamy viruses. In Topley & Wilson's Microbiology and Microbial Infections: Virology (ter Meulen, V. and Mahy, B. W. J., eds), pp. 1304–1321, Hodder Arnold, London
6 Oroszlan, S. and Luftig, R. B. (1990) Retroviral proteinases. Curr. Top. Microbiol. Immunol. **157**, 153–185
7 Dunn, B. M., Goodenow, M. M., Gustchina, A. and Wlodawer, A. (2002) Retroviral proteases. Genome Biol. **3**, reviews3006.1–reviews3006.7
8 Katoh, I., Yasunaga, T., Ikawa, Y. and Yoshinaka, Y. (1987) Inhibition of retroviral protease activity by an aspartyl proteinase inhibitor. Nature **329**, 654–656
9 Katoh, I., Ikawa, Y. and Yoshinaka, Y. (1989) Retrovirus protease characterized as a dimeric aspartic proteinase. J. Virol. **63**, 2226–2232

10 Pearl, L. H. and Taylor, W. R. (1987) A structural model for the retroviral proteases. Nature **329**, 351–354
11 Tessmer, U. and Krausslich, H. G. (1998) Cleavage of human immunodeficiency virus type 1 proteinase from the N-terminally adjacent p6* protein is essential for efficient gag polyprotein processing and viral infectivity. J. Virol. **72**, 3459–3463
12 Louis, J. M., Wondrak, E. M., Kimmel, A. R., Wingfield, P. T. and Nashed, N. T. (1999) Proteolytic processing of HIV-1 protease precursor, kinetics and mechanism. J. Biol. Chem. **274**, 23437–23442
13 Louis, J. M., Weber, I. T., Tozser, J., Clore, G. M. and Gronenborn, A. M. (2000) HIV-1 protease: maturation, enzyme specificity, and drug resistance. Adv. Pharmacol. **49**, 111–146
14 Pettit, S. C., Gulnik, S., Everitt, L. and Kaplan, A. H. (2003) The dimer interfaces of protease and extra-protease domains influence the activation of protease and the specificity of GagPol cleavage. J. Virol. **77**, 366–374
15 Chiu, H. C., Wang, F. D., Chen, Y. M. and Wang, C. T. (2006) Effects of human immunodeficiency virus type 1 transframe protein p6* mutations on viral protease-mediated gag processing. J. Gen. Virol. **87**, 2041–2046
16 Louis, J. M., Ishima, R., Torchia, D. A. and Weber, I. T. (2007) HIV-1 protease: structure, dynamics, and inhibition. Adv. Pharmacol. **55**, 261–298
17 Wondrak, E. M., Nashed, N. T., Haber, M. T., Jerina, D. M. and Louis, J. M. (1996) A transient precursor of the HIV-1 protease: isolation, characterization, and kinetics of maturation. J. Biol. Chem. **271**, 4477–4481
18 Cherry, E., Liang, C., Rong, L., Quan, Y., Inouye, P., Li, X., Morin, N., Kotler, M. and Wainberg, M. A. (1998) Characterization of human immunodeficiency virus type-1 (HIV-1) particles that express protease–reverse transcriptase fusion proteins. J. Mol. Biol. **284**, 43–56
19 Tang, C., Louis, J. M., Aniana, A., Suh, J. Y. and Clore, G. M. (2008) Visualizing transient events in amino-terminal autoprocessing of HIV-1 protease. Nature **455**, 693–696
20 Hartl, M. J., Wöhrl, B. M., Rösch, P. and Schweimer, K. (2008) The solution structure of the simian foamy virus protease reveals a monomeric protein. J. Mol. Biol. **381**, 141–149
21 Iwahara, J. and Clore, G. M. (2006) Detecting transient intermediates in macromolecular binding by paramagnetic NMR. Nature **440**, 1227–1230
22 Tang, C., Iwahara, J. and Clore, G. M. (2006) Visualization of transient encounter complexes in protein-protein association. Nature **444**, 383–386
23 Volkov, A. N., Worrall, J. A., Holtzmann, E. and Ubbink, M. (2006) Solution structure and dynamics of the complex between cytochrome c and cytochrome *c* peroxidase determined by paramagnetic NMR. Proc. Natl. Acad. Sci. U.S.A. **103**, 18945–18950
24 Hartl, M. J., Wöhrl, B. M. and Schweimer, K. (2007) Sequence-specific ^{1}H, ^{13}C and ^{15}N resonance assignments and secondary structure of a truncated protease from simian foamy virus. Biomol. NMR Assign. **1**, 175–177
25 Hartl, M. J., Kretzschmar, B., Frohn, A., Nowrouzi, A., Rethwilm, A. and Wöhrl, B. M. (2008) AZT resistance of simian foamy virus reverse transcriptase is based on the excision of AZTMP in the presence of ATP. Nucleic Acids Res. **36**, 1009–1016
26 Findlay, J. W. and Dillard, R. F. (2007) Appropriate calibration curve fitting in ligand binding assays. AAPS J. **9**, E260–E267
27 Cigler, P., Kozisek, M., Rezacova, P., Brynda, J., Otwinowski, Z., Pokorna, J., Plesek, J., Gruner, B., Doleckova-Maresova, L., Masa, M. et al. (2005) From nonpeptide toward noncarbon protease inhibitors: metallacarboranes as specific and potent inhibitors of HIV protease. Proc. Natl. Acad. Sci. U.S.A. **102**, 15394–15399
28 Lawrence, J. J., Berne, L., Ouvrier-Buffet, J. L. and Piette, L. H. (1980) Spin-label study of histone H1–DNA interaction. comparative properties of the central part of the molecule and the N and C-amino tails. Eur. J. Biochem. **107**, 263–269
29 Jahnke, W., Rudisser, S. and Zurini, M. (2001) Spin label enhanced NMR screening. J. Am. Chem. Soc. **123**, 3149–3150
30 Iwahara, J., Tang, C. and Marius Clore, G. (2007) Practical aspects of ^{1}H transverse paramagnetic relaxation enhancement measurements on macromolecules. J. Magn. Reson. **184**, 185–195
31 Sun, I. C., Shen, J. K., Wang, H. K., Cosentino, L. M. and Lee, K. H. (1998) Anti-AIDS agents: synthesis and anti-HIV activity of betulin derivatives. Bioorg. Med. Chem. Lett. **8**, 1267–1272
32 Quere, L., Wenger, T. and Schramm, H. J. (1996) Triterpenes as potential dimerization inhibitors of HIV-1 protease. Biochem. Biophys. Res. Commun. **227**, 484–488
33 Wlodawer, A. and Gustchina, A. (2000) Structural and biochemical studies of retroviral proteases. Biochim. Biophys. Acta **1477**, 16–34
34 Wlodawer, A., Miller, M., Jaskolski, M., Sathyanarayana, B. K., Baldwin, E., Weber, I. T., Selk, L. M., Clawson, L., Schneider, J. and Kent, S. B. (1989) Conserved folding in retroviral proteases: crystal structure of a synthetic HIV-1 protease. Science **245**, 616–621
35 Ishima, R., Torchia, D. A., Lynch, S. M., Gronenborn, A. M. and Louis, J. M. (2003) Solution structure of the mature HIV-1 protease monomer: insight into the tertiary fold and stability of a precursor. J. Biol. Chem. **278**, 43311–43319
36 Koh, Y., Matsumi, S., Das, D., Amano, M., Davis, D. A., Li, J., Leschenko, S., Baldridge, A., Shioda, T., Yarchoan, R. et al. (2007) Potent inhibition of HIV-1 replication by novel non-peptidyl small molecule inhibitors of protease dimerization. J. Biol. Chem. **282**, 28709–28720
37 Koh, Y., Nakata, H., Maeda, K., Ogata, H., Bilcer, G., Devasamudram, T., Kincaid, J. F., Boross, P., Wang, Y. F., Tie, Y. et al. (2003) Novel bis-tetrahydrofuranylurethane-containing nonpeptidic protease inhibitor (PI) UIC-94017 (TMC114) with potent activity against multi-PI-resistant human immunodeficiency virus in vitro. Antimicrob. Agents Chemother. **47**, 3123–3129
38 Poppe, S. M., Slade, D. E., Chong, K. T., Hinshaw, R. R., Pagano, P. J., Markowitz, M., Ho, D. D., Mo, H., Gorman, 3rd, R. R., Dueweke, T. J. et al. (1997) Antiviral activity of the dihydropyrone PNU-140690, a new nonpeptidic human immunodeficiency virus protease inhibitor. Antimicrob. Agents Chemother. **41**, 1058–1063
39 Reference deleted
40 Kosen, P. A. (1989) Spin labeling of proteins. Methods Enzymol. **177**, 86–121
41 Wlodawer, A. and Gustchina, A. (2000) Structural and biochemical studies of retroviral proteases. Biochim. Biophys. Acta **1477**, 16–34
42 Ishima, R., Ghirlando, R., Tozser, J., Gronenborn, A. M., Torchia, D. A. and Louis, J. M. (2001) Folded monomer of HIV-1 protease. J. Biol. Chem. **276**, 49110–49116
43 Ishima, R., Torchia, D. A., Lynch, S. M., Gronenborn, A. M. and Louis, J. M. (2003) Solution structure of the mature HIV-1 protease monomer: insight into the tertiary fold and stability of a precursor. J. Biol. Chem. **278**, 43311–43319
44 Ishima, R., Torchia, D. A. and Louis, J. M. (2007) Mutational and structural studies aimed at characterizing the monomer of HIV-1 protease and its precursor. J. Biol. Chem. **282**, 17190–17199
45 Kovalevsky, A. Y., Liu, F., Leshchenko, S., Ghosh, A. K., Louis, J. M., Harrison, R. W. and Weber, I. T. (2006) Ultra-high resolution crystal structure of HIV-1 protease mutant reveals two binding sites for clinical inhibitor TMC114. J. Mol. Biol. **363**, 161–173
46 Louis, J. M., Nashed, N. T., Parris, K. D., Kimmel, A. R. and Jerina, D. M. (1994) Kinetics and mechanism of autoprocessing of human immunodeficiency virus type 1 protease from an analog of the gag-pol polyprotein. Proc. Natl. Acad. Sci. U.S.A. **91**, 7970–7974
47 Louis, J. M., Clore, G. M. and Gronenborn, A. M. (1999) Autoprocessing of HIV-1 protease is tightly coupled to protein folding. Nat. Struct. Biol. **6**, 868–875

Received 16 September 2009/21 January 2010; accepted 8 February 2010
Published as BJ Immediate Publication 8 February 2010, doi:10.1042/BJ20091451

13 Publication G

Maximilian J. Hartl and Birgitta M. Wöhrl (2009): Regulation of foamy virus protease by RNA – a unique mechanism among retroviruses. *in preparation*.

Regulation of Foamy Virus Protease Activity by RNA – a Unique Mechanism Among Retroviruses

Maximilian J. Hartl and Birgitta M. Wöhrl*

Universität Bayreuth, Lehrstuhl für Struktur und Chemie der Biopolymere & Research Center for Biomacromolecules, 95440 Bayreuth, Germany

* Corresponding author, Mailing address for B.M. Wöhrl: Universität Bayreuth, Lehrstuhl Biopolymere, Universitätsstr. 30, D-95447 Bayreuth, Germany; Phone: +49 921 55-3542; Fax: +49 921 55-3544; E-mail: birgitta.woehrl@uni-bayreuth.de

Abbreviations

E. coli, Escherichia coli; HIV, human immunodeficiency virus; IPTG, isopropyl-thiogalactoside; LTR, long terminal repeat; PFV, prototype foamy virus; SFVmac, simian foamy virus from macaques; SHAPE, selective 2' hydroxyl acylation analyzed by primer extension; EMSA, electrophoretic mobility shift assay; NMIA, N-methylisatoic anhydride;

Abstract

The foamy virus Pol protein is translated independently from Gag from a separate mRNA. Thus, in contrast to orthoretroviruses no Gag-Pol precursor protein is synthesized. Only the integrase domain is cleaved off from Pol resulting in a mature reverse transcriptase harboring the protease domain at the N-terminus (PR-RT). We have demonstrated recently that FV protease is an inactive monomer with a very weak dimerization tendency and postulated protease activation through dimerization. Protease activity has to be strictly regulated in order to avoid its premature stimulation before Pol has been taken up into the virus. Here, we analyzed the CasI and CasII sequences of the pregenomic viral RNA and determined their impact on protease activity. CasII harbors the cPPT, which consists of the four purine rich elements A-D. Our data show that an RNA comprising the AB-elements is sufficient for protease stimulation. Electrophoretic mobilty shift assays and crosslinking reactions demonstrate an oligomeric binding of PR-RT to RNA. Although RNA is also bound non-specifically, only RNA sequences containing the A- and B-element result in significant activation of the protease. Structure analysis of AB-RNA by selective 2' hydroxyl acylation analyzed by primer extension predicts a distinct RNA folding, which is necessary for protease activation and thus virus maturation.

Key words: foamy virus, Pol, protease activation, polypurine tract, CasI CasII

Introduction

The replication of spumaretroviruses or foamy viruses (FVs) differs in several aspects from that of the orthoretroviruses. One important deviation from the replication strategy concerns the time point of reverse transcription, which in FVs takes place before the virus particles leave the cell, whereas orthoretroviruses reverse transcribe their RNA genome shortly after they have entered the host cell [1-3] (for reviews see [4-6]). As a consequence, FVs possess a double stranded DNA instead of a single stranded RNA genome. However, it has been shown that part of the DNA genome is still single stranded, indicating that plus strand DNA synthesis is not complete once progeny viruses are budding [7,8]. Another difference is the mode of *pol* expression. In orthoretroviruses, in addition to the Gag polypeptide a Gag-Pol fusion protein is synthesized at a ratio of approximately 1:20. Both polypeptides are taken up into the virus particle by interaction of the Gag region with the viral RNA (reviewed in [9]). In contrast FV Pol is synthesized from a separate mRNA independently from Gag, leading to a Pol precursor protein [10-12]. Consequently the uptake mechanism for FV Pol must be different. It has been shown that the C-terminus of FV Gag as well as parts of the FV genome contain determinants important for Pol uptake [13-16].

Once assembly of the viral components has taken place, the viral protease (PR) processes the Gag and Pol precursor proteins into mature structural and functional proteins. In FV only the viral integrase is cut off from Pol, whereas the protease (PR) remains covalently linked to the RT domain, thus leading to a mature protease-reverse transcriptase (PR-RT) protein [17]. It has been shown previously that the PFV and SFVmac PR-RT as well as the SFVmac PR domain are monomeric [18-20]. The PR domain forms only transient dimers, which constitute a very small fraction (< 5 %) of PR molecules [21]. Retroviral PRs have been shown to be active as homodimers [22].

Consequently, since they are predominantly monomeric proteins, SFVmac PR and PR-RT lack proteolytic activity under physiologically relevant conditions *in vitro*. So far, the regulatory mechanism for PR activation is not understood. Activation of the PR either in the separate PR domain or in the context of PR-RT could be achieved at very high NaCl concentrations of 2 – 3 M [19-21]. It is obvious that these conditions do not reflect the situation in living cells but somehow create an environment that facilitates dimerization, probably by hydrophobic interaction of two monomers.

To identify the factors that might be important for PR stimulation *in vivo* we set out to analyze relevant regions of the pregenomic viral RNA that might be able to stimulate PR

dimerization and thus activity. We postulated that RNA regions, which are essential for virus replication and/or Pol uptake might play a stimulatory role in PR activation as well.

In previous studies two cis-acting sequences, CasI and CasII, have been shown to play a role in the transfer of FV vectors [13,23-25], indicating an important role in virus assembly. CasI spans the region from nucleotide 1-645 and CasII from 3869-5884 of the pregenomic RNA from prototype FV (PFV). It has been demonstrated that FVs harbor a second, so called central polypurine tract (cPPT) in addition to the 3' PPT [8,16,26,27]. The latter is located upstream of the 3' long terminal repeat (LTR) and is required for plus strand DNA synthesis. FV share this feature of two PPTs with the lentiviruses, although they are members of different subfamilies. The cPPT is located in the *pol* open reading frame of the pregenomic viral RNA and thus is part of the CasII sequence. In FVs it is comprised of four purine rich regions (elements A-D, Figure 1) [26]. The A and B elements play a role in Pol protein encapsidation, whereas the C element is required for regulation of gene expression. Although only the sequence of the D element is 100 % identical to the 3' PPT region, no definite function could be determined. Mutations in D resulted in 50 % reduction of the virus titer [26].

We thus analyzed the influence of an *in vitro* transcribed RNA containing the CasI and CasII elements on PR activity. Our data show that cleavage of a model substrate by the PR-RT of PFV and simian FV from macaques (SFVmac) is strongly activated by an RNA fragment comprising the A and B elements of the cPPT, whereas the C and D elements exhibited only minor stimulation of PR activity.

Materials and Methods

Purification of SFVmac and PFV PR-RT. SFVmac and PFV PR-RTs, and the GB1-GFP PR substrate were purified as described previously [19,20,28].

RNA synthesis. Synthesis of all RNAs used in this study was done with the T7 or T3 MEGAscript® Kit (Applied Biosystems, Austin, USA). To obtain ^{32}P labeled RNA, 20 µCi α[^{32}P]-UTP (Hartmann Analytic GmbH, Braunschweig, Germany) were included in the *in vitro* transcription assay. All RNAs were purified over MicroSpin columns (GE Healthcare, Munich, Germany). The integrity of the RNAs was checked by denaturing gel electrophoresis (5 to 10 % polyacrylamid, 7 M urea). RNA folding was performed in the corresponding buffers used for the experiments by incubation for 2 min at 95 °C, followed by 10 min at 65 °C and slow cooling to 30 °C within 45 to 60 min directly before use.

PR activity assays. PR activity assays were performed as described previously [19] with minor changes. In summary, 10 µM of the GB1-GFP substrate, containing the SFVmac RT-IN cleavage site of the Pol polyprotein (ATQGSYVVH↓CNTTP) between GB1 and GFP, were incubated with 2.5 µM PR-RT and 0.5 µM DNA or RNA as indicated for 2 h at 37 °C in 50 mM Na_2HPO_4/NaH_2PO_4 pH 6.4 and 100 mM NaCl in a total volume of 20 µl. The products were then separated by electrophoresis on 10 % BisTris gels (Invitrogen, Karlsruhe, Germany) in 50 mM MES buffer pH 7.3, 50 mM Tris base, 0.1 % SDS, 1 mM EDTA.

Protein-Protein crosslinking. For crosslinking reactions 2 µM PFV or SFVmac PR-RT was incubated with 0.1 mM bis-sulfosuccinimidyl suberate (BS^3) (Sigma-Aldrich Chemie GmbH, Taufkirchen, Germany) in the presence or absence of 0.5 µM RNA as indicated, for 15 min at room temperature in 50 mM Na_2HPO_4/NaH_2PO_4 pH 6.4, 100 mM NaCl in a total volume of 5 µl. For each condition, control reactions were performed without BS^3. The reactions were stopped by the addition of an equal volume of 1 M Tris pH 9. To hydrolyze the RNA, the mixture was then incubated for 15 min at 45 °C. Reaction products were separated by electrophoresis on 10 % BisTris gels (Invitrogen, Karlsruhe, Germany) in 50 mM MES buffer pH 7.3, 50 mM Tris base, 0.1 % SDS, 1 mM EDTA.

Electrophoretic mobility shift assay. For electrophoretic mobility shift assays (EMSAs) 0.5 µM sense or antisense [^{32}P] labeled RNA-AB was mixed with 0 to 2.5 µM PFV or SFVmac PR-RT as indicated in 50 mM Na_2HPO_4/NaH_2PO_4 pH 6.4, 100 mM NaCl and 10 %

glycerol in a total volume of 10 µl. The mixture was incubated at room temperature for 5 min. Half of the mixture was loaded on a 6% DNA Retardation Gel (Invitrogen, Karlsruhe, Germany). Electrophoresis was carried out in 0.5 x TBE buffer (89 mM Tris/HCl pH, 8.0 89 mM borate and 20 mM EDTA) at 100 V for 3 h at 4 °C. RNA bands were visualized using a phosphoimaging device (FLA 3000, raytest, Straubenhardt, Germany).

5'-end labeling of DNA oligonucleotides. 100 pmol of 3'AB primer (5'-GGTCTTCCTACTAGCAGTTTAGTTAAAAGTCGTTTTATATC) (IBA, Göttingen, Germany) were labeled with 100 µCi γ [^{32}P]-ATP (Hartmann Analytic GmbH, Braunschweig, Germany) and 4 U T4 polynucleotide kinase (New England Biolabs, Frankfurt, Germany) in a total volume of 20 µl at 37 °C for 1 h, followed by inactivation of the kinase for 20 min at 65 °C. The labeled primer was finally purified via a MicroSpin column (GE Healthcare, Munich, Germany).

SHAPE. Selective 2' hydroxyl acylation analyzed by primer extension (SHAPE) [29-31] was used to determine the secondary structure of RNA-AB. In principle, the protocol developed by Wilkinson *et al.* [32] was used. A total of 2 pmol RNA-AB in 12 µl 0.5 x TE buffer (10 mM Tris/HCl pH 8.0 and 1 mM EDTA) was heated to 95 °C for 2 min and then put on ice for 2 min. Folding of the RNA was completed by the addition of 6 µl RNA folding mix (333 mM HEPES pH 8.0, 20 mM $MgCl_2$ and 333 mM NaCl) and incubation for 20 min at 37 °C. Half of the mixture was removed and modified by adding 18 mM N-methylisatoic anhydride (NMIA; Invitrogen, Karlsruhe, Germany), dissolved in 100 % DMSO, and incubation for 45 min at 37 °C. The other half served as a control and was treated with DMSO only. Both samples were ethanol precipitated and the resulting pellet was dissolved in 10 µl 0.5 x TE buffer.

For primer annealing 100 nM [^{32}P]-labeled 3'AB primer was incubated for 5 min at 65 °C. The reaction mixture was then slowly cooled down to 35 °C within 1 h. Reverse transcription was carried out in 50 mM Tris/HCl pH 8.3, 50 mM KCl, 3 mM $MgCl_2$, 5 mM DTT and 500 µM of each dNTP for 10 min in a total volume of 20 µl. The reaction mixture was preincubated for 1 min at 52 °C. Then the reaction was started by the addition of 200 U of Superscript III reverse transcriptase (Invitrogen, Karlsruhe, Germany) and further incubation at 52 °C for 10 min. Subsequently, to degrade the RNA template, 1 µl of 4 M NaOH was

added and the mixture was incubated for 5 min at 95 °C. Finally, an equal volume of 8 M urea in 1 M Tris/HCl pH 8.0, 50 mM boric acid and 50 mM EDTA, containing traces of bromophenol blue and xylene cyanol, was added. 8 µl samples were analyzed by denaturing gel electrophoresis (10 % polyacrylamide, 7 M urea). The reaction products were visualized and quantified by densitometry using a phosphoimaging device (FLA 3000, raytest, Straubenhardt, Germany) and the software AIDA (version 4.15; raytest, Straubenhardt, Germany).

For calculation of relative SHAPE intensities the difference between the integrated band intensities of the reactions with and without NMIA was divided by the highest measured value in the experiment. Relative SHAPE intensities higher than 0.35 were considered significant. The RNA secondary structure was predicted using RNAfold [33,34]. Nucleotides (nt) showing significant SHAPE intensities (for exceptions see results) were assumed not to pair.

Sequencing. To assign the SHAPE reaction products, sequencing reactions were run in parallel using the same [^{32}P] endlabeled 3'AB primer and a vector harboring the CasI-CasII DNA sequences as a template. Sequencing reactions were performed with the Sequenase 7-deaza-dGTP Sequencing Kit (usb, Cleveland, USA) using the ^{32}P endlabeled 3' AB primer.

Results

To analyze the PR activity, we used the recombinant PR-RTs of PFV and SFVmac purified from *Escherichia coli* (*E. coli*) [20,28] and added different RNAs containing either the complete CasI and CasII sequences or shorter versions thereof, as indicated in Figure 1.

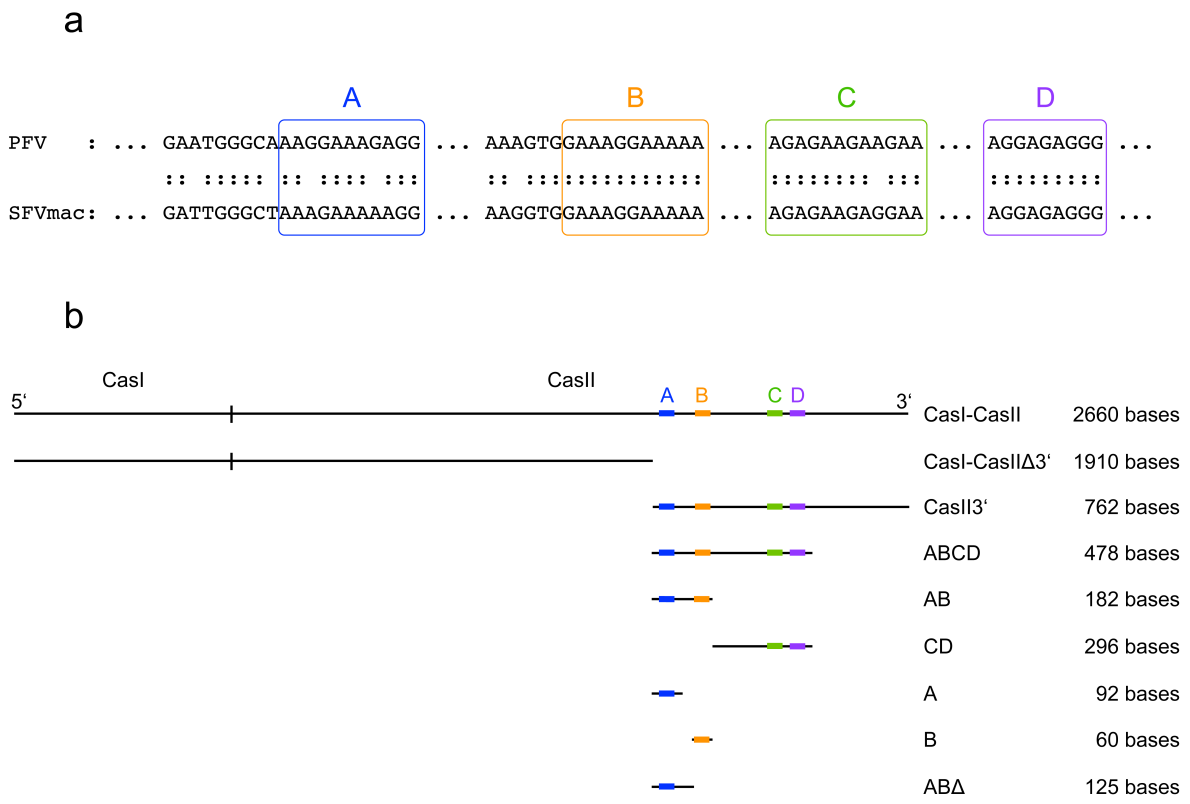

Figure 1: **Sequence comparison of PFV and SFVmac purine rich elements and schematic representation of RNA fragments used in this study.**
(a), Purine rich sequences of the PFV and SFVmac cPPT are shown. The core sequences are highlighted. **(b)**, Overview of the RNAs examined for PR activation. The relative positions of the polypurine rich sequences A to D and the lengths of the different RNAs are displayed.

PR activity was examined using a model substrate described previously, which contains the natural PR cleavage site in the Pol precursor between the GB1 and GFP protein domains [19]. We showed previously that in the absence of other factors, PR could only be activated at high NaCl concentrations of 2 - 3 M [19,20]. Here, we decreased the NaCl concentration to 100 mM, to achieve conditions that are biologically more relevant. Analysis of the cleavage products by SDS-PAGE reveals that the CasI-CasII RNA can stimulate PR activity (Figure 2). To identify the RNA sequence sufficient for stimulation we created two shorter RNA fragments CasI-CasIIΔ3', and CasII-3' harboring the cPPT (Figure 1). Since the stimulatory

effect of CasII-3' was much more pronounced, we created 5' deletions in CasII-3' to determine the minimal region necessary for PR stimulation. The *in vitro* transcribed RNAs harbored various regions of the cPPT A-D elements of PFV: ABCD; AB; CD; A; B and ABΔ, which contains a deletion of the 3' region of the B element. In addition, antisense RNAs of CasI-CasII (=anti-CasI-CasII) and of AB (=anti-AB) were tested (Figure 1). We used these RNAs to investigate the PR activities of both, PFV and SFVmac PR-RT.

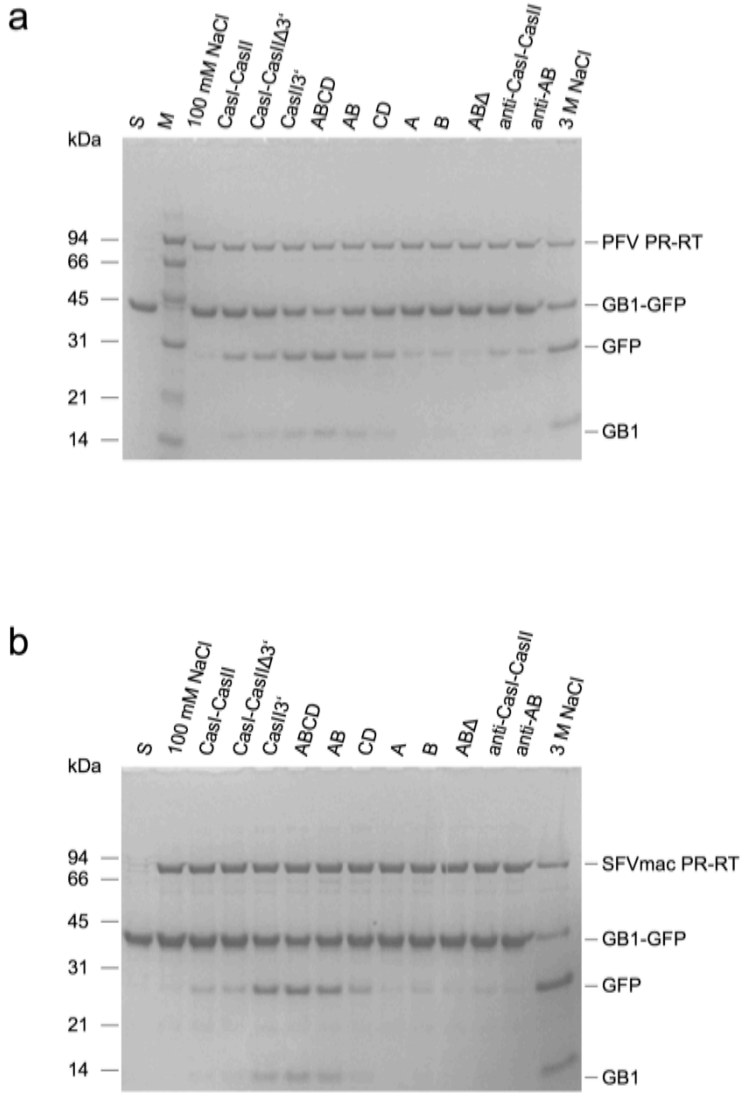

Figure 2: **Proteolytic activities of PR-RT in the presence of various RNAs.**
Activity assays with different RNAs were performed with (**a**) PFV and (**b**) SFVmac PR-RT. 10 µM GB1-GFP substrate was incubated with 2.5 µM PR-RT and 0.5 µM RNA as indicated at 37°C for 2 h in 50 mM Na_2HPO_4/NaH_2PO_4 pH 6.4, 100 mM NaCl. Reaction products were analyzed by 10 % BisTris gels. S: uncleaved substrate; M, molecular weight standard. The sizes of the standard proteins are indicated on the left.

Figure 2 shows that the cleavage activity of both enzymes in the presence of AB is comparable with that of the ABCD or the CasII 3' RNAs, whereas neither A nor B alone could not stimulate PR in a similar manner. Also truncation of AB at the 3' end (ABΔ) by

57 nt resulted in a weaker PR activity, which was similar to that of anti-AB. Obviously, RNA in general had a weak stimulatory effect on PR activity, whereas we could not observe any change in PR activity when DNA-CasI-CasII, -ABCD or –AB was added (data not shown). However, strong activation appeared to be dependent on the presence of AB-RNA, whereas CD-RNA resulted only in weak stimulation. Interestingly, the PFV AB-RNA stimulated SFVmac PR-RT to a similar extent, although the sequence of the A-element differs by two bases (Figure 1a). Addition of 6 mM $MgCl_2$ to the reaction mixture or refolding of the RNAs after *in vitro* transcription and purification did not change the results (data not shown).

Secondary structure prediction of the PFV cPPT AB-RNA reveals a molecule with several hairpin loop structures (data not shown). To determine the actual structure of the PFV AB-RNA we performed SHAPE analyses. NMIA preferentially reacts with conformationally flexible nucleotides, e.g. nucleotides that are not base paired, at the 2' OH of the ribose. Sequencing reactions of RNA treated with NMIA will stop at positions modified with NMIA. Thus, nucleotides showing significantly higher band intensities in sequencing reactions after treatment with NMIA correspond to single-stranded RNA regions.

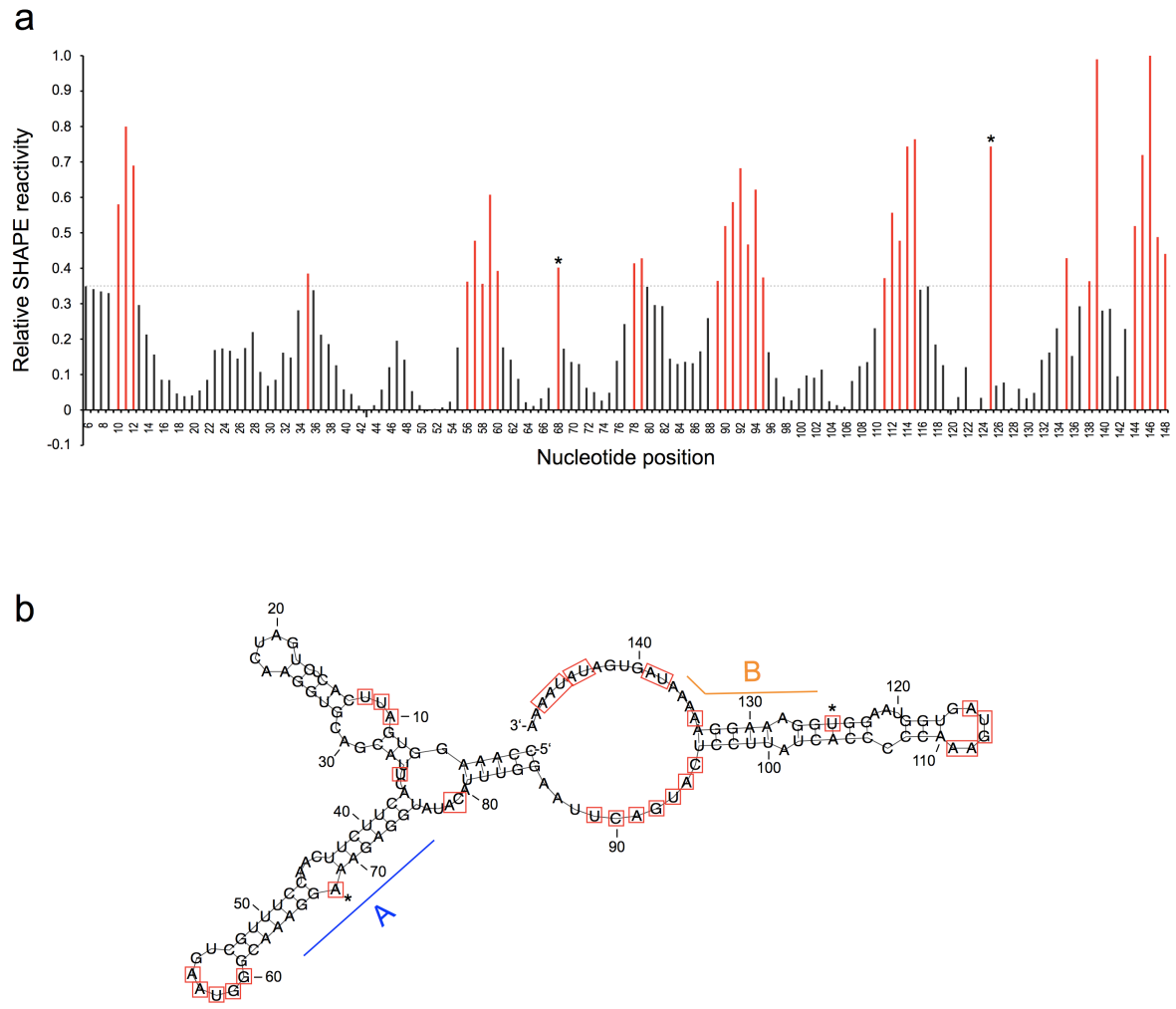

Figure 3: SHAPE analysis of RNA-AB.
(**a**) Relative SHAPE intensities as a function of nucleotide position. (**b**) RNA secondary structure model of RNA-AB using SHAPE constraints. Bases with relative SHAPE intensities higher than 0.35 are highlighted in purple. (*): significant intensities were only measured at NMIA concentrations higher than 14 mM NMIA and the corresponding bases not constrained in the RNA secondary structure calculation.

Our data (Figure 3A) indentified several regions in the RNA-AB sequence, which were unpaired. Calculations of the RNA secondary structure including constraints for the unpaired regions (Figure 3B) confirmed the predicted RNA secondary structure to a great extent. The RNA consists of three hairpin loop structures and a central as well as a 3' unpaired region (nt 86 to 95 and 134 to 150). The A and B elements are each located in a hairpin of approximately 15 nt in length. Upstream of the A- as well as the B-element an accumulation of purines can be observed starting at the beginning of the loop. Thus, in both cases the region 3' of the loop almost exclusively consists of purines.

Two nt (68 and 125) showed an unusual behavior. Only NMIA concentrations higher than 14 mM resulted in strong signals at these nt, implying that they were in an unpaired region,

whereas lower NMIA concentrations did not show this effect (Table 1). Thus, nt 68 and 125 were not considered to be unpaired in our secondary structure calculations.

Table 1: Relative SHAPE reactivity of selected nucleotides.

nt	11 mM NMIA	14 mM NMIA	18 mM NMIA
68	0.07	0.10	0.40
94	0.49	0.55	0.62
97	0.07	0.11	0.09
125	0.04	0.06	0.74

To confirm the hypothesis that the PR-RTs bind to RNA-AB in order to enhance PR activity, we performed EMSAs with PFV PR-RT and RNA-AB as well as anti-AB (Figure 4). Our experiments with AB indicated that RNA binding might be a prerequisite for PR activation. Not surprisingly, since RTs are nucleic acid binding proteins, that bind to RNA or DNA also non-specifically, anti-AB RNA was shifted, too.

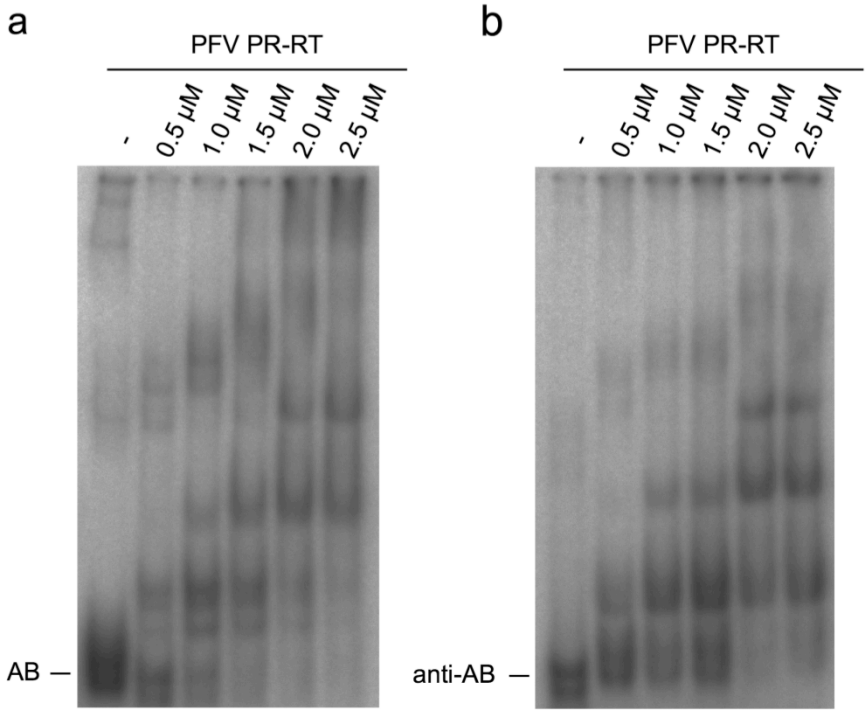

Figure 4: Electrophoretic mobility shift assay with different RNAs.
500 nM of a radioactively labeled RNA (**a**) AB or (**b**) anti-AB was incubated with increasing concentrations of PFV PR-RT in 50 mM Na_2HPO_4/NaH_2PO_4 pH 6.4, 100 mM NaCl and 10 % glycerol at RT for 5 min. Complexes were separated on 6 % DNA retardation gels at 4 °C.

Multiple shift bands indicated that dimers and higher multimers were formed. However, binding to AB appeared to be slightly stronger than for anti-AB. Similar results were obtained with SFVmac PR-RT (data not shown).

Since dimerization of the PR domain is a prerequisite for PR activity, we analyzed whether binding to AB-RNA or anti-AB actually initiated PR-RT dimerization. PFV PR-RT, was crosslinked with the corsslinking reagent BS^3 in the presence or absence of RNA-AB or anti AB, respectively. To exclude crosslinking of PR-RT to RNA, RNA hydrolysis under alkaline conditions was performed before the samples were analyzed by SDS-PAGE (Figure 5).

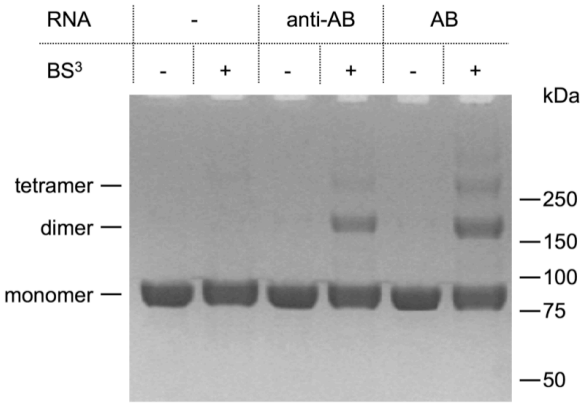

Figure 5: **Protein crosslink of PFV PR-RT.**
Crosslinking reactions were performed with 2 µM PFV PR-RT and 0.1 mM BS^3 in the presence or absence of different RNAs (0.5 µM) as indicated for 15 min at RT in 50 mM Na_2HPO_4/NaH_2PO_4 pH 6.4, 100 mM NaCl. After RNA hydrolysis, reaction products were separated on 10 % BisTris gels. The proposed oligomerization state is indicated on the left, the sizes of the standard proteins are displayed the right.

Clearly, dimers and, however to a much lower extent, tetramers of PFV PR-RT could be detected with the samples containing RNA. No dimers or multimers are visible in the control assays without RNA. Again, dimerization in the presence of RNA-AB is slightly more pronounced as compared to anti-AB. Comparable results were obtained using SFVmac PR-RT (data not shown). The protein crosslink proves that FV PR-RTs dimerize when binding to RNA. Specific RNA sequences appear to stimulate binding and dimerization of the PR-RTs to a greater extent than RNAs that do not harbor the AB sequences (Figure 4, 5).

Discussion

It has been shown previously that PFV as well as SFVmac PR-RT behave like monomers under biologically relevant conditions [18-20]. Although dimerization is needed for a catalytically active PR [22], only a small fraction (< 5 %) was dimerized [21]. Activation of FV PR *in vitro* could be accomplished at high salt concentrations (2 – 3 M NaCl) [19,20]. However, how dimerization is achieved during the viral life cycle remained unclear.

Orthoretroviral PRs investigated so far are present in the virion as rather stable dimers with catalytic activity [22,35]. Recently, a study showed that the HIV-1 PR domain can form transient dimers in the Gag-Pol precursor protein [36]. Thus, premature activation of PR can be prevented before virus assembly. Packaging of the Pol proteins in HIV-1 is mediated by RNA binding of Gag within the Gag-Pol polyprotein (reviewed in [9]) and this process probably activates PR. Since FVs express Gag and Pol independently, Pol packaging and PR regulation have to be different.

The C-terminus of Gag as well as the A and B elements of the FV cPPT have been identified as determinants for Pol uptake [14-16]. Here, we show that CasI-CasII RNA enables PR-RT to form a proteolytically active dimer. Truncating the CasI-CasII RNA at the 5' and 3' ends allowed us to define the minimum sequence needed for PR activation (Figure 2). Our data indicate that important interactions between Pol and the A and B elements of the cPPT occur during virus assembly and maturation [26]. Therefore, RNA binding of Pol is not only required for Pol encapsidation, but for PR activation as well.

Secondary structure analysis by SHAPE showed similar folds of the A and B elements (Figure 3). Each sequence is part of a hairpin loop structure. The loop and the 3' sequence of the stem are formed almost exclusively by purines. The polypurine sequences of the HIV RNA/DNA hybrid have been associated with bent structures and deviations from Watson-Crick base pairing have been reported [37,38].

Unusual behavior of nt 68 and 125 of the AB-element of the PFV PPT was observed. While low NMIA concentrations predicted paired bases, high NMIA concentrations indicated that they were not paired (Table 1). We cannot exclude that high NMIA concentrations themselves caused changes in RNA folding and led to a modification of the 2' OH ribo-group of the two nt. Noticeably, only nt 68 and 125 were affected. Both are located in the center of a polypurine hairpin loop structure. This might indicate that indeed a distinct RNA tertiary structure was formed, which is recognized by PR-RT, leading to the formation of a proteolytically active PR-RT dimer upon binding. Thus, even though the PFV PPT is built by

double stranded RNA, its structure reveals similar abnormal behavior as the RNA/DNA hybrid of the HIV PPT [37,38].

EMSA analyses proved PR-RT binding to RNA (Figure 4). PR-RT appears to bind to RNA independently of the sequence. Shifts corresponding to multiple binding of PR-RT were obtained for RNA-AB and anti-AB with only minor differences. Crosslinking experiments revealed similar results (Figure 5). Without RNA PR-RT is monomeric as has already been shown previously [18-20]. In the presence of RNA-AB as well as anti-AB, dimers and even tetramers could be detected. EMSA and protein crosslinking are in good agreement with PR activity assays, where all RNA sequences had at least a low stimulatory effect on PR activity. In conclusions, our data indicate that PR-RT dimerizes upon RNA binding. However, RNA containing the A and B elements with a distinct RNA folding appears to be required to form a stabile PR-RT dimer with high catalytic activity.

We propose that PR in FVs is inactive after expression within the Pol polyprotein due to inefficient dimerization [21]. Packaging of Pol is achieved through binding of Pol via the PR-RT domain to the A- and B- RNA sequences of the FV cPPT [13,26], whereas Gag is recruited via its C-terminus [14]. Only PR-RT bound to the cPPT RNA is able to form proteolytically active dimers thus allowing cleavage of Pol and Gag, which results in mature virus particles.

Acknowledgements

The project was funded by the Deutsche Forschungsgemeinschaft DFG (Wo630/7-3), the Graduate School in the Elite Network of Bavaria “Lead Structures of Cell Functions” and the University of Bayreuth.

References

1 Moebes, A., Enssle, J., Bieniasz, P. D., Heinkelein, M., Lindemann, D., Bock, M., McClure, M. O. and Rethwilm, A. (1997) Human foamy virus reverse transcription that occurs late in the viral replication cycle. J. Virol. **71**, 7305-7311

2 Yu, S. F., Sullivan, M. D. and Linial, M. L. (1999) Evidence that the human foamy virus genome is DNA. J. Virol. **73**, 1565-1572

3 Rethwilm, A. (2003) The replication strategy of foamy viruses. Curr. Top. Microbiol. Immunol. **277**, 1-26

4 Rethwilm, A. (2005) Foamy viruses. In Topley & Wilson's Microbiology and Microbial Infections - Virology (ter Meulen, V. and Mahy, B. W. J., eds.), pp. 1304-1321, Hodder Arnold, London

5 Rethwilm, A. (2007) Foamy virus vectors: An awaited alternative to gammaretro- and lentiviral vectors. Curr. Gene Ther. **7**, 261-271

6 Linial, M. (2007) Foamy viruses. In Fields Virology (Knipe, D. M. and Howley, P. M., eds.), pp. 2245-2262, Lippincott Williams & Wilkins, Philadelphia

7 Schweizer, M., Renne, R. and Neumann-Haefelin, D. (1989) Structural analysis of proviral DNA in simian foamy virus (LK-3)-infected cells. Arch. Virol. **109**, 103-114

8 Kupiec, J. J., Tobaly-Tapiero, J., Canivet, M., Santillana-Hayat, M., Flügel, R. M., Peries, J. and Emanoil-Ravier, R. (1988) Evidence for a gapped linear duplex DNA intermediate in the replicative cycle of human and simian spumaviruses. Nucleic Acids Res. **16**, 9557-9565

9 Goff, S. P. (2007) Retroviridae: The retroviruses and their replication. In Fields Virology (Knipe, D. M. and Howley, P. M., eds.), pp. 1999-2069, Lippincott Williams & Wilkins, Philadelphia

10 Enssle, J., Jordan, I., Mauer, B. and Rethwilm, A. (1996) Foamy virus reverse transcriptase is expressed independently from the gag protein. Proc. Natl. Acad. Sci. U. S. A. **93**, 4137-4141

11 Jordan, I., Enssle, J., Guttler, E., Mauer, B. and Rethwilm, A. (1996) Expression of human foamy virus reverse transcriptase involves a spliced pol mRNA. Virology. **224**, 314-319

12 Löchelt, M. and Flügel, R. M. (1996) The human foamy virus pol gene is expressed as a pro-pol polyprotein and not as a gag-pol fusion protein. J. Virol. **70**, 1033-1040

13 Heinkelein, M., Leurs, C., Rammling, M., Peters, K., Hanenberg, H. and Rethwilm, A. (2002) Pregenomic RNA is required for efficient incorporation of pol polyprotein into foamy virus capsids. J. Virol. **76**, 10069-10073

14 Lee, E. G. and Linial, M. L. (2008) The C terminus of foamy retrovirus gag contains determinants for encapsidation of pol protein into virions. J. Virol. **82**, 10803-10810

15 Stenbak, C. R. and Linial, M. L. (2004) Role of the C terminus of foamy virus gag in RNA packaging and pol expression. J. Virol. **78**, 9423-9430

16 Peters, K., Wiktorowicz, T., Heinkelein, M. and Rethwilm, A. (2005) RNA and protein requirements for incorporation of the pol protein into foamy virus particles. J. Virol. **79**, 7005-7013

17 Pfrepper, K. I., Rackwitz, H. R., Schnolzer, M., Heid, H., Löchelt, M. and Flügel, R. M. (1998) Molecular characterization of proteolytic processing of the pol proteins of human foamy virus reveals novel features of the viral protease. J. Virol. **72**, 7648-7652

18 Benzair, A. B., Rhodes-Feuillette, A., Emanoil-Ravicovitch, R. and Peries, J. (1982) Reverse transcriptase from simian foamy virus serotype 1: Purification and characterization. J. Virol. **44**, 720-724

19 Hartl, M. J., Wöhrl, B. M., Rösch, P. and Schweimer, K. (2008) The solution structure of the simian foamy virus protease reveals a monomeric protein. J. Mol. Biol. **381**, 141-149

20 Hartl, M. J., Mayr, F., Rethwilm, A. and Wöhrl, B. M. (2009) Biophysical and enzymatic properties of the simian and prototype foamy virus reverse transcriptase. *submitted*. Publication A

21 Hartl, M. J., Schweimer, K., Reger, M. H., Schwarzinger, S., Bodem, J., Rösch, P. and Wöhrl, B. M. (2009) Formation of transient dimers by a retroviral protease. *Biochemical Journal, in revision*. Publication F

22 Pearl, L. H. and Taylor, W. R. (1987) A structural model for the retroviral proteases. Nature. **329**, 351-354

23 Heinkelein, M., Dressler, M., Jarmy, G., Rammling, M., Imrich, H., Thurow, J., Lindemann, D. and Rethwilm, A. (2002) Improved primate foamy virus vectors and packaging constructs. J. Virol. **76**, 3774-3783

24 Linial, M. L. and Eastman, S. W. (2003) Particle assembly and genome packaging. Curr. Top. Microbiol. Immunol. **277**, 89-110

25 Erlwein, O., Bieniasz, P. D. and McClure, M. O. (1998) Sequences in pol are required for transfer of human foamy virus-based vectors. J. Virol. **72**, 5510-5516

26 Peters, K., Barg, N., Gärtner, K. and Rethwilm, A. (2008) Complex effects of foamy virus central purine-rich regions on viral replication. Virology **33**, 51-60

27 Tobaly-Tapiero, J., Kupiec, J. J., Santillana-Hayat, M., Canivet, M., Peries, J. and Emanoil-Ravier, R. (1991) Further characterization of the gapped DNA intermediates of human spumavirus: Evidence for a dual initiation of plus-strand DNA synthesis. J. Gen. Virol. **72**, 605-608

28 Hartl, M. J., Kretzschmar, B., Frohn, A., Nowrouzi, A., Rethwilm, A. and Wöhrl, B. M. (2008) AZT resistance of simian foamy virus reverse transcriptase is based on the excision of AZTMP in the presence of ATP. Nucleic Acids Res. **36**, 1009-1016

29 Wilkinson, K. A., Gorelick, R. J., Vasa, S. M., Guex, N., Rein, A., Mathews, D. H., Giddings, M. C. and Weeks, K. M. (2008) High-throughput SHAPE analysis reveals structures in HIV-1 genomic RNA strongly conserved across distinct biological states. PLoS Biol. **6**, e96

30 Merino, E. J., Wilkinson, K. A., Coughlan, J. L. and Weeks, K. M. (2005) RNA structure analysis at single nucleotide resolution by selective 2'-hydroxyl acylation and primer extension (SHAPE). J. Am. Chem. Soc. **127**, 4223-4231

31 Mortimer, S. A. and Weeks, K. M. (2007) A fast-acting reagent for accurate analysis of RNA secondary and tertiary structure by SHAPE chemistry. J. Am. Chem. Soc. **129**, 4144-4145

32 Wilkinson, K. A., Merino, E. J. and Weeks, K. M. (2006) Selective 2'-hydroxyl acylation analyzed by primer extension (SHAPE): Quantitative RNA structure analysis at single nucleotide resolution. Nat. Protoc. **1**, 1610-1616

33 Mathews, D. H., Sabina, J., Zuker, M. and Turner, D. H. (1999) Expanded sequence dependence of thermodynamic parameters improves prediction of RNA secondary structure. J. Mol. Biol. **288**, 911-940

34 Gruber, A. R., Lorenz, R., Bernhart, S. H., Neubock, R. and Hofacker, I. L. (2008) The vienna RNA websuite. Nucleic Acids Res. **36**, W70-4

35 Dunn, B. M., Goodenow, M. M., Gustchina, A. and Wlodawer, A. (2002) Retroviral proteases. Genome Biol. **3**, 1465-6914

36 Tang, C., Louis, J. M., Aniana, A., Suh, J. Y. and Clore, G. M. (2008) Visualizing transient events in amino-terminal autoprocessing of HIV-1 protease. Nature. **455**, 693-696

37 Fedoroff, O. Y., Ge, Y. and Reid, B. R. (1997) Solution structure of r(gaggacug):D(CAGTCCTC) hybrid: Implications for the initiation of HIV-1 (+)-strand synthesis. J. Mol. Biol. **269**, 225-239

38 Sarafianos, S. G., Das, K., Tantillo, C., Clark, A. D.,Jr., Ding, J., Whitcomb, J. M., Boyer, P. L., Hughes, S. H. and Arnold, E. (2001) Crystal structure of HIV-1 reverse transcriptase in complex with a polypurine tract RNA:DNA. EMBO J. **20**, 1449-1461

14 Acknowledgement

I would like to gratefully and sincerely thank Prof. Dr. Birgitta Wöhrl for her guidance, understanding, patience, and most importantly, for encouraging me to grow as an independent thinker. Thank you for trying hard in finding positive remarks first.
Moreover, I thank Dr. Kristian Schweimer for spending so many hours explaining the miraculous world of NMR ... and then explaining all over again.
I would like to thank Prof. Dr. Axel Rethwilm, Dr. Jochen Bodem and Benedikt Kretzschmar for endless discussions, skepticism and sharing newest results.
I am also grateful for a unique working atmosphere – thanks to all Biopoles and Prof. Dr. Paul Rösch. A special thanks to Ulrike Persau, Andrea Hager, Ramona Heissmann, Britta Zimmerman, Katrin Weiß, Violaine Zigan and Gudrun Wagner for their support in everyday matters and Dr. Stephan Schwarzinger for taking care of all these BIGSS things. Dr. Stefan Prasch, Dr. Hanna Berkner, Sabine Wenzel, Philipp Weiglmeier, Luisa Ströh, Claudia Knake, Florian Mayr, Berit Leo, Sophie Pleißner and Björn Burmann deserve many thanks for high-level discussions at coffee break and for the one or two drinks after work.
Furthermore, many thanks to Martin Reger for showing me this other side of scientific work and all the other friends of mine I cannot mention personally.
My family has been a constant source of support – emotional and moral. Special, special thanks to my grandparents, my dear brothers and parents. Thank you so much Susi und Wilfried, especially for inculcating in me the dedication and discipline to do whatever I undertake well.
Finally, and most importantly, I would like to thank my loved piratess Olli. You are my joy, my pillar and my guiding light. Thank you for the happiness and music in my life.

15 Erklärung

Hiermit erkläre ich, dass ich diese Arbeit selbstständig verfasst und keine anderen als die von mir angegebenen Quellen und Hilfsmittel benutzt habe.

Ferner erkläre ich, dass ich anderweitig mit oder ohne Erfolg nicht versucht habe, diese Dissertation einzureichen. Ich habe keine gleichartige Doktorprüfung an einer anderen Hochschule endgültig nicht bestanden.

Bayreuth, den 21. April 2010